International PhD Program in Neurosciences

XXIX Cycle

DYNAMIC EXPRESSION OF AQUAPORINS IN PHYSIOLOGICAL AND PATHOPHYSIOLOGICAL *IN VITRO* MODELS

PhD Thesis

Rosanna Avola

Coordinator: Prof. Salvatore Salomone

Tutor: Prof. Venera Cardile

Department of Biomedical and Biotechnological Sciences

University of Catania - Medical School

Year 2016

To Gloria

With encouragement to aim as high as possible

and with the belief that everything in life

can be achieved if you believe and work

hard enough for it.

TABLE OF CONTENTS

ACKNOWLEDGEMENTS

The years of PhD program have been a precious experience, an exciting journey that I could not have undertaken without the enduring support of my Tutor, Colleagues and Family.

I wish to thank my Tutor, Prof. Venera Cardile, University of Catania, for welcoming me in her laboratory, who introduced me to the world of cells physiology and the complexities of stem cells science. I have greatly appreciated her support, without which, I would have never successfully completed this project.

I am very grateful to Prof. Filippo Drago and Prof. Salvatore Salomone, University of Catania; they gave me the opportunity to take part to this PhD program.

I wish to thank Dr. Adriana Carol Eleonora Graziano and Dr. Giovanna Pannuzzo, for sharing with me their knowledge, they were able to give me good advices and technical supports.

I want to thank also all Professors, colleagues and friends of the Section of Physiology of University of Catania.

Finally, I would like to thank my family and Giuseppe for their love and support kept me going, especially those difficult days when things do not seem to work.

Thank you everyone for making my PhD such a wonderful journey!

LIST OF ABBREVIATIONS

6-OHDA	6-hydroxydopamine
ADH	Antidiuretic hormone
Ag	Antigen
ANP	Atrial natriuretic peptide
AQP1	Aquaporin-1
AQP2	Aquaporin-2
AQPs	Aquaporins
ar/R	Aromatic/arginine
ASCs	Adult stem cells
AT-MSCs	Mesenchymal stem cells from adipose tissue
BBB	Blood Brain Barrier
BDNF	Brain-derived neurontrophic factor
BHA	Butylated hydroxyanisole
BM- MSCs	Bone marrow mesenchymal stem cells
BME	β-mercaptoethanol
CFU-F	Colony-forming-unit fibroblastic cells
CGMP	Cyclic guanosine monophosphate
CHIP 28	Channel like Intrinsic Protein of 28 kDa
CNS	Central Nervous System
CP	Choroid plexus
CSF	Cerebro Spinal Fluid
DA	Dopamine transporter
DMSO	Dimethyl sulfoxide
ECS	Brain extracellular space
EGF	Epidermal growth factor
ER	Reticulum endoplasmatic
ESCs	Embryonic stem cells
FAK	Focal adhesion kinase
FGF-β	Basal fibroblast growth factor
FSCs	Fetal stem cells
G1-G3	Glycerol molecules

GALC	Enzyme galactosylceramidase
GLD	Globoid cell leukodystrophy
GlpF	Glycerol facilitator
HGF	Hepatocyte growth factor
IGF	Insulin-like growth factor
ISCT	International Society for Cellular Therapy
KD	Krabbe disease
kDa	Kilodalton
Kir4.1	Rectifyng potassium channel 4.1
MIP	Major Intrinsic Protein
MPA	Phorbol 12-Myristate 13-acetate
MPP^+	1-methyl-4-phenylpyridinium
MPTP	1-methyl-4-phenyl-1, 2, 3, 6-tetrahydropyridine
NGF	Nerve growth factor
NPA	Asn-Pro-Ala conserved motif
NSCs	Neural stem cells
OECs	Olfactory ensheathing cells
P	Passage
PAS	Periodic acid-Schiff
PD	Parkinson's disease
PDGF	Platelet-derived growth factor
PLA	Lipoaspirate
PNS	Peripheral nervous system
RA	Retinoic acid
RBC	Red blood cells
ROS	Reactive oxygen species
RT-PCR	Reverse transcriptase-polymerase chain reaction
SNpc	Substantia nigra pars compacta
SVF	Stromal-vascular fraction
TM	Transmembrane domains
VEGF	Vascular endothelial growth factor

ABSTRACT

Water is the main component of biological fluids and a prerequisite of all organisms living. In 1987, Agre and coworkers isolated a new integral membrane protein acting as a channel that mediates the water flux and uncharged solutes across biological membranes. This protein was called aquaporin1 and ever since its discovery, more than 300 homologues have been identified in many phyla, including animal, bacteria and plant. So far, in human have been discovered 13 aquaporins (AQPs) isoform (AQP0-AQP12) widely distributed in various epithelia and endothelia where are important actors of fluid homeostasis maintenance in secretory and absorptive processes in response to an osmotic or pressure gradient. In the human brain nine aquaporin subtypes (AQP1, 2, 3, 4, 5, 7, 8, 9, and 11) have been recognized and partially characterized, but only three aquaporins (AQP1, 4, and 9) have been clearly identified *in vivo*. This discovery highlighted the concept of the important role of AQPs in all brain functions and of the dynamics of water molecules in the cerebral cortex. Additionally, AQPs releaved an important role in glial control and neuronal excitability, such as in brain structure and general development. However, a clearer understanding of specific function and distribution of water channels in adult or in development brain requires a more detailed elucidation. Some of these findings are limited from the complexity of direct investigation, inaccessibility of the neural tissue, and hence difficulty in obtaining a brain biopsy, until after the death of an individual. In this sense, several past and present *in vitro* models have been used to provide important clues about many processes, such as brain development, neurotoxicity, inflammation, neuroprotection, pathogenic mechanisms of the diseases and potential pharmacological targets.

In the Chapter I, we have reviewed some *in vitro* approaches used to investigate the mechanisms involved in Krabbe disease with particular regard to the cellular systems employed to study processes of inflammation, apoptosis and angiogenesis. Moreover, in this study, we used some *in vitro* methods with the aim to update the knowledge on stem cells biology and to provide a relationship between aquaporins expression and cellular differentiation. In particular, we have analysed the differentiation of human mesenchymal stem cells from adipose tissue (AT-MSCs) into neural phenotypes and SH-SY5Y neuroblastoma cell line into physiological and pathophysiological dopaminergic neurons.

Thus, in the Chapter II, we have reported the results of the expression of AQP1, 4, 7, 8 and 9 at 0, 14, and 28 days in AT-MSCs during the neural differentiation by performing immunocytochemistry, RT-PCR and Western blot analysis. Our studies demonstrated that AT-MSCs could be differentiated into neurons, astrocytes and oligodendrocytes, showing reactivity not only for the typical neural markers, but also for specific AQPs in dependence from differentiated cell type. Our data revealed that at 28 days AT-MSCs express AQP1, astrocytes AQP1, 4 and 7, oligodendrocytes AQP1, 4 and 8, and finally neurons AQP1 and 7. In the Chapter III, we have examined the possible involvement of AQPs in a Parkinson's disease-like cell model. For this purpose, we used SH-SY5Y, a human neuroblastoma cell line, differentiated in dopaminergic neurons with retinoic acid (RA) and phorbol 12-myristate 13-acetate (MPA) alone or in association. The vulnerability to dopaminergic neurotoxin 1-methyl-4-phenyl-1, 2, 3, 6-tetrahydropyridine (MPTP) and H_2O_2 was evaluated and compared in all cell groups. We found that the vulnerability of cells was linked to dynamic changes of AQP4 and AQP9. The data described here provides fundamental insights on the biology of the human mesenchymal stem cells and significant evidences on the involvement of AQPs in a variety of physiological and pathophysiological processes. This suggests their possible application as markers, which may be helpful in diagnosing as well as in the understanding of neurodegenerative diseases for future therapeutical approaches.

INTRODUCTION

Water is a prerequisite of all organisms living and it is an essential component for the biologic activity of proteins [1].Water accounts for approximately 60% of our body weight, (which translates to about 42 L in a 70 kg person). Of this, 65% is found inside the cells, while the remaining 35% constitutes the extracellular fluid. At the extracellular level, water is the main component of biological fluids, allowing, for instance, the long distance trafficking of important solutes such as sugars and ions in human blood. At the extracellular/intracellular interface, water exchange through the plasma membrane maintains the osmolality of the cytoplasm and thus the integrity of the cell. At the molecular level, water is involved in the configuration of some important molecules. Indeed, water molecules are polar, which allows them to easily form hydrogen bonds with each other and with other molecules. They serve as excellent solvents for a variety of polar substances in the cells. Water provides solvent shells around charged groups of biopolymers. A striking property of most human tissues is their capacity for extremely rapid and highly regulated transport of water through cellular membranes, processes essential to human health [2, 3]. Until the 1990, little was known about the molecular mechanism regulating total body water content and the distribution of water between the extracellular and intracellular space.

The discovery of the plasma membrane in the 1920s started the discussion on how water can be transported across this membrane. Such trans-tissue water flow is possible by two routes: transcellular water flow across both basal and apical membranes, which occurs in response to the osmotic stimuli [2], created by salt transport [4] or paracellular flow across cell–cell junctions into intercellular spaces, driven by salt or solute gradients [4]. Transcellular water flow is dependent on the permeability of the plasma membrane to water molecules. The biological membrane surrounding living cells is not a pure lipidic bilayer and although have a measurable permeability to water, the simple diffusion of water is insufficient for the high flux rates needed in specialized tissue throughout the body, including organs such as brain, kidney, vascular system, lungs and others. Long-standing experimental evidence suggests that cellular membranes had a higher permeability to the water, that not could be explained by diffusion alone [5], nor the low energy activation observed for such phenomena [6, 7]. Historically, these observations led to the

hypothesis that the specialized water permeable cells must have 'water channels'. The discovery of intrinsic membrane proteins acting as water channels aquaporins (AQPs) mediate the water flux across biological membranes is the fundamental discovery in biology of the twentieth century [8-10]. Water movement by osmosis may be through the lipid bilayer, by passive co-transport with other ions and solutes [11] or through aquaporins (AQPs) water channels [12]. This discovery became a very hot area of research in molecular cell biology with increasing physiological and medical implications.

Discovery of aquaporins

The possible existence of water channels was predicted for a long time. The first studies on water transport started in the late 1950s on mammalian red blood cells (RBC). These pioneer studies demonstrated that water permeability in these cells was much higher than predicted by simple water diffusion through the bilayer [13], and water flux could be inhibited by addition of mercuric chloride in a reversible fashion by adding a reducing agent [14]. However, in 1986 Benga's group discovered the presence and location of the water channel protein among the polypeptides migrating in the region of 35-60 kDa on the electrophoretogram of RBC membrane proteins and labeled with 203Hg-PCMBS in the conditions of specific inhibition of water diffusion [10]. In 1987, Agre and coworkers isolated a new integral membrane protein from the RBC membrane, having a non-glycosylated component of 28 kDa and a glycosylated component migrating as a diffuse band of 35-60 kDa [15]. Agre's team suggested that the new protein, called CHIP 28 (Channel like Intrinsic Protein of 28 kDa), may play a role in linkage of the membrane skeleton to the lipid bilayer. In the 1992s, using a Xenopus oocyte expression assay, Agre and co-workers [10] demonstrated that CHIP28, a functional unit of membrane water channels abundant in RBC and renal proximal tubules, was water permeable [9]. By reconstitution in liposomes, it was demonstrated that CHIP28 is a water channel itself rather than a water channel regulator. In 1993, CHIP28 was renamed aquaporin-1 (AQP1) [16]. In parallel, studies on the antidiuretic hormone (ADH) responsive cells in amphibian urinary bladder led to the discovery of the second water channel protein, called today aquaporin-2 (AQP2). The corresponding cDNA was cloned and the deduced amino acid sequence related to the ancient family of membrane channels, MIP for Major Intrinsic Protein [17].

Ever since their discovery, more than 300 homologues of MIP members have been identified in many phyla, including animal, bacteria and plant. The increase of the identified member has supported their importance for life [18]. In October 2003, The Royal Swedish Academy of Sciences awarded the Nobel Prize in Chemistry "for discoveries concerning channels in cell membranes", with one-half of the prize to Peter Agre for the discovery of aquaporins (AQPs). The seminal contributions from 1986 of the Benga's group were mentioned in several comments on the 2003 Nobel Prize.

Structural features of aquaporins

The MIP family has fundamental significance in biology and comprise around 1000 members with a widespread distribution in all kingdoms of life. MIPs members have a relatively small size are less than 300 amino acids in length, with average molecular weights between 28 and 30 kDa [19]. Electronic crystallography and, more recently, molecular dynamics revealed that AQPs are relatively high homology and common general structure [20] indicating that they all may descend from an ancestral aquaporin prototype and probably have appeared in a very early state of evolution. MIPs share a specific three-dimensional structure embedded in the phospholipidic bilayer. In the native membrane, MIP are organized in 6 transmembrane (TM) domains connected by five loops, the N- and C- termini being cytoplasmic and grouped into homotetramers [21], where each monomer is a functional unit and contains a single water channel. This creates a central pore in the middle of the four monomers (Figs. 1 and 2).

Figure 1. Aquaporin structure

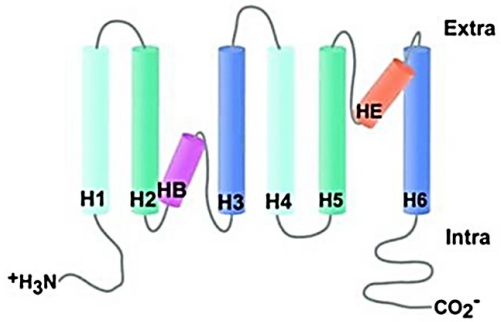

Generalized schematic of AQP family proteins expanded to show connectivity. (From Huber et al. 2012).

Figure 2. Atomic model of AQP1

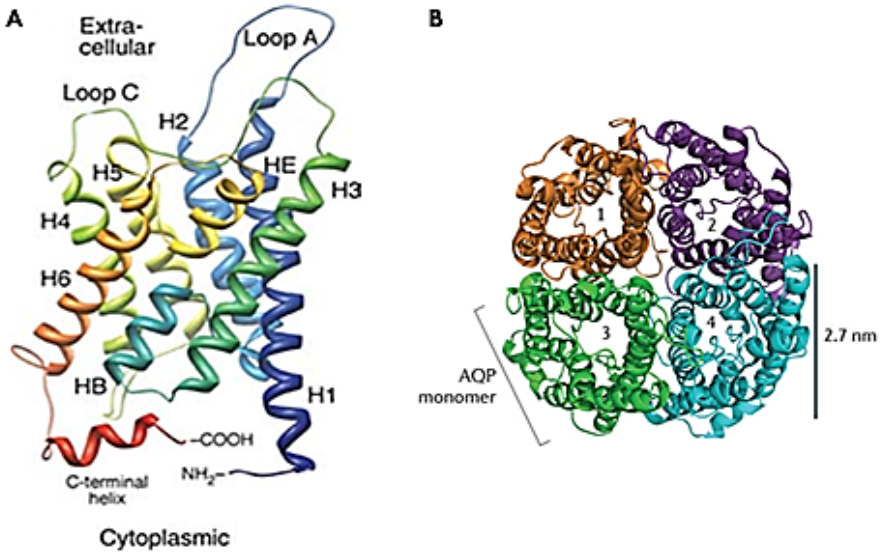

(A) AQP1 monomer viewed in the direction parallel to the membrane. Membrane-spanning helices are denoted as H1–H6, loops are denoted as A–E, and the two pore helices formed by loops B and E as HB and HE, respectively.
(B) AQP1 tetramer viewed from the extracellular surface, with monomers labelled 1–4, based on the X-ray structure of bovine AQP1 (Protein Data Bank (PDB) code: 1J4N).
(Adapted from Gonen et al., 2006 and Verkman et al., 2014).

At the center of the pore, highly conserved NPA (Asn-Pro-Ala) motifs, located at the loops B and E that form short hydrophobic helices, in which the asparagine is bonded back with the NH group of the main chain by a carbonyl group, and it enters the membrane from the extracellular side or cytoplasmic side in an opposite orientation. [22, 23]. This organization formed what has come to be known as the 'hour-glass model' (Fig. 3A), characterised by wide external openings to the channel with a narrow central constriction where the NPA motifs interact, forming the functional water pore. The primary structure can be divided into 2 similar halves (TM1–3, hemipore-1 and TM4–6, hemipore-2) that probably arose by gene duplication during evolution [24, 25].

In spite of a general highly conserved structure, differences at key areas of the MIP sequences provide a channel selectivity and two constriction points within the pore,

referred to as the NPA constriction and the aromatic/arginine (ar/R) selectivity filter (Fig. 3 B), respectively and the selection is done through mechanisms of charge, polar and size exclusions [26, 27].

Figure 3. 'Hour-glass model'

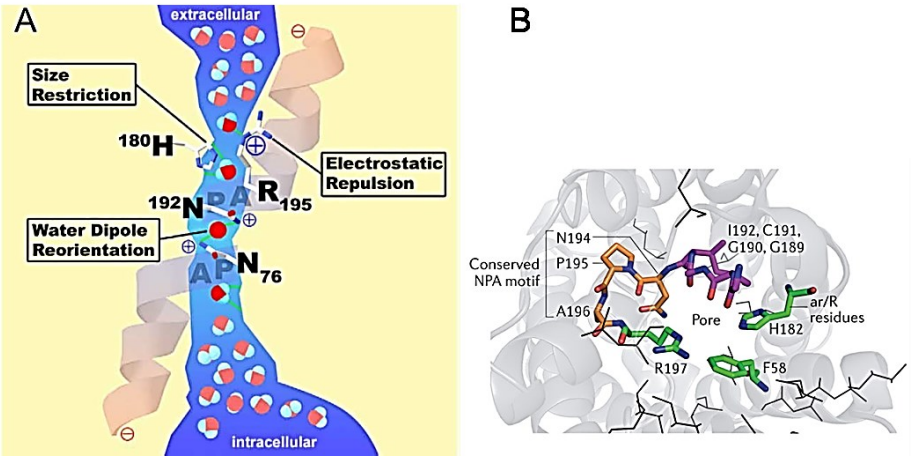

(A) Schematic diagram representing channel pore in same orientation.
(B) The constriction region (in green) is made up of aromatic and arginine residues (known as the ar/R constriction; residues Phe58, His182 and Arg197); extracellular Asn-Pro-Ala (NPA) residues (Asn194, Pro195 and Ala196) are shown in orange.
(Adapted from Agre et al., 2003 and Verkman et al., 2014).

In the center of the pore, located at the end of loop B and E, as previously described, two conserved Asn-Pro-Ala motifs (NPA filter) are responsible of generation of electric field and provoke the reorientation of 180 degree of the water molecule that destroyed H-bonds between adjacent water molecules and promote the proton exclusion (Fig. 4).
The aromatic/arginine (ar/R)-constriction region is the second filter located at the extracellular side, it impairs the entrance of high molecular weight substrates (~2.8 Å in AQPs) but it is also a checkpoint site for uncharged molecules in AQPs [27]. The ar/R constriction is formed by the interaction of four amino acids within the pore.

Figure 4. The proton exclusion mechanism

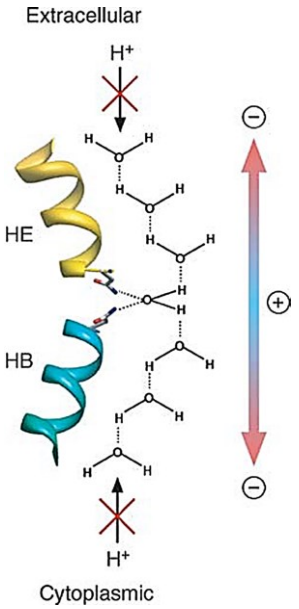

The asparagine residues of the two NPA motifs orient the water molecule in the center of the pore with the two hydrogen atoms perpendicular to the pore axis, dividing the pore into two half channels. The electrostatic field in the pore causes the water molecules in the two half channnels to be oriented in opposite directions, thus preventing proton conduction through the pore.
(From Gonen et al., 2006)

In 1990s was recognized a new AQP family the GlpF is the glycerol facilitator in E. coli. GlpF has a much lower water permeability, but it is permeable to glycerol, urea and glycine [28, 29]. The structure of GlpF was determined to 22 Å resolution by X-ray crystallography [30, 31] showing the same right-handed bundle of six α-helices seen in AQP1 [32-34], but also revealed three glycerol molecules (G1–G3) in the pore. The main differerences in the structures of AQP1 and GlpF are found in the extracellular loops (Fig. 5).

Figure 5. Glycerol molecules in the GlpF pore

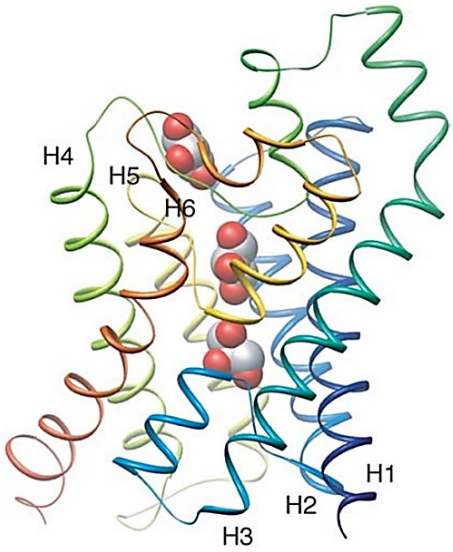

GlpF containing three glycerol molecules shown in space-filling representation. The glycerol molecule in the center occupies the constriction, while the lowest one is located at the height of the two NPA motifs.
(From Gonen et al., 2006)

Loop A is much shorter in GlpF than in AQP1. Loop E, the NPA-carrying loop in the second tandem repeat, is longer in GlpF than in AQP1 and forms a one-turn helix before connecting with transmembrane helix 6. The ar/R constriction region of GlpF pore has to be larger and more hydrophobic than that in the pore of AQP1. This is accomplished by a number of substitutions in residues forming the constriction site of GlpF. In particular Trp48, Gly191 and Arg 205 instead of Phe56, His180, Cys189 and ARg195 in AQP1. A much smaller glycine residue Gly191 replaces His182, which is preserved among water-specific AQPs. The much more hydrophobic Phe200 and Phe58 replace Cys191 of AQP1. These substitutions have critical effects on the characteristics of the GlpF ar/R constriction region: they increase the size in GlpF pore (3.4 Å), increase the hydrophobicity [34] and the conduction is not sensitive to mercurials.

The GlpF channel lining is strongly amphipathic, with oxygens and nitrogens lined up on one side and carbons on the opposite side of the lumen surface.

This amphipathic channel uniquely matches the chemical structure of glycerol, which is a composite of the polar hydroxyl group arranged on a non-polar alkyl backbone [30].

Aquaporin classification and selectivity

The AQPs family arose by tandem gene duplication [24]. Since bacteria such as E. coli contain both a glycerol facilitator (GlpF) and a specific water pore (AQPZ), the gene duplication appears to have occurred early in evolution. So far, in mammalian have been discovered 13 AQPs isoform (AQP0-AQP12). Phylogenetic analysis showed that the members of the AQP family have sequence identity that ranges from about 25 to 40%, and can be classified into three major functional subfamily according to their transport capability: aquaporins, aquaglyceroporins and S-aquaporins (Fig 6) [35-37]. AQPs (AQP0, AQP1, AQP2, AQP4, AQP5, AQP6 and AQP8) are a mainly water selective or specific water channels, also named by various authors as "orthodox", "ordinary", "conventional", "classical", "pure", "normal", or "sensu strictu" aquaporins. AQP0, AQP1 and AQP6 are considered water channels, but they are also permeate nitrate and chloride ions, and AQP8 ammonia. Water diffusion through AQPs is inhibited by mercury, except AQP4, which is mercury-intensive aquaporin [38]. The aquaglyceroporins (AQP3, AQP7, AQP9 and AQP10) are permeable to water, but also to other small-uncharged molecules, in particular glycerol and urea. AQP10 is an aquaglyceroporin permeable to water, but not to glycerol and urea [39]. AQP9 was also named “neural channel” that facilitates the water diffusion, but also polyols (glycerol, mannitol, and sorbitol), purines (adenine), pyrimidines (uracil and chemotherapeutic agent 5-fluorouraricil) and monocarboxylates (lactates and β-hydroxybutirrate). In addition, AQP9 facilitates metalloid transport, suggesting that AQP9, like AQP7may be a major route of arsenite intake uptake into mammalian cells [40]. S-aquaporins (AQP11 and AQP12), the third subfamily of little conserved amino acid sequences around the NPA boxes, unclassifiable to the first two subfamilies. They are also named "superaquaporins", "subcellular aquaporins", or "sip-like aquaporins". Both unusual AQPs are intracellular proteins, which display a crucial role in endoplasmic reticulum (ER) integrity maintenance; in particular, AQP11 has a C-terminal extremity with a putative ER-related retention signal even AQP12 that lacks this ER retention signal.

Figure 6. Phylogenetic tree of mammalian AQPs and AQPs of known atomic structure

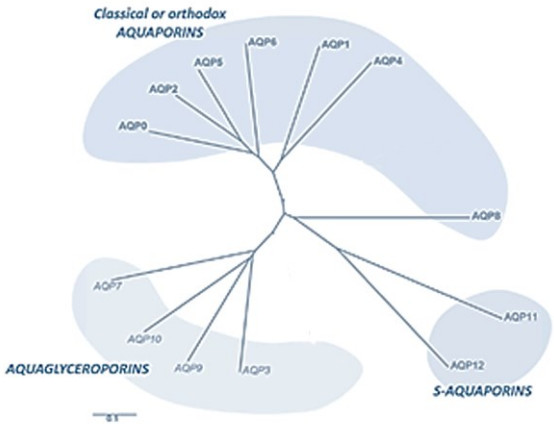

(Adapted from Gonen et al., 2006)

Aquaporin distribution and physiological function

In human, aquaporins are widely distributed in various epithelia and endothelia of tissues involved in fluid transport such as kidney, brain, eye, skin, fat and exocrine glands, suggesting their involvement in major organ functions and disease processes, including urinary concentrating, brain swelling, epilepsy, glaucoma, cancer and obesity [41]. In general, AQPs increase water membrane permeability, they are important actors of fluid homeostasis maintenance in secretory and absorptive processes in response to an osmotic or pressure gradient. However, their specific distribution in certain cell types of an organ often reflects a precise function (Fig. 7A). Tissue distribution and regulation studies have provided indirect evidence for the involvement of AQPs in a variety of physiological processes.

Fluid secretion

AQPs are express in many epithelia, such as kidney tubules, glands, choroid plexus, ciliary body and alveoli, where they increase transepithelial water permeability and are responsible of fluid secretion and absorption.

Reduced epithelial cell osmotic water permeability can consequently impair active fluid transport and osmotic water equilibration, resulting in the secretion (or absorption) of a reduced volume of inappropriately hypertonic fluid [42] (Fig. 7B).

Figure 7. Aquaporins distribution in human body and their physiological functions

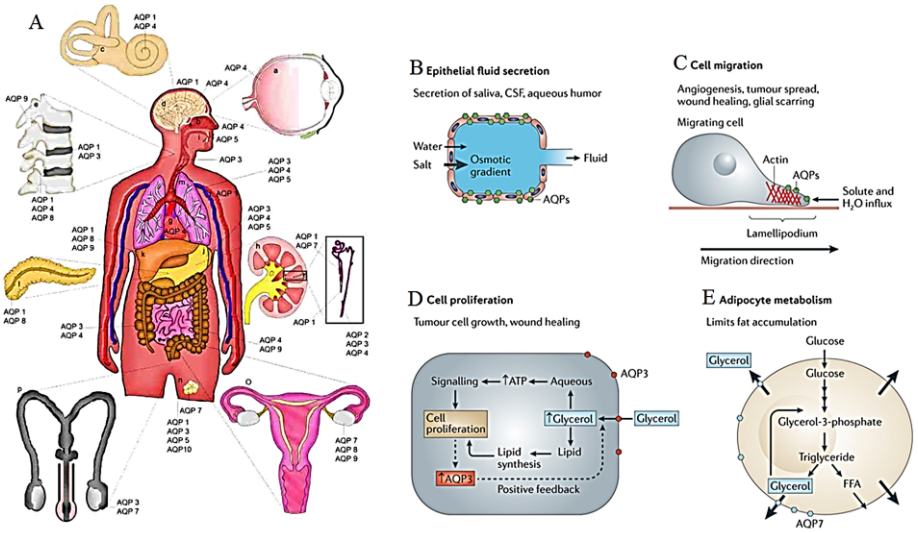

(A) Schematic rappresentation of AQPs in human body.
(B) Expression of AQPs in epitelium of secretion: AQP deficiency reduces transepithelial water permeability, preventing osmotic equilibration of lumenal fluid and impairing urinary concentrating ability.
(C) Proposed mechanism of AQP-facilitated cell migration, showing water entry into protruding lamellipodia in migrating cells.
(D) Proposed mechanism of AQP3-facilitated cell proliferation involving increased cellular glycerol and consequent increased ATP energy and biosynthesis.
(E) AQP7 facilitates glycerol escape from adipocytes: adipocyte hypertrophy is seen in AQP7 deficiency, possibly because of impaired AQP7-dependent glycerol escape from adipocytes, resulting in cellular glycerol accumulation and increased triglyceride content.
(Adapted from Day et al., 2013 and Verkam et al., 2014)

Cell migration

Migration is a fundamental property of cells that occurs during many physiological and pathological processes including organogenesis in the embryo, repair of

damaged tissue after injury, the inflammatory response, formation of new blood vessels, and the spread of cancer. In migrating cells, AQP1 and AQP4 become polarized to the front end of cells and they are associated with increased turnover of cell membrane protrusions, suggesting an important role for AQPs at the leading edge of migrating cells [43, 44] (Fig. 6C).

Glycerol metabolism

For many years, the physiological significance of glycerol transport by the aquaglyceroporins was unclear. AQP7 is expressed in the plasma membrane of adipocytes where are involved in efflux of glycerol, in AQP7 deficiency, the plasma membrane of adipocytes showed a reduced glycerol permeability contemporary with an accumulation of glycerol in adipocyte cytoplasm, resulting in increased glycerol-3-phosphate and triglyceride biosynthesis. AQP9 expressed in liver (which facilitate the uptake of glycerol and thereby the availability of glycerol for *de novo* synthesis of glucose and triglyceride), have an important role in controlling glycerol metabolism in both adipose tissue and liver [45] (Fig. 6D).

Cell proliferation

Another important aspect is the implication of same AQPs, in particular AQP3 and AQP5 to enhance cell proliferation in epidermal cells and the cell growth in cancer condition [46-48] (Fig. 6E).

Aquaporin in brain

Considering that about 80% of the brain is water, AQPs play an important role in the production, circulation and homeostasis of the cerebrospinal fluid (CSF). Fluid balance (secretion, removal, fluxes and homeostasis of salts) is important for the brain survival but also neuronal excitability [49].The knowledge of the distribution and regulation of water channels in the brain is important to understand water homeostasis and their correlation with physiopathological condition. To date, nine aquaporin subtypes (AQP1, 2, 3, 4, 5, 7, 8, 9, and 11) have been recognized and partially characterized in human brain cell function, but only three aquaporins (AQP1, 4, and 9) have been clearly identified in brain cells *in vivo* [50].

Figure 8. Aquaporin distribution in brain

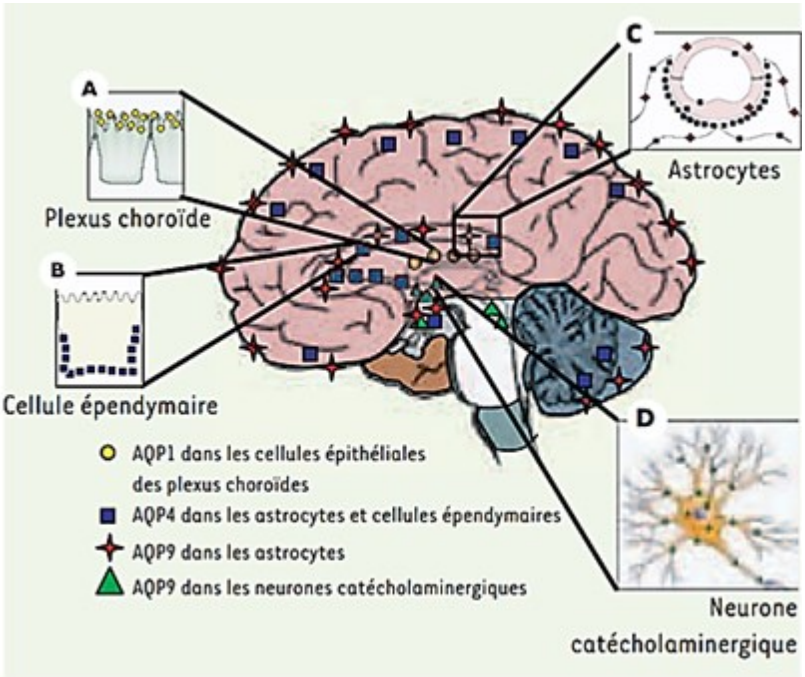

A) AQP1 is mainly express in the apical pole of choroid plexus (CP).
B) AQP4 and AQP9 are co-express in astrocytes.
C) AQP4 is express in ependymal surfaces.
D) AQP9 is express in catecolaminergic neurons.

(Form Guérin et al., 2005)

AQP1

In the central nervous system, AQP1 is mainly express in the apical pole of choroid plexus (CP) (Fig. 8A) in the lining of the cerebral ventricles in primate and in human astrocytes [51-53]. This protein was proposed to be the major water-transporting protein in choroid plexus and to play a role in cerebrospinal fluid formation and in governing the rate of net fluid secretion. The CP is essential for the brain from the earliest stages of the development through the passages into old age. One might speculate that AQP1 is express contemporary with the CP formation and is enables the CP cells to sense the osmolality of the CSF and thereby initiate the appropriate adjustments of transport rates [54]. The ion channel activity of AQP1 is dependent on intracellular cGMP. Activation of AQP1 cation channel by cGMP signaling (activated by the atrial natriuretic peptide, ANP) decreased the rate of net fluid flow from basolateral to apical in confluent layers of cultured rat choroid plexus, and the effect was reversed by application of a blocker of the AQP1 cation channel [55].

CFS traditionally has been considered a cushion providing a physical protection of the brain, a reservoir of salt and nutrient, a drainage system of removal waste products and metabolites, and in generally have a role into the development, homeostasis and repair of CNS. During the life, a progressive functional decline of CP in the aging increase the risk for development of late-onset diseases such as Alzheimer's disease [56]. This could suggest a hypothetical relationship between AQP1 expreesion and increased risk of Alzheimer's disease. In the peripheral nervous system, AQP1 is expressed in a subpopulation of primary sensory neurons of dorsal root and nodose ganglia in mice [57] plus enteric neurons and it has been proposed to play a role in cerebrospinal fluid formation and in mice and rats [58-60]. Moreover, AQP1 mRNA or immunoreactivity has been observed in trigeminal ganglion neurons in rodents [58, 61-65]. These results indicate that AQP1 could play a relevant role in trigeminal neurotransmission. Interestingly, AQP1 is express in capillary endothelial cells in the systemic circulation [64], but it is not found in the capillaries of cerebrovascular system in normal condition [66]. Conversely, vascular AQP1 immunolabeling was observed in various tumor cell lines (mammary carcinomas and glioblastomas) implanted in the rat brain [43].

AQP4

Aquaporin-4 (AQP4) is the main water channel in the neuropil of the central nervous system and is highly polarized in expression [67]. It is primarily found on astrocytes (Fig. 8C), particularly on the astrocytic end-feet surrounding capillaries and the blood brain barrier as well as the glia limitans [68-70]. AQP4 exists in the end-feet adjacent to the capillary, with lower density found on the end-feet adjacent to neurons; the large surface area of the end-feet near neurons compensates for this lower density. AQP4 is highly abundant at sites of fluid transport, including pial and ependymal surfaces (Fig. 8B) in contact with cerebrospinal fluid (CSF), subarachnoid space, and the ventricular system [67]. AQP4 is also present in vasopressin-secretory neurons in supraoptic and paraventricular nuclei of the hypothalamus, and in Purkinje cells of cerebellum [67, 71, 50]. AQP4 expression has also been reported in neural stem cells obtained from human and murine subventricular zone and in their glial progeny in culture [72]. Based on its location and expression, the first functional role of the AQP4 has been suggested to be an involvement in bidirectional fluid exchange between both the blood and CSF compartments and the brain [68]. In fact, the highly polarized AQP4 expression (in glial membranes that are in direct contact with capillaries and pia) indicates that it mediates the flow of water between glial cells and the cavities filled with CSF and the intravascular space (i.e. across the BBB and blood–CSF barrier). The location of the AQP4 follows the distribution of the inwardly rectifying potassium channel 4.1 (Kir4.1) [68]. Although no functional relationship was clearly shown between AQP4 and Kir4.1, the absence of the AQP4 resulted in delaying the reuptake of the extracellular potassium in epileptic conditions possibly due to an increase of the extracellular space [73]. Water transport via AQP4 in brain is involved in the control of neuronal activity and linked to this activity is the spatial K^+ buffering/K^+ siphoning [74, 75]. In AQP4 deleted mice was observed an altered neuronal activity explained by altered K^+ kinetics in brain extracellular space (ECS) [76, 50].

It was found that AQP4-null mice have delayed K^+ clearance from brain ECS after local electrical stimulation [73] and during cortical excitation by spreading depression [77, 50]. AQP4 similarly with other AQPs enhance cells migration, in particular AQP4 deficiency impairs the migration of cultured astrocytes [78].

AQP9

AQP9 is an aquaglyceroporin with a broad selectivity transporting carbamides (urea, thiourea), ammonia, polyols (glycerol, mannitol, and sorbitol), purines and pyrimidines (adenine, uracil) and monocarboxyates (lactate, β-hydroxybutyrate) [79, 80]. In the brain, AQP9 was first detected in astrocytic cultures [79] and confirmed by immunocytochemical studies in rodent brain [81, 82]. To date, AQP9 expression has been observed in three cell types: glial cells, in particular tanycytes and astrocytes (Fig. 8C) [81-83], endothelial cells of sub-pial vessels [82] and in neurons (Fig. 8D) [82, 84]. The AQP9 expression was observed both on neuronal cell bodies and their processes as well as on the noradrenergic processes present in the adventitia of pial vessels [82]. The distribution of AQP9-ir in neurons and astrocytes is indicated on the schematic drawing of a sagittal rat brain section. The presence of AQP9 in the ependymal lining of the cerebral ventricles raises the possibility that this water channel may be involved in the extrachroideal production and the extra arachnoid reabsorption of the cerebrospinal fluid. AQP4 is also present in these regions in the mouse, suggesting that AQP9 contributes with AQP4 to the facilitation of water movements between CSF and brain parenchyma. Indeed, these channels can facilitate the diffusion of glycerol and lactate, which can serve as energetic substrates [85-89]. In the “lactate shuttle model” [88], glucose is converted into lactate in astrocytes and can then be used as fuel for neurons. In addition, AQP4 and AQP9 labeling on astrocytes was found in white matter tracts, hippocampus and several hypothalamic nuclei. In general, AQP9 is involved in brain energy metabolism as a metabolite channel. Since AQP9 is abundant in glucose-sensing neurons in the brainstem, it could also participate in the regulation of the whole body energy balance. In agreement with this hypothesis, the presence of AQP9 protein was recently demonstrated in mitochondria of astrocytes and dopaminergic neurons [90].

Other brain aquaporins

The presence of other members of AQPs family in the brain has been reported, but their functional role remains to be established [37].

AQP7 protein was found during perinatal development of mouse brain and in particular was observed in choroid plexus in parallel with the AQP1 expression. Moreover, despite it was detected in ependyma, pia and some blood vessels of the brain few functional information are yet available [91].

AQP8 was discovered in 1997 and the first studies in the brain showed its expression only by Northern blot analysis, AQP8 mRNA was not detected. However, Yamamoto et al., [92] observed AQP8 expression in oligodendrocytes.

Later, Oshio et al., [69] found the AQP8 expression in the spinal cord, in particular in the ependymal cells lining the central canal and observed a faint staining in cells surrounding the canal suggesting that AQP8 could play a role in concert with AQP4 and AQP9 facilitating the water transport into the central canal [93].

***In vitro* models for neurological research**

The studies of the central nervous system are beset with the complexity of direct investigation because of the inaccessibility of the neural tissue, and hence the difficulty in obtaining a brain biopsy, until after the death of the affected individual. Neuronal cell development is a complex and dynamic processes, which generates new neurons of different phenotypes. The neurogenic function from undifferentiated stem and progenitor cells starts at very early stages of development and continues in discrete regions of the mammalian nervous system throughout life. Understanding mechanisms underlying neuronal cell development, biology, function, and interaction with other cells, especially in the neurogenic niches of fully developed adults, is important to provide fundamental insight into the neuroscience. On the other hand, many common and rare neurological diseases can be modelled in rodents, in many cases these animal models do not faithfully reproduce the human syndrome at either the molecular or anatomical levels - perhaps owing to important species differences. Therefore, the employ of *in vitro* models would be extremely important to understand the brain development, the normal brain functions, the pathological processes involved in neurodegeneration, and finally, to explore therapeutic options for disorders of the CNS, including cells replacement. *In vitro* models offer advantages over *in vivo* models in several aspects. First, it is possible to study the role of isolated cells of one particular type in a controlled environment that simulates the disease allowing the exploring in a fast and reproducible manner the single pathogenic mechanisms a possible deleterious or protective role of specific molecules and compounds related damage to the brain. Second, screening for potential actions of drugs is also facilitated [94]. In this sense, *in vitro* models of neurodegenerative processes have been used to provide important clues about mechanisms of the diseases and potential pharmacological targets. Several studies with neuronal and non-neuronal primary cultures and cell lines have investigated many processes, such as neurotoxicity, inflammation, neuroprotection, and therapeutic approaches. For example, several past and present approaches *in vitro* have allowed identification of some pathogenic mechanisms involved in Krabbe's leukodystrophy (Fig.9). Krabbe disease (KD), also known as Globoid cell leukodystrophy (GLD, OMIM #245200), is a metabolic disorder of the white matter of the central and peripheral nervous systems (CNS and PNS) caused by inborn genetic defects. In particular, it is an autosomal recessive inherited

neurodegenerative disorder caused by deficient lysosomal enzyme galactosylceramidase (GALC) [95, 96], that leads to a progressive deterioration of oligodendrocytes in the CNS and Schwann cells in the PNS [97]. In any case, studies with primary cultures and cell lines of neurons, microglia, astrocytes, and oligodendrocytes have been used to investigate many processes such as neurotoxicity, inflammation, and neuroprotection and to screen for novel therapies to treat neurodegenerative disorders, including KD [98].

Figure 9. Pathways involved in Krabbe's leukodystrophy

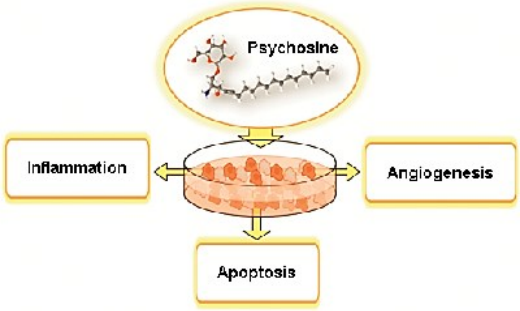

The *in vitro* systems described the direct and/or indirect roles of psychosine in the release of cytokines, ROS and NO and in the activation of kinases, caspases, and angiogenic factors. (From Avola et al., 2016).

The *in vitro* approaches have been widely used, not only to increase knowledge on rare neurodegerative disorders, but also to analyze molecular pathways involved in most common neurodegenerative disease, like Parkinson's disease.

Parkinson's disease (PD) is a common progressive neurodegenerative disease clinically characterized by motor impairment, namely bradykinesia, rigidity, resting tremor, and postural instability [99]. Synaptic and axonal degeneration within the striatum followed by loss of dopaminergic neurons in the substantia nigra pars compacta (SNpc) leads to reduced levels of dopamine in the nigrostriatal circuitry [100]. Despite the several information about the clinical progression, the pathogenesis of PD and the involved-molecular mechanisms are not yet completely understood. To clarify these two aspects and consequently provide the means for therapeutic strategies remain indispensable. In the recent years a growing interest

has been addressed to neuroinflammation and oxidative stress as key aspects of pathogenesis of disease-associated nigrostriatal degeneration in PD animal models as well in clinical [99, 100]. Usually, PD studies are limited because of the inaccessibility of the neural tissue and hence the difficulty in obtaining a brain biopsy, until the death of the affected individual. The perfect cell culture system needs to be homogeneous, easily expanded in order to generate large numbers of neuronal precursor cells and easily directed towards a post-mitotic state in a synchronized manner with a mature neuronal (dopaminergic) phenotype. In this kind of system, the specific molecular pathways and the genes/proteins at the basis of the progression of PD should be studied (Fig 10) [101]. Up to now, an *in vitro* model widely used in the field of PD research is the SH-SY5Y human neuroblastoma cell line. These cells are easy to differentiate into a post-mitotic mature dopaminergic state and widely used to study mechanisms of neurodegeneration [102].

Figure 10. Parkinson's disease *in vitro* model

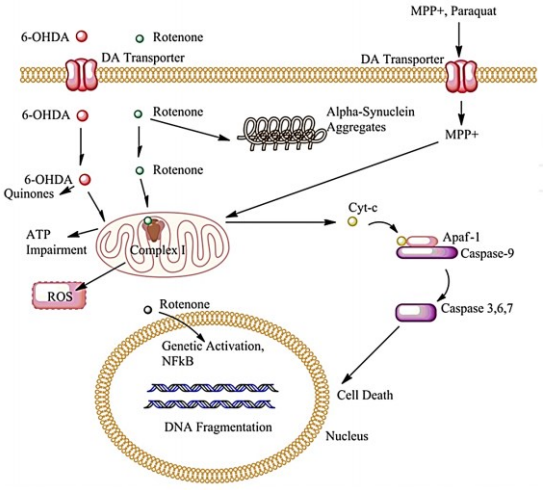

Many molecules are currently used in cellular models of PD, including pesticides as paraquat or rotenone and neurotoxins such as 6-hydroxydopamine (6-OHDA) and 1-methyl-4-phenylpyridinium (MPP^+). Paraquat, 6-OHDA and MPP^+ easily cross cell membrane through the dopamine transporter (DA) thus inducing the formation of α-synuclein aggregates and mitochondrial impairment with the subsequent production of ROS, inhibition of mitochondrial complex I and the release of proapoptotic molecules. (From Cabezas et al., 2013).

Stem Cells

The term "Stem cells" appears for the first time in the scientific literature as early as 1868 by Ernst Haeckel (German biologist), that used the term "Stammzelle" (German for stem cell) to designate an unicellular organism that he considered the evolutionary ancestor of multicellular organism from which he presumed all multicellular organisms evolved. Subsequently he used the same term to designate the fertilized egg distinguishing it sharply from maternal egg. (Fig. 11) [103].

Figure. 11 First representations of an early embryo (bottom) from which the term *Stammzelle,* stem cell.

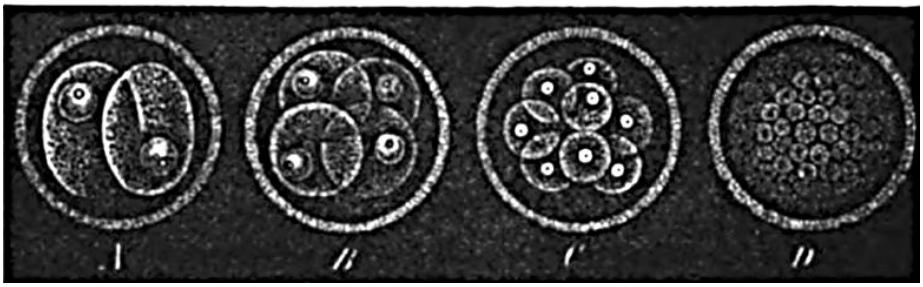

(From Federico Calegari, Claudia Waskow 2014)

Today, the term "stemness" includes the ability of self-renewal (replication capacity), clonality, and potency. These capabilities make the stem cells, the heart of some of the most fascinating questions in biology and medicine and can be defined as single cells capable of generating daughter cells identical to their mother as well as long-term survival. They have the potential to divide asymmetrically and eventually becoming a functionally mature cell to differentiating into multiple specific cell types, including neuronal and glial cell lineages [104]. They were found in all multicellular organisms. A hierarchy classification of stem cells can be obtained based or on their time of onset or their differentiation potency. According to their time of onset may be sourced from the blastocyst in the developing embryo prior to implantation, derived from inner cell mass (embryonic stem cells, ESCs) or derived from the fetus (fetal stem cells, FSCs) or, from blood and tissues postnatally (adult or somatic stem cells, ASCs) [105, 106]. Stem cells can best understood in terms of how committed they are to becoming any particular type of cells. Their developmental versatility includes cells capable of differentiating into any cell type

in the body including embryonic and extra-embryonic tissues, defined totipotent. According to this definition, the zygote (fertilized egg) is the only totipotent stem cell. Pluripotent stem cells, are descendants of the totipotent stem, and include embryonic stem cells, embryonic germ cells and cord blood-derived stem cells capable to differentiate into cell types of all three germ layers: ectoderm, mesoderm and endoderm. Substantially, they can develop into each of the more than 200 cell types of the adult body [107] but cannot produce the extra-embryonic tissues or the placenta [108]. The offspring of the pluripotent cells become antecedents of specialized cells able to differentiate into a limited range of cells within a tissue type. At this stage, they are multipotent with a more constraint differentiation potential and capacity for self-renewal; this category includes adult stem that are undifferentiated cells present in differentiated tissue and used to replace cells that have died or lost function. It renews itself and can specialize to yield all cell types present in the tissue from which it originated. So far, adult stem cells have been identified for many different tissue types such as hematopoetic (blood), neural, endothelial, muscle, mesenchymal, gastrointestinal, and epidermal cells. Finally, progenitor cells with a very limited differentiation potential and able to produce only one cell type are definited unipotent such as the erythroid progenitor cells that differentiate only into red blood cells (Fig.12).

Figure 12. Potency and source of stem cells

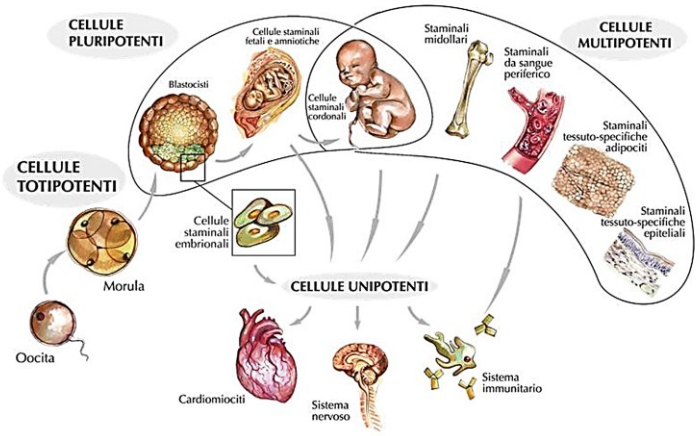

(From Martini et al., 2011)

Mesenchymal stem cells

Mesenchymal stem cells (MSCs) are ASCs with mesodermal and neuroectodermal origin [109].The hypothesis about their existence goes back to 1867, but MSCs were first isolated and defined by Friedenstein and co-workers as plastic-adherent, colony-forming-unit fibroblastic cells (CFU-F) [110]. Later, these cells were named "marrow stromal cells" due to their possible use as a feeder layer for hematopoietic stem cells [111]. MSCs possess an extended degree of plasticity compared to other ASCs populations. In fact, they have been shown to differentiate under appropriate conditions, into adipocytes, chondrocytes, osteocytes or muscle and might be able to differentiate also into endodermal and ectodermal cell lineages with neuronal cells electrically excitable [112] and into glial phenotypes [113]. In addition, it seems that few cells that were capable of engrafting into the nervous tissue fused with endogenous cells and thereby acquired the phenotype of the partner host cell [114]. Human MSCs are generally isolated from bone marrow (BM) aspirate harvested from the superior iliac crest. Moreover, they have also been found in other BM cavities such as vertebrae bodies [115]. BM-MSCs have been considered the gold standard, but many more recent reports describe the presence of MSCs in a variety of fetal, perinatal and adult tissues, including peripheral blood, umbilical cord Wharton's Jelly and blood, fetal liver and lung, adipose tissue, skeletal muscle, amniotic fluid, synovium and circulatory system where they work as supportive cells and maintain tissue homeostasis. Recently it was shown that MSCs are recruited from perivascular niches, which represent a tight network throughout the vasculature of the whole body. Current research on MSCs is mainly focused on their self-renewal capacity, multi-lineage differentiation potential, surface markers, and immune regulation. Considering the rising interest in the biology of MSCs, the International Society for Cellular Therapy (ISCT) describes a set of standards to define human MSC for both laboratory-based scientific investigations and for pre-clinical studies [116]:

1) Adherence to plastic in standard culture condition;
2) Specific surface antigen (Ag) expression: phenotype positivity (≥ 95 %+) for CD105, CD73, CD90; phenotype negative (≤ 2 %+) for CD45, CD34, CD14 or CD11b, CD79 α or CD19, and HLA-DR;
3) Multipotent differentiation *in vitro* potential to endodermal and ectodermal cell lineages (Fig. 13).

MSCs from different tissues also display significant differences in proliferative potential and their capacity of mature differentiation and integration in the host tissue are not yet clear. This suggested that the functional difference between MSCs from different sources might be related to the origin of the cells.

Figure 13. Mesenchymal from bone marrow and adipose tissue

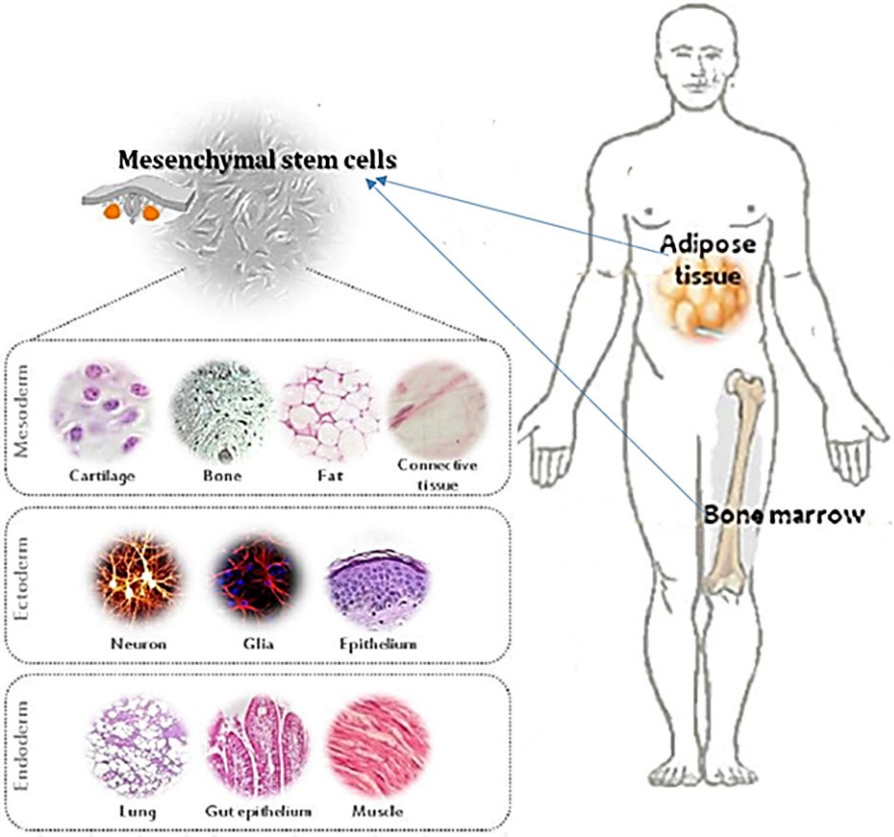

Cell fate that have been demonstrated for adult stem cells regarding the mesodermic, endodermic or ectodermic cell lineage.
(Adapted from Neirinckx et al., 2013).

Mesenchymal stem cells from adipose tissue

Recent studies have shown that subcutaneous adipose tissue provides a clear advantage over other MSCs sources due to the ease with which adipose tissue can be accessed as well as to the ease of isolating stem cells in abundant quantities [117, 118]. One gram of adipose tissue yields approximately 5,000 stem cells, whereas the yield from BM-MSCs is 100 to 1,000 cells/mL of marrow [119]. AT-MSCs were first isolated by Zuk et al. [120] through an initial enzymatic digestion of the harvested adipose tissue, which yields a mixture of stromal and vascular cells (preadipocytes, fibroblasts, vascular smooth muscle cells, endothelial cells, resident monocytes/macrophages, lymphocytes, and AT-MSCs [121], referred to as the stromal-vascular fraction (SVF) [122]. SVF is a rich source of pluripotent AT-MSCs [123, 120], which were first named processed lipoaspirate (PLA) cells [120, 124].

Morphologically, AT-MSCs are fibroblast like cells and preserve their shape after *in vitro* expansion [125, 126, and 120]. Average doubling time of tissue-cultured AT-MSCs is between three [120] to five days [127]. AT-MSCs in long-term culture showed the manifestation of senescent feature at passage (P) 15 and P20 and all the results showed that *in vitro* culture beyond P10 favors senescence pathways and therefore limits their clinical use [128]. They phenotypically express over 90 % of MSCs markers CD13, CD29, CD44, CD71, CD90, CD105/SH2, SH3, and STRO-1. AT-MSCs also share cell surface antigens with fibroblasts and pericytes, in contrast, no expression of the hematopoietic lineage markers: CD14, CD16, CD31, CD34, CD45, CD 56, CD 61, CD 62E, CD 104, and CD106 and for the endothelial markers: CD31, CD144, and von Willebrand factor was observed [129, 130, 124]. This observation results not only in a more homogeneous cell population with extended culturing but also in changes in AT-MSCs features: $CD34^+$ cells have a greater proliferative capacity whereas $CD34^-$ cells have a higher plastic adherence. Moreover, telomerase activity seems to be superior in AT-MSCs compared with BM-MSCs that indicates maintenance of the capacity for self-renewal and proliferation ability in culture and after transplantation [131]. AT-MSCs are of particular interest because they demonstrated properties that could be helpful in cell therapy: angiogenicity [132-134], immunomodulation [137], and promotion of tissue remodeling [134-136]. In fact, they are able to secrete growth factors promoting angiogenesis (VEGF, HGF, PDGF, FGFb, IGF, ecc.) [134, 138-140]. Therefore, the use of AT-MSCs is highly justified to induce the tissue revitalization or

reconstruction. Furthermore, AT-MSCs have anti-inflammatory, low immunogenic characteristics [141] making them useful also in allotransplant without immunosuppression [142, 143]. They not display transformation in teratoma [144], and there are few ethical issues surrounding their clinical application [145-147]. These unique features make AT-MSCs the ideal candidate for very different neurological diseases associated with degeneration and inflammation. Anyway, the complexity of the mechanisms involved in survival, differentiation and immunomodulation is not yet completely understood.

Neural differentiation of AT-MSCs

AT-MSCs are traditionally considered capable of differentiating into cell types of their own original lineage, but also in ectodermal and endodermal tissues or organs in the fields of gastroenterology, neurology, orthopedics, reconstructive surgery, and related clinical disciplines [124]. We and many other groups have showed that *in vitro* AT-MSCs can be capable of chrondrocyte, adipocyte, and neural phenotypes differentiations [148-153]. Given their ability to differentiate both morphologically and functionally into neurons, astrocytes and oligodendrocytes they are currently under investigation for neurological diseases, for brain injury, stroke, neuronal protection, and peripheral nerve injury. In general, the processes of proliferation, allocation, and lineage-specific terminal differentiation are regulated by a complex interplay involving stem cell transcription factors (molecular rheostats), cell-specific transcription factors, and a wide variety of cellular kinases, growth factors, and receptors. Neural differentiation of AT-MSCs has been reported in numerous studies, by using a variety of protocols. Some used simple chemical agent, treated AT-MSCs with conditioned media or mixture of growth factors, or maintained in co-culture with other neural cells. Earlier studies that utilized certain agent such as β-mercaptoethanol (BME), dimethyl sulfoxide (DMSO), and butylated hydroxyanisole (BHA) [154] reported that AT-MSCs could differentiate into cells of neuronal morphology within few hours, and therefore, these cells may be feasible for transplantation. However, the reversible morphological nature of differentiated neuronal cells [155] and the toxicity of the chemical substance employed limit their use in clinical trials [156]. Differentiation of AT-MSCs towards the neuronal lineage was also induced using conditioned media obtained from cultured rat olfactory ensheathing cells (OECs) or human B104 neuroblastoma cells [150]. In both cases,

AT-MSCs acquire morphological features of neuronal-like cells and, in a time-dependent manner, they express nestin, protein gene product 9.5 (PGP 9.5) and MAP-2. In other studies, AT-MSCs were turned into multipotent stage and then induced into neural cell lineages, by exposing them to appropriate neural differentiation conditions [156-158]. Different protocol using growth factors, as basal fibroblast growth factor (bFGF), FGF-β, nerve growth factor (NGF), brain-derived neurontrophic factor (BDNF) has been translated from the neural stem cells (NSCs) culture method [159-161]. NSCs are traditionally grown in induction media added of EGF and FGF-β forming floating aggregation called neurosphere [162]. After neurosphere dissociation, culture medium was supplemented with BDNF and retinoic acid. Following this treatment, about half of AT-MSCs showed morphological, immunocytochemical and electrophysiological evidence of initial neuronal differentiation. Neural modified AT-MSCs by the cultivation in neurodifferentiative conditions, in contrast to native AT-MSCs, express several neural progenitor and mature neural markers demonstrated by real time RT-PCR, Western blot and immunocytochemistry. The most cited proteins include S100β, SOX-2, GFAP, O4, β-tubulin-III, PGP 9.5 and NeuN. Moreover, with appropriate neural induction protocols, AT-MSCs could produce mature neuran-like cells that exhibit multiple neuronal properties and traits, such as action potential, synaptic transmission, secretion of neurotrophic factors and dopamine, and demonstration of spontaneous post-synaptic current.

Stem cells and aquaporins

SCs pass through a complex gauntlet of cell behaviors, such as proliferation, differentiation, and migration. Recently, a growing interest has been addressed to highly controlled movement of several ions and small molecules by AQPs that trigger numerous, complex signaling pathways that underscore the regulation of these behaviors. Despite it is clear that AQPs governing the water homeostasis and the considerable amount of water into or out of the cells to achieve rapid volume regulation during stem cells differentiation [163], only a small number of studies indicated the expression and function of AQPs in stem cells [72, 164-167]. AQP3 was found in human and rat progenitor cells surface and glandular airway epithelium [165, 168]. AQP4, AQP8, and AQP9 were expressed in murine adult neural stem cells [164-72] that normally replace neurons and/or glia in the adult brain and spinal cord. AQP8 is a general feature characterizing stem cells observed in mouse embryonic stem cells [169] and in intracellular membrane systems, probably corresponding to mitochondria of murine adult neural stem cells where might play a critical role in proliferation and differentiation [164]. In fact, AQP8 are involved in the mediations of water between the cytoplasm and the mitochondrial compartment, thus adjusting mitochondrial volume homeostasis pivotal for the activity of the electron-transport chain [170]. AQP4 and AQP9 expression was found in the adult forebrain periventricular region [171, 172], where the NSCs pool resides, but their expression levels and cellular localization were differentially regulated during murine adult neural stem cells differentiation into neurons and glial cells [72]. Following cell differentiation there was an increase in the overall levels of AQP4 mRNA and a concomitant redistribution of the protein, which localized in a high proportion of differentiated glial cells. In contrast to AQP4, only 30% of the cells in the differentiated cultures showed AQP9 positivity. AQPs protein levels seem to be progressively downregulated in the NSCs post commitment phases, on the contrary, using AQP4 knockout (KO) mice, it was demonstrated that AQP4 deletion reduced the proliferation, migration, survival, and neuronal differentiation of neural stem cells of adult mice [166]. An observed impairment in neurosphere formation in AQP4 KO mice was attributed to both increased cell apoptosis and decreased cell proliferation due to cell cycle arrest in G2/M phase [173]. AQP1 and AQP5 were expressed in mouse BM-MSCs in the plasma membrane pattern [167]. AQP1 promotes MSCs migration into the fracture sites by upregulating the expression of

β-catenin and focal adhesion kinase (FAK) [174]. AQP5-mediated high plasma membrane water permeability enhances the apoptosis rate of differentiating mouse BM-MSCs, thus decreasing their differentiation capacity [167].

AIMS OF THE RESEARCH

AQPs are expressed in a specific age-dependent manner, concomitantly with the intracellular and extracellular water content changes reaching a crucial role during the early postnatal period. In particular, water balance involving AQPs might be important during the neurogenesis, accompaning the entire developmental age and maintaining cell and tissue homeostasis. In the brain the electrical activity and the survival of neurons is strictly correlated to water, glycerol and lactate balance; alteration or genetic defect in AQPs expression are associated with several human disease and neurodegenerative disorders.

AQPs may contribute also in stem cell differentiation, as stem cells transport considerable amount of water into or out of the cells to achieve rapid volume regulation during differentiation. Nevertheless, until now, only a small number of studies has been published on expression and function of AQPs in stem cells.

Thus, the aim of the present study was to identify the gene and protein expression profile of AQPs in two different cell models, which allowed reproducing *in vitro* some physiological and pathophysiological conditions of nervous cells.

Additionally, during the initial phase of this research to look for the most appropriate experimental protocol to use for the proposed aims, a preliminary study of protocols about the *in vitro* models of some neurodegenerative diseases such as Krabbe leukodystrophy was carried out.

As regards the experimental part of the proposed objectives, the first model evaluated the dynamic expression of aquaporins during the differentiation of human mesenchymal stem cells from adipose tissue (AT-MSCs) toward neural phenotypes. The objective was to determine when and which AQPs are produced during differentiation of AT-MSCs into astrocytes, oligodendrocytes and/or neurons. The second model has reproduced *in vitro* oxidative and inflammatory conditions of the neurons present in the brain of patients suffering from Parkinson's disease (PD). Usually, PD researches are limited by the inaccessibility of the neural tissue and hence the difficulty in obtaining a brain biopsy, until the death of the affected individual. Therefore, a human neuroblastoma cells line (SH-SY5Y) was differentiated into dopaminergic neurons with retinoic acid (RA) and phorbol 12-myristate 13-acetate (MPA) alone or in association and subjected to treatment with the neurotoxin 1-methyl-4-phenyl-1,2,3,6-tetrahydropyridine (MPTP) and the

hydrogen peroxide to strongly mimic the oxidative environment that characterize PD neurons *in vivo*. The aim was to verify a primary involvement of AQP4 and AQP9 in the behavior of dopaminergic neurons in presence of oxidative stress and PD neurotoxin suggesting their possible application in diagnosing as well as in the understanding of PD during life.

CHAPTER I

J Neurosci Res. 2016 Nov; 94(11):1284-92. doi: 10.1002/jnr.23846.

KRABBE'S LEUKODYSTROPHY: APPROACHES AND MODELS IN VITRO

Rosanna Avola, Adriana Carol Eleonora Graziano, Giovanna Pannuzzo, Elisa Alvares, Venera Cardile

Department of Biomedical and Biotechnological Sciences, Section of Physiology, University of Catania, Via S. Sofia 64, 95125 Catania, Italy

Running title: **Cell models and Krabbe disease**

Key words: Apoptosis; Angiogenesis; Cell models; Globoid Cell Leukodystrophy; Inflammation; In vitro experiment.

Abstract

This Review describes some *in vitro* approaches used to investigate the mechanisms involved in Krabbe's disease, with particular regard to the cellular systems employed to study processes of inflammation, apoptosis, and angiogenesis. The aim was to update the knowledge on the results obtained from *in vitro* models of this neurodegenerative disorder and provide stimuli for future research. For a long time, the nonavailability of established neural cells has limited the understanding of neuropathogenic mechanisms in Krabbe's leukodystrophy. More recently, the development of new Krabbe's disease cell models has allowed the identification of neurologically relevant pathogenic cascades, including the major role of elevated psychosine levels. Thus, direct and/or indirect roles of psychosine in the release of cytokines, reactive oxygen species, and nitric oxide and in the activation of kinases, caspases, and angiogenic factors results should be clearer. In parallel, it is now understood that the presence of globoid cells precedes oligodendrocyte apoptosis and demyelination. The information described here will help to continue the research on Krabbe's leukodystrophy and on potential new therapeutic approaches for this disease, that even today, despite numerous attempts, is without cure.

Significance Statement

This Review describes some past and present approaches *in vitro* that have allowed identification of the pathogenic mechanisms involved in Krabbe's leukodystrophy. Several studies with neuronal and non-neuronal primary cultures and cell lines have investigated many processes, such as neurotoxicity, inflammation, neuroprotection, and therapeutic approaches. Here particular attention is focused on some cellular systems used to investigate processes of inflammation, apoptosis, and angiogenesis in Krabbe's disease. The knowledge on models and mechanisms obtained through in vitro experiments can be a stimulus for further research both *in vitro* and *in vivo*.

Introduction

Krabbe's disease (KD) is an autosomal recessively inherited neurodegenerative disorder characterized by demyelination in the central nervous system (CNS) and peripheral nervous system (PNS) with the consequent loss of all cognitive and nerve functions until death (Suzuki and Suzuki, 1970). Diffuse demyelination, gliosis, loss of oligodendrocytes, and presence of globoid cells are the "hallmarks" of the pathology. For this reason, KD is also called *globoid cell leukodystrophy* (GLD) for the presence in the white matter of phagocyte-lineage cells, the globoid cells, characteristic of galactocerebroside accumulation, which can be identified by the presence of periodic acid–Schiff (PAS)-positive material (Wenger et al., 1997).

Ranked among the lipidosis, KD is caused by genetic defects in the activity of galactosylceramidase (GALC), the lysosomal enzyme (hydrolase) that degrades two important components, galactosylceramide (gal-cer) and galactosylsphingosine (psychosine; Hideki and Suzuki, 1984; Graziano and Cardile, 2015). The inadequate degradation of these glycosphingolipids involves an accumulation of uncatabolized products. Despite the GALC deficiency, gal-cer does not dramatically increase in the brain of patients with KD. On the contrary, psychosine accumulates in the brain (Miyatake and Suzuki, 1972; Vanier and Svennerholm, 1976; Svennerholm et al., 1980; Suzuki, 1998), causing apoptotic death of myelingenerating cells, oligodendrocytes in CNS, and Schwann cells in PNS (Hannun and Bell, 1987; Tanaka and Webster, 1993). Until now, the exact mechanism of psychosine cytotoxicity has not yet been fully elucidated, and several different mechanisms have been postulated to account for its cytotoxic action.

Over the last years, many advances in understanding the normal brain functions and the pathological processes involved in neurodegeneration have emerged from work undertaken in *in vitro* models. Thus, studies with primary cultures and cell lines of neurons, microglia, astrocytes, and oligodendrocytes have been used to investigate many processes such as neurotoxicity, inflammation, and neuroprotection and to screen for novel therapiesy to treat neurodegenerative disorders, including KD (Gibbons and Dragunow, 2010).

To update the knowledge on cell models and methods used to study molecular mechanisms and so to provide specific stimuli for future research, this review presents a mix of past and present *in vitro* investigations on KD. We focus our

attention on some in vitro approaches with particular regard to the cell systems used to investigate processes of inflammation, apoptosis, and angiogenesis.

Krabbe disease and inflammation

Activation of the immune system with inflammatory components has been shown to be present in mice with KD (Matsushima et al., 1994; Wu et al., 2001), and several groups have reported the expression of proinflammatory cytokines (IL-6, TNF-α) and chemokines (MCP-1, IP-10, MIP-1α MIP-1β and RANTES) in both twitcher mouse brain and cell cultures (LeVine and Brown, 1997; Wu et al., 2001; Giri et al., 2002; Haq et al., 2003). To understand the inflammatory phenomena of KD better, psychosine has been added to neuronal, oligodendrocyte, Schwann, and/or fibroblast cell cultures and high levels of psychosine have been shown to induce several signaling responses, which mimic KD/twitcher disease condition *in vivo*.

It was hypothesized that, in KD, the toxicity of supraphysiologic levels of psychosine kills oligodendrocytes or inhibits their maturation (Won et al., 2013), resulting in severe demyelination. However, when oligodendrocytes from twitcher mice were transplanted to shiverer mice, another mouse model for demyelination, the twitcher oligodendrocytes were capable of myelinating the shiverer axons (Kondo et al., 2005). This suggests that demyelination in KD is not attributable exclusively to oligodendrocytes dying by lipid accumulation, based on their capability to myelinate axons in different cellular environment.

With regard to oligodendrocytes, cell death induction by proinflammatory cytokines such as TNF-α IL-6 (Taniike et al., 1999; Jatana et al., 2002; Haq et al., 2003), and inducible nitric oxide synthase (iNOS) activation and further potentiating the nuclear translocation of AP-1 and C/EBP without modulating the cytokinemediated transcription activity of nuclear factor-*k*B (NF*k*B) have been described (Giri et al., 2002). Giri et al. reported for the first time the induction of iNOS in KD brain and the potentiation of the cytokine-mediated induction of iNOS and production of NO in psychosinetreated cultured C6 glial cells and rat primary astrocytes. This research indicated a role for MAP kinases and transcription factors AP-1 and C/EBP in psychosinemediated induction of iNOS (Giri et al., 2002). Therefore, psychosine potentiated the LPS-induced expression of iNOS and the production of proinflammatory cytokines (IL-1, TNF-α, and IL-6) in a dose-dependent manner in rat primary astrocytes. Upregulation of cytokine/LPS-mediated induction of iNOS

protein and production of NO by psychosine was due to sustained synthesis of iNOS mRNA. These observations indicate that psychosine, which accumulates in KD because of the mutation in galactocerebrosidase enzyme, under inflammatory conditions leads to the production of NO, which plays a role in the pathogenesis of the disease. Induction of NO by psychosine under inflammatory conditions may be the basis for the oligodendrocyte loss, because $ONOO^-$ generated by the reaction of NO and O_2^- is known to modify cellular components (protein, lipids, and DNA) leads to inactivation of cellular functions and, finally, to cell death.

Moreover, the same authors documented that psychosine-induced oligodendrocyte death is mediated via generation of lysophosphatidylcholine (LPC) and arachidonic acid (AA) by the activation of secretory phospholipase A2 (sPLA2; PLA2 at low-molecular-mass: 13.5–16.8 kDa). LPC is recognized to act as a chemoattractant for monocytes and T lymphocytes and as an enhancer for the production of INF-γ by activated T cells, thus promoting an inflammatory reaction (Giri et al., 2006).

Mohri et al. (2006 a, b) described upregulation of lipocalin-type prostaglandin (PG) D synthase (L-PGDS), a dually functional protein acting both as a PGD2-synthesizing enzyme and as an extracellular transporter of various lipophilic small molecules in the CNS of twitcher mice. Using primary cultures of mouse microglia and astrocytes, the authors demonstrated that psychosine-activated microglia produces a large amount of PGD2 synthesized by HPGDS and that astrocytes express both DP1 and DP2 receptors activated by PGD2. Pharmacological blockade of HPGDS or genetic ablation of DP1 in the twitcher mouse resulted in decreased astrogliosis and microgliosis, accompanying by less demyelination. This was the first example of a PGD2-mediated microglia–astrocyte interaction that enhances neuroinflammation and demyelination. It was demonstrated that *in vitro* glycosphingolipids such as D-galactosyl-beta1-1'-sphingosine and D-glucosyl-beta1-1'-sphingosine damage human natural killer (NK) cells, inducing apoptosis, globoid-like formation, and multinucleation (Maghazachi et al., 2004). Besides direct actions of psychosine, pathology in twitcher mice is thought to be mediated, in part, by activated macrophages/microglia independent of lymphocyte infiltration into the CNS (Matsushima et al., 1994). Myelin and/or oligodendrocyte debris produced by oligodendrocyte death in KD activates microglial cells, which are the primary mediators of neuroinflammation (Farooqui et al., 2007). Activated microglia become phagocytic and secrete a variety of cytokines, including the

proinflammatory cytokines TNF-α, IL-1β and INF-γ. These cytokines augment and perpetuate microgliosis (Merrill and Benveniste, 1996) and induce astrocytes to become hypertrophic and undergo reactive astrocytosis (Back and Volpe, 1998). Activated macrophages/microglia can produce reactive metabolites, such as NO (Zielasek et al.,1992; Banati et al., 1993) and TNF-α (Glabinski et al., 1995; Renno et al., 1995) that are cytotoxic to oligodendrocytes and/or myelin *in vitro* (Selmaj and Raine, 1988; Zajicek et al., 1992; Merrill et al., 1993) and play a pathogenic role in KD (Matsushima et al., 1994). In addition to TNF-α, other cytokines are involved. For example, IL-6 expression can be induced in astrocytes (Benviste et al., 1990; Norris et al., 1994) or microglia when TNF-α (Benviste et al., 1990; Norris et al., 1994) or myelin debris (Williams et al., 1994) is added to the culture medium, respectively.

An emerging trend in understanding the neurodegenerative diseases of the CNS is the increasing prominence of the role of astrocytes, no longer a passive support network for neurons, but the abundant population of astrocytes in the CNS has been documented to have a primary role in a variety of neurological conditions.

This topic was well described in a recent review (Verkhratsky et al., 2012) in which it was reported that dysfunction of astrocytes underlies development of CNS inflammation (Sharma et al., 2010). Astrocytes regulate fundamentally important functions to maintain CNS homeostasis. Altered astrocytic function is now recognized as a primary contributing factor to an increasing number of neurological diseases.

Recently, astrocytes were implicated in the pathogenesis of neuropathology in KD. It was determined that astrocytic expression of matrix metalloproteinase (MMP)-3, an extracellular protease, is dramatically increased at the time of clinical disease onset in twitcher mice. Furthermore, its expression continues to rise with disease progression (Ijichi et al., 2013). This astrocytic MMP3, which potentially targets myelin protein proteolytically, is a primary mediator of the formation of multinucleated globoid cells and highly activated phagocytes and a hallmark of KD pathology (Ijichi et al., 2013). Thus, astrocytic reactivity in the CNS of KD may not represent a secondary response to demyelination but rather may be a primary response to accumulated psychosine that can contribute significantly to the pathogenesis of KD (Claycomb et al., 2013). Claycomb et al. concluded that further

study on the regulation of astrocyte reactivity in this disease might represent a new avenue for understanding the etiology of neuropathology in KD.

It is now almost certain that elevated levels of psychosine elicit unique cellular reactions, such as formation of multinucleated cells (globoid cells) from resident microglia/macrophages and reactive astrogliosis. Activated glial cells produce various inflammatory cytokines and related mediators and chemokines, including macrophage chemoattractant protein-1, which are likely to play an important role in recruiting peripheral macrophages into the brain. These recruited macrophages further upregulate the inflammatory disease and participate in the progressive demyelinating process in KD and in twitcher mice.

Some authors have described how, when psychosine is added to the human myelomonocyte cell line U937, cleavage furrows formed either incompletely or almost completely. Moreover, psychosine has the ability to inhibit cytokinesis and to induce the formation of multinuclear globoid-like cells in U937 cells (Kanazawa et al., 2000). For a long time, globoid cells have been thought to be a secondary consequence of chronic demyelination.

However, some studies examining the temporal association of globoid cells to the white matter pathology of KD have identified the presence of globoid cells preceding oligodendrocyte apoptosis and overt demyelination (Pollanen and Brody, 1990). The temporal sequence of development of the neuropathology in KD suggests that globoid cells are formed in advance of demyelination (Martin et al., 1981). Thus, more recently, Claycomb et al. (2014) provided a template for the development of a protocol for the study of globoid cell formation using primary mixed glial cultures, which include both astrocytes and microglia. This cell model represents an important advantage for its utility in assessing the contributions and interplay between astrocytes and microglia (Claycomb et al., 2014). Because glycosphingolipids, such as psychosine and several other sphingolipids, are poorly expressed in cells and tissue other than those originating from the nervous system. Ribbens et al. (2014) developed and characterized a new cell model for KD. They obtained brain samples from twitcher mice, the natural mouse model with GALC deficiency, and immortalized the primary neuroglial cultured cells with SV40 large T antigen, generating the 145M-Twi and the 145C-Wt cell lines from twitcher and control mice, respectively. Both cell lines expressed specific oligodendrocyte markers, including A2B5 and GalC (Ribbens et al., 2014). These established 145M-

Twi cells can be a powerful research tool for investigating the neurologically relevant pathways in KD.

Krabbe disease and apoptosis

Cytotoxicity of psychosine *in vitro* and the fatal effects of intracranial-injected psychosine led to the conclusion (known as the psychosine hypothesis) that progressive accumulation of psychosine is the critical biochemical pathogenetic mechanism of cell death in KD brain (Suzuki, 1998). Several groups have reported that the mode of oligodendrocyte death induced by psychosine is apoptosis. DNA fragmentation, a marker of apoptosis, was detected in MOCH-1 (glia-derived) cells and cultured fibroblasts that were incubated with psychosine (Tohyama et al., 2001). The percentage of glia-derived cells that underwent apoptosis was significantly higher than that of fibroblasts, which suggests a susceptibility of oligodendrocytes to apoptosis (Tohyama et al., 2001). It was demonstrated that psychosine is a potent inhibitor of protein kinase C (PKC) *in vitro* (Hannun and Bell, 1987). PKC is a family of protein kinases with many biological functions, including regulation of cell growth, regulation of transcription, and modification of membrane structure. Disruption of the signal transduction pathways involved in these functions could eventually lead to cell death (Hannun and Bell, 1987).

A study by Yamada et al. (1996) showed that growth and proliferation of twitcher Schwann cells in response to a number of growth factors that act through the PKC pathway were reduced compared with normal Schwann cells. This is in agreement with the study by Hannun and Bell (1987) indicating impairment of PKC signaling by psychosine. However, this inhibition of PKC contrasts somewhat with more recent research showing that psychosine mediates the activation of sPLA2 in the brains of both KD patients and twitchers (Giri et al., 2006). sPLA2 hydrolyzes phospholipids to generate fatty acids, which have been shown to enhance activation of PKC (Nishizuka, 1995).

An important mediator of apoptotic signaling is the c-Jun N-terminal kinase/stress-activated protein kinase (JNK/SAPK), a subgroup of mitogen-activated protein kinases (MAPKs; Sorger et al., 1997; Widmann et al., 1999; Lin et al., 2003). It was observed that psychosine treatment resulted in the upregulation of AP-1 phosphorylation and, hence, activation of JNK. Activated JNK, in turn, resulted in the activation of c-jun through phosphorylation of the latter, which is a transcription

factor of the AP-1 family. The results of a electrophoretic mobility shift assay (EMSA) clearly showed that psychosine upregulates the AP-1 transcription machinery.

These observations were confirmed by transfection studies using the dominant negative form of c-jun, which showed that the apoptotic effect of psychosine was less prominent in the human oligodendrocyte cells expressing dominant negative c-jun (Haq et al., 2003). A different study reported that psychosine downregulates the phosphoinositide 3-kinase (PI3K)-Akt survival pathway inhibiting the phosphorylation of Akt and Erk1/Erk2 (Erk1/2), which are the main antiapoptotic pathways of the IGF-1 receptor (IGF-1R; Zaka et al., 2005).

Another important regulator of apoptosis is thought to be NF-kB. Accumulating evidence suggests that NF-kB has either a proapoptotic or an antiapoptotic function, depending on the cell type and the death stimulus (Lin et al., 1995, 1998; Beg and Baltimore, 1996; van Antwerp et al., 1996). Several proapoptotic genes, such as c-myc, p53, Fas ligand, and the IL-1β-converting enzyme caspase 1, have NF-kB binding sequences in their promoter regions (La Rosa et al., 1994; Wu and Lozano, 1994; Baeuerle and Baltimore, 1996; Qin et al., 1999), indicating that NF-kB acts as a proapoptotic transcription factor. In contrast, NF-kB activity appears to be necessary for the activation of genes that suppress some type of apoptosis.

Antiapoptotic genes that are regulated by NF-kB include manganese superoxide dismutase (Wang et al., 1996) and the zinc finger protein (Opipari et al., 1992). However, the precise factors that determine the ability of NF-kB to regulate these divergent biological actions are unknown. Treatment of oligodendrocytes with psychosine was found to reduce both nuclear translocation and DNA binding of NF-kB (Haq et al., 2003). In that study, cultured oligodendrocyte cells were treated with LPS, an inducer of NF-kB activation, which resulted in increased DNA binding activity of NF-kB. However, the addition of psychosine to LPS-treated cells reduced this DNA binding activity and resulted in a higher concentration of cytosolic IkBα, a member of a family of cellular proteins that function to inhibit NF-kB. As reported above, the same study established that the DNA binding activity of AP-1, a downstream product of the JNK signaling cascade, was increased in psychosine-treated cells, suggesting that psychosine also upregulates the JNK signal transduction pathway (Haq et al., 2003). Together, upregulation of the JNK pathway and downregulation of NF-kB by psychosine could result in cell apoptosis. In

summary, the data described here are consistent with the proposal that MAPKs mediate a central role in psychosine-induced apoptosis, in part by downregulating the prosurvival (NF-kB) and upregulating the stress-mediated (JNK/AP-1) signal transduction pathways.

Apoptotic cells and expression of apoptosis-related molecule such as TNF-α and its receptor 1 was observed in twitcher mouse brains and in brains of KD patients, underscoring the hypothesis that induction of inflammation during progressive accumulation of psychosine is one of the main biochemical and pathogenetic mechanisms of cell death in the KD brain (Giri et al., 2008). This same study, performed with rat primary astrocytes, primary oligodendrocytes, and oligodendrocyte cell line (MO3.13), delineated an explicit role for AMPK in psychosine induced inflammation in astrocytes without directly affecting the cell death of oligodendrocytes. It was documented that psychosine mediates inactivation of AMPK, which results in lipid alteration both in astrocytes and oligodendrocytes.

Although AMPK activator did not rescue oligodendrocytes from psychosine-mediated cell death, in primary astrocytes it downregulated psychosine-mediated production of NO and expression of proinflammatory cytokines and mediators (iNOS and Cox-2), suggesting a specific role of AMPK in oligodendrocytes and astrocytes (Giri et al., 2008).

As described above, inflammatory cytokines are known to induce the PLA2 enzyme system. PLA2s hydrolyze phospholipids at the sn-2 position and generate lysolipids and free fatty acids, including AA. These mediators are critically involved in the regulation of several physiological events, including cell death (Capper et al., 2001; Dennis, 1994). Psychosine mediates its proapoptotic signaling through the PLA2 pathway rather than as the originally suggested consequence of its lytic activity (psychosine hypothesis; Giri et al., 2006). LPC is a well-known lysolipid, responsible for inducing demyelination in an animal model and cell death of mature oligodendrocytes and their progenitors *in vitro*. Giri et al. showed that the mechanism of action of psychosine-mediated oligodendrocyte cell death is via activation of sPLA2 and generation of LPC and AA. These effects of psychosine were independent of the presumed receptor of psychosine, T-cell death-associated gene 8 (TDAG8).

In contrast, Im et al. (2001) previously reported that TDAG8 is a putative receptor for psychosine and that its overexpression results in the formation of multinuclear cells by psychosine.

PPAR-α regulates the transcription of peroxisomal enzymes, and this receptor was also found to be decreased in twitcher brains (Haq et al., 2006). This is somewhat contradictory to the fact that sPLA2-IIA has been reported to exert its effect through PPAR−α activation (Farooqui et al., 2007).

That is, if the sPLA2 activated by psychosine is sPLA2-IIA, then there should be increased levels of PPAR-α rather than decreased levels.

Inhibition of sPLA2 reduced the degree of downregulation of PPAR-α in psychosine-treated oligodendrocytes (Haq et al., 2006), indicating that dysfunction of peroxisomal functions in the twitcher may be due to psychosine-mediated activation of sPLA2. Given the important role of many peroxisomal enzymes in reactive oxygen species (ROS) synthesis and degradation (Schrader and Fahimi, 2004), dysfunction of these organelles could lead to alterations in the expression of these enzymes to favor either a net increase or a net decrease in ROS. The former outcome is supported by depleted levels of glutathione in both psychosine-treated oligodendrocytes and the twitcher brain (Haq et al., 2003; Khan et al., 2005). Voccoli et al. (2014) addressed the role of calcium dynamics during psychosine-induced cell death. Using the human oligodendrocyte cell line MO3.13, they reported that cell death by psychosine is accompanied by robust cytosolic and mitochondrial calcium (Ca^{2+}) elevations and by mitochondrial ROS production.

One of the characteristic biochemical events associated with apoptosis is the activation of caspases, a family of cysteine proteases with specificity for aspartate residues in the target proteins. Psychosine led to the activation of caspases 9 and 3, but not caspase 8, which suggests that psychosine can directly act at the level of mitochondria.

To prove this point, isolated mitochondria were treated directly with psychosine. and this treatment resulted in the release of cytochrome c. The fact that the incubation of mitochondria with psychosine induced release of cytochrome c suggests that psychosine by itself could initiate apoptosis without the requirement for additional molecules.

The facts that cytochrome c has multiple lipid binding sites and that lipid-bound cytochrome c shows a lower affinity for attachment to artificial membranes (Subramanian et al., 1998) strengthen this hypothesis.

This observation was further supported by the finding that treatment of whole cells with psychosine also led to the release of cytochrome c and to the cleavage of procaspase 3, as observed by the appearance of the cleaved form of the enzyme.

More recently, psychosine-induced apoptosis in cultured cells has been found to involve activation of caspases 9, 8, and 3 (Haq et al., 2003; Zaka and Wenger, 2004; Giri et al., 2006, 2008).

Caspase 9 was activated by binding to a protein cofactor, called Apaf-1, in the presence of cytochrome c (Li et al., 1997). The finding that cells incubated with psychosine release cytochrome c from mitochondria is in agreement with this (Haq et al., 2003).

However, cytochrome c release from mitochondria can also occur in the late stages of apoptosis, after caspase activation (Hengartner, 2000). Activation of caspase 9 in turn activates caspase 3 (Li et al., 1997), and apoptosis results. Caspase 8 is activated in a manner different from that of caspase 9, usually by a variety of death receptors, including type 1 tumor necrosis factor receptor (TNF-R1) and the Fas receptor (Earnshaw et al., 1999). Caspase 8 is also known to activate caspase 3 *in vitro* (Stennicke et al., 1998) which may explain why no other downstream caspases have yet been detected in psychosine-mediated apoptosis.

The presence of both caspase 8 and caspase 9 indicates that more than one apoptotic pathway may be mediated by psychosine. Moreover, psychosine was found to change the mitochondrial membrane potential and activate caspase 9. These effects of psychosine were reversed when cells were pretreated with the antioxidant molecules N-acetyl-L-cysteine (NAC) or procysteine (Singh et al., 1998; Pannuzzo et al., 2010; Voccoli et al., 2014). To determine the nature of the cell death induce by psychosine in MO3.13 cells, the occurrence of internucleosomal degradation of nuclear DNA, a typical biochemical marker of apoptosis, was investigated. Nuclear degradation was first analyzed with a TUNEL assay. To confirm the internucleosomal DNA cleavage characteristic of apoptosis, cytoplasmic DNA isolated from cells treated in a similar manner was subjected to agarose gel electrophoresis. To ascertain whether caspase 3 might be activated by proteolysis of the inactive proenzyme, the level of caspase 3 proenzyme and its degradation

product formation during psychosine-induced apoptosis was analyzed by Western blot analysis (Haq et al., 2003).

Ribbens et al. (2014), using 145M-Twi cells, showed biochemical and cellular disturbances related to KD neuropathogenesis, including remarkable caspase 3 activation, release of cytochrome c into the cytosol, and expansion of the lysosomal compartment. Under treatment with glycosphingolipids, 145M-Twi cells showed increased levels of LC3B, a marker of autophagy.

Recently, it was confirmed that PI3K is involved in the apoptotic effects of psychosine in wild type and twitcher oligodendrocyte progenitors through a downstream pathway involving the activation of PTEN and caspase-3 and the subsequent activation of the proapoptotic Bcl-2 family protein Bad. The research showed that psychosine induces an increase of connexin (Cx) 43 levels, too (Graziano et al., 2016). Cx43 is known for its effects on cell death or survival. Capable of a direct interaction with α- and β- tubulin, a key role in programmed cell death induction has been described for Cx43 by interacting with Bax to initiate the mitochondrial apoptotic pathway (Sun et al., 2012).

Krabbe disease and angiogenesis

Angiogenesis, the growth of new blood vessels from preexisting ones, plays a pivotal role in various physiological and pathological conditions (Carmeliet and Jain, 2011). The effects of GALC deficiency on CNS microvascularization and angiogenesis have been investigated in twitcher mice and cortical brain biopsies from KD patients (Belleri et al., 2013). GALC deficiency, with consequent psychosine accumulation, induces significant defects in the endothelium of the postnatal brain of twitcher mice. Moreover, twitcher endothelium shows a progressively reduced capacity to respond to proangiogenic factors. In addition, RNA interference-mediated GALC gene silencing hampers the proangiogenic response of human endothelial cells to vascular endothelial growth factor (VEGF). More recently, microvascular corrosion casting followed by scanning electron microscopy morphometry confirmed the presence of significant alterations of the functional angioarchitecture of the brain cortex of twitcher mice with reduction in microvascular density, vascular branch remodeling, and intussusceptive angiogenesis.

Intussusceptive microvascular growth, confirmed by histological analysis, was paralleled by alterations of the expression of intussusception-related genes in twitcher brain (Giacomini et al., 2015). These observations suggest that GALC deficiency affects not only the glial/neuronal compartment of the neurovascular brain unit but also its vascular moiety. Neovascularization plays an important role in the development of the CNS and protects it from neurological disorders (Greenberg and Jin, 2005; Segura et al., 2009). The tight cross talk among glial, neuronal, and endothelial cells in the CNS is underscored by the capacity of angiogenic factors, including VEGF-A and fibroblast growth factor-2 (FGF2), to modulate neurogenesis and neuroprotection (Ment et al., 1997; Greenberg and Jin, 2005; Zacchigna et al., 2008; Segura et al., 2009). In turn, neurotrophic factors may regulate angiogenesis. To investigate the effect of GALC deficiency and psychosine accumulation on CNS microvascularization and the angiogenic process, studies have been conducted with endothelial cells. The data demonstrate that psychosine is endowed with antiangiogenic activity by causing actin cytoskeleton disassembly (Belleri et al., 2013).

Previous observations had shown the ability of psychosine to affect actin reorganization, leading to the formation of multinuclear globoid cells (Kanazawa et al., 2000; Kozutsumi et al., 2002). On this basis, the effect of psychosine on different components of the endothelial cell cytoskeleton was evaluated. In particular, the capacity of psychosine to affect different steps in the angiogenesis process, including endothelial cell migration and extracellular matrix invasion, was investigated. Migration of endothelial cells following the mechanical wounding of a cell monolayer was characterized by the repositioning of the cell microtubule organization center from a random distribution to a biased localization in front of the nucleus, toward the direction of cell migration (Ueda et al., 1997).

Psychosine has been identified as an endothelial actindisassembling agent endowed with antiangiogenic activity in vitro and in vivo. Psychosine inhibits, in murine aortic endothelial cells and brain microvascular endothelial cells, different steps of the angiogenesis process *in vitro*, including endothelial cell proliferation and migration and extracellular matrix invasion and sprouting and hampers the activity exerted in vivo by the potent proangiogenic factor FGF2 in the chick embryo chorioallantoic membrane (CAM) and murine Matrigel plug assays (Belleri et al., 2013).

The results by Belleri et al. (2013) revealed a new neuropathogenic aspect of globoid cell leukodystrophy in which the deficiency of GALC activity affects the ability of the blood microvasculature to respond to angiogenic stimuli not only in the nervous system but also in somatic organs. This may contribute to worsening KD evolution and may adversely affect therapeutic interventions, including bone marrow repopulation following haematopoietic stem cell transplantation (Visigalli et al., 2010).

Finally, it remains challenging to establish whether vascular alterations in KD represent the outcome of the astrocytic/neuronal injury, with a consequent deficiency in the production of trophic angioneurins (Lee et al., 2009) or are due to a direct damage of endothelial cell functions.

Conclusion

Since 1916, the year in which KD was described for the first time as the presence of globoid cells in the brain, a number of experimental in vitro approaches have been used to understand the mechanisms causing and contributing to the neurological processes of KD and to test the mechanistic role of psychosine.

In summary, it was shown that psychosine 1) is an inhibitor of PKC (Strasberg, 1986; Hannun and Bell, 1987; White et al., 2009); 2) disrupts mitochondrial function (Taketomi and Nishimura, 1964; Li et al., 1997; Hengartner, 2000; Haq et al., 2003; Voccoli et al., 2014) and the integrity of membranes (Vartanian et al., 1989); 3) disrupts the architecture of lipids rafts, disturbing plasma membrane integrity and inhibiting PKC translocation to the plasma membrane (Giri et al., 2006; White et al., 2009; Zigdon et al., 2014); 4) causes the processes, but not the soma, of oligodendrocytes to disintegrate (Hawkins-Salsbury et al., 2013); 5) affects neurofilament phosphorylation in a motor neuron cell line, leading to impaired axonal transport (Cantuti-Castelvetri et al., 2012); 6) produces multinucleation of microglia resembling the characteristic globoid cells (Claycomb et al., 2014); 7) inhibits in murine aortic endothelial cells and brain microvascular endothelial cells different steps of the angiogenesis process *in vitro* (Belleri et al., 2013); and 8) induces apoptosis through activation of caspases 9, 8, and 3 (Haq et al., 2003; Zaka and Wenger, 2004; Giri et al., 2006, 2008).

Thus, direct and/or indirect roles of psychosine in the release of cytokines, ROS and NO and in the activation of kinases, caspases, and angiogenic factors results are now clearer.

However, numerous processes and mechanisms involved in KD have still to be clarified, such as the temporal sequence of the development of events involved in KD or the contributions and interplay among astrocytes, microglia, and oligodendrocytes. The novel *in vitro* systems described in this Review may be useful models in which to study the formation and function of psychosine, and the results here summarized could be useful stimuli for further researches both *in vitro* and *in vivo*.

Conflict of interest statement

All authors disclose that they have no known or potential conflict of interest.

Role of authors

All authors had full access to all the data in the study and take responsibility for the integrity of the data and the accuracy of the data analysis. Study concept and design: RA and ACEG; Acquisition of data: RA, ACEG, GP, and EA; Analysis and interpretation of data: ACEG and VC; Drafting of the manuscript: VC; Study supervision: VC; Obtained funding: VC.

References

Back S, Volpe J. 1998. Mechanisms of oligodendrocyte death in cell death and diseases of the nervous system. Ed. Koliatsos V, Rattan R. Humana Press Inc. 409-418.

Baeuerle PA, Baltimore D. 1996. NF-kB: ten years after. Cell 87:13–20.

Banati RB, Gehrmann J, Schubert P, Kreutzberg GW. 1993. Cytotoxicity of microglia. Glia 7: 111-118.

Beg AA, Baltimore D. 1996. An essential role for NF-κB in preventing TNF-α–induced cell death. Science 274: 782–784.

Belleri M, Ronca R, Coltrini D, Nico B, Ribatti D, Poliani PL, Giacomini A, Alessi P, Marchesini S, Santos MB, Bongarzone ER, Presta M. 2013. Inhibition of angiogenesis by β-galactosylceramidase deficiency in globoid cell leukodystrophy Brain 136: 2859–2875.

Benviste EN, Sparacio SM, Norris JG, Grenett HE, Fuller GM. 1990. Induction and regulation of interleukin-6 gene expression in rat astrocytes. J Neuroimmunol 30: 201-212.

Cantuti-Castelvetri L, Zhu H, Givogri MI, Chidavaenzi RL, Lopez-Rosas A, Bongarzone ER. 2012. Psychosine induces the dephosphorylation of neurofilaments by deregulation of PP1 and PP2A phosphatases. Neurobiol Dis 46: 325–335.

Capper EA, Marshall LA. 2001. Mammalian phospholipases A(2): mediators of inflammation, proliferation and apoptosis. Prog Lipid Res 40: 167–197.

Carmeliet P, Jain RK. 2011. Molecular mechanisms and clinical applications of angiogenesis. Nature 473: 298–307.

Claycomb KI, Johnson KM, Bongarzone ER, Crocker SJ. 2014. An in vitro model for the study of cellular pathophysiology in globoid cell leukodystrophy. J Vis Exp 92: 1-6.

Claycomb KI, Johnson KM, Winokur PN, Sacino AV, Crocker SJ. 2013. Astrocyte Regulation of CNS Inflammation and Remyelination. Brain Sci 3: 1109–1127.

Dennis EA. 1994. Diversity of group types, regulation, and function of phospholipase A2. J Biol Chem 269: 13057–13060.

Earnshaw WC, Martins LM, Kaufmann SH. 1999. Mammalian caspases: Structure, activation, substrates, and functions during apoptosis. Annual Rev Biochem. 68: 383-424.

Farooqui AA, Horrocks LA, Farooqui T. 2007. Modulation of inflammation in brain: a matter of fat. J Neurochem 101: 577-599.

Giacomini A, Ackermann M, Belleri M, Coltrini D, Nico B, Ribatti D, Konerding MA, Presta M, Righi M. 2015. Brain angioarchitecture and intussusceptive microvascular growth in a murine model of Krabbe disease. Angiogenesis 18: 499-510.

Gibbons HM, Dragunow M. 2010. Adult human brain cell culture for neuroscience research. Int J Biochem Cell Biol 42: 844-856.

Giri S, Jatana M, Rattan R, Won JS, Singh I, Singh AK. 2002. Galactosylsphingosine (psychosine)-induced expression of cytokine-mediated inducible nitric oxide synthases via AP-1 and C/EBP: implications for Krabbe disease. FASEB J 16: 661-672.

Giri S, Khan M, Nath N, Singh I, Singh AK. 2008. The role of AMPK in psychosine mediated effects on oligodendrocytes and astrocytes: Implication for Krabbe Disease. J Neurochem 105: 1820–1833.

Giri S, Khan M, Rattan R, Singh I, Singh AK. 2006. Krabbe disease:psychosine-mediated activation of phospholipase A" in olygodendrocyte cell death. J.Lipid Res 47: 1478-1492.

Glabinski A, Mirecka M, Pokoca L. 1995. Tumor necrosis factor alpha but not lymphotoxin is overproduced by blood mononuclear cells in multiple sclerosis. Acta Neurol Scand 91: 276-279.

Graziano AC, Cardile V. 2015. History, genetic, and recent advances on Krabbe disease. Gene 555: 2–13.

Graziano AC, Parenti R, Avola R, Cardile V. 2016. Krabbe disease: involvement of connexin43 in the apoptotic effects of sphingolipid psychosine on mouse oligodendrocyte precursors. Apoptosis 21: 25-35.

Greenberg DA, Jin K. 2005. From angiogenesis to neuropathology. Nature 438: 954–959.

Hannun YA, Bell RM. 1987. Lysosphingolipids inhibit protein kinase C: implications for the sphingolipidoses. Science 235: 670-674.

Haq E, Contreras MA, Giri S, Singh I, Singh AK. 2006. Dysfunction of peroxisomes in twitcher mice brain: a possible mechanism of psychosine-induced disease. Biochem Biophys Res Comm 343: 229-238.

Haq E, Giri S, Singh I, Singh AK. 2003. Molecular mechanism of psychosine-induced cell death in human olygodendrocyte cell line. J Neurochem 86: 1428-1440.

Hawkins-Salsbury JA, Parameswar AR, Jiang X, Schelsinger PH, Bongarzone ER, Ory DS, Demchenko AV, Sands MS. 2013. Psychosine, the cytotoxic sphingolipid that accumulates in globoid cell leukodystrophy, alters membrane architecture. J Lipid Res 54: 3303-3311.

Hengartner MO. 2000. The biochemistry of apoptosis. Nature 407: 770-776.

Hideki I, Suzuki K. 1984. Progressive accumulation of toxic metabolite in a genetic leukodystrophy. Science 224: 753-755.

Ijichi K, Brown GD, Moore CS, Lee JP, Winokur PN, Pagarigan R, Snyder EY, Bongarzone ER, Crocker SJ. 2013. MMP-3 mediates psychosine-induced globoid cell formation: Implications for leukodystrophy pathology. Glia 61: 765–777.

Im DS, Heise CE, Nguyen T, O'Dowd BF, Lynch KR. 2001. Identification of a molecular target of psychosine and its role in globoid cell formation. J Cell Biol 153: 429–434.

Jatana M, Giri S, Singh AK. 2002. Apoptotic positive cells in Krabbe brain and induction of apoptosis in rat C6 glial cells by psychosine. Neurosci Lett 330: 183-187.

Kanazawa T, Nakamura S, Momoi M, Yamaji T, Takematsu H, Yano H, Sabe H, Yamamoto A, Kawasaki T, Kozutsumi Y. 2000. Inhibition of cytokinesis by a lipid metabolite, psychosine. J Cell Biol 149: 943-950.

Khan M, Haq E, Giri S, Singh I, Singh AK. 2005. Peroxisomal participation in psychosine mediated toxicity: implications for Krabbe's disease. J Neurosci Res 80: 845-854.

Kondo Y, Wenger DA, Gallo V, Duncan ID. 2005. Galactocerebrosidase-deficient oligodendrocytes maintain stable central myelin by exogenous replacement of the missing enzyme in mice. Proc Natl Acad Sci USA 102: 18670–18675.

Kozutsumi Y, Kanazawa T, Sun Y, Yamaji T, Yamamoto H, Takematsu H. 2002. Sphingolipids involved in the induction of multinuclear cell formation. Biochim Biophys Acta 1582: 138–143.

La Rosa FA, Pierce JP, Sonenshein GE. 1994. Differential regulation of the c-myc oncogene promoter by the NF-κB Rel family of transcription factors. Mol Cell Biol 14: 1039–1044.

Lee HS, Han J, Bai HJ, Kim KW. 2009. Brain angiogenesis in developmental and pathological processes: regulation, molecular and cellular communication at the neurovascular interface. FEBS J 276: 4622–435.

LeVine SM, Brown DC. 1997. IL-6 and TNFalfa expression in brains of twitcher, quaking and normal mice. J Neuroimmunol 73: 47-56.

Li P, Nijhawan D, Budihardjo I, Srinivasula S M, Ahmad M, Alnemri ES, Wang X D. 1997. Cytochrome c and dATP-dependent formation of Apaf-1/caspase-9 complex initiates an apoptotic protease cascade. Cell 91: 479-489.

Lin A. 2003. Activation of the JNK signaling pathway: breaking the brake on apoptosis. Bioessays 25:17-24.

Lin KI, Baraban JM, Ratan RR. 1998. Inhibition versus induction of apoptosis by proteasome inhibitors depends on concentration. Cell Death Differ 5: 577-583.

Lin KI, Lee SH, Narayanan R, Baraban JM, Hardwick JM, Ratan RR. 1995. Thiol agents and Bcl-2 identify an alphavirus-induced pathway that requires activation of the transcription factor NF-κB. J Cell Biol 131: 1149–1161.

Maghazachi AA, Knudsen E, Jin Y, Jenstad M, Chaudhry FA. 2004. D-galactosyl-beta1-1'-sphingosine and D-glucosyl-beta1-1'-sphingosine induce human natural killer cell apoptosis. Biochem Biophys Res Commun 320: 810-815.

Martin JJ, Leroy JG, Ceuterick C, Libert J, Dodinval P, Martin L. 1981. Fetal Krabbe leukodistrophy. A morphologic study of two cases. Acta Neuropathol 53: 87-91.

Matsushima GK, Taniike M, Glimcher LH, Grusby MJ, Frelinger JA, Suzuki K, Ting JP-Y. 1994. Absence of MHC class II molecules reduces CNS demyelination, microglial/macrophage infiltration, and twitching in murine globoid cell leukodystrophy. Cell 78: 645-656.

Ment LR, Stewart WB, Fronc R, Seashore C, Mahooti S, Scaramuzzino D, Madri JA. 1997. Vascular endothelial growth factor mediates reactive angiogenesis in the postnatal developing brain. Brain Res Dev Brain Res 100: 52–61.

Merril JE, Ignarro LJ, Sherman MP, Melinek J, Lane TE. 1993. Microglial cell cytotoxicity of oligodendrocytes is mediated through nitric oxide. J Immunol 151: 2132-2141.

Merrill JE, Benveniste EN. 1996. Cytokines in inflammatory brain lesions: Helpful and harmful. Trends in Neurosci 19: 331-338.

Miyatake T, Suzuki K. 1972. Globoid cell leukodystrophy: additional deficiency of psychosine galactosidase. Biochem Biophys Res Commun 48: 538-543.

Mohri I, Taniike M, Okazaki I, Kagitani-Shimono K, Aritake K, Kanekiyo T, Yagi T, Takikita S, Kim HS, Urade Y, Suzuki K. 2006a. Lipocalin-type prostaglandin D synthase is up-regulated in oligodendrocytes in lysosomal storage disease and binds gangliosides. J Neurochem 97: 641-651.

Mohri I, Taniike M, Taniguchi H, Kanekiyo T, Aritake K, Inui T, Fukumoto N, Eguchi N, Kushi A, Sasai H, Kanaoka Y, Ozono K, Narumiya S, Suzuki K, Urade Y. 2006b. Prostaglandin D2-mediated microglia/astrocyte interaction enhances astrogliosis and demyelination in twitcher. J Neurosci 26: 4383-4393.

Nishizuka Y. 1995. Protein kinase C and lipid signaling for sustained cellular responses. FASEB J 9: 484-496.

Norris JG, Tang LP, Sparacio SM, Benveniste EN. 1994. Signal transduction pathways mediating astrocyte IL-6 induction by IL-1 beta and tumor necrosis factor-alpha. J Immunol 152: 841-850.

Opipari AW Jr, Hu HM, Yabkowitz R, Dixit VM. 1992. The A20 zinc finger protein protects cells from tumor necrosis factor cytotoxicity. J Biol Chem 267: 12424–12427.

Pannuzzo G, Cardile V, Costantino-Ceccarini E, Alvares E, Mazzone D, Perciavalle V. 2010. A galactose-free diet enriched in soy isoflavones and antioxidants results in delayed onset of symptoms of Krabbe disease in twitcher mice. Mol Gen Metabol 100: 234–240.

Pollanen MS, Brody BA. 1990. Fetal globoid cell leukodistrophy. Arch Pathol Lab Med 114: 213-216.

Qin ZH, Chen RW, Wang Y, Nakai M, Chuang DM, Chase TN. 1999. J. Neurosci 19: 4023-4033.

Renno T, Krakowski M, Piccirillo C, Lin JY, Owens T. 1995. TNF-alpha expression by resident microglia and infiltrating leukocytes in the central nervous system of mice with experimental allergic encephalomyelitis. Regulation by Th1 cytokines. J Immunol 154: 944-953.

Ribbens JJ, Moser AB, Hubbard WC, Bongarzone ER, Maegawa GHB. 2014. Characterization and application of a disease-cell model for neurodegenerative lysosomal disease. Mol Genet Metab 111: 172-183.

Schrader M, Fahimi HD. 2004. Mammalian peroxisomes and reactive oxygen species. Histochem Cell Biol 122: 383-393.

Segura I, De Smet F, Hohensinner PJ, Ruiz de Almodovar C, Carmeliet P. 2009. The neurovascular link in health and disease: an update. Trends Mol Med 15: 439–451.

Selmaj KW, Raine CS. 1988. Tumor necrosis factor mediates myelin and oligodendrocyte damage in vitro. Ann Neurol 23: 339-346.

Sharma R, Fischer MT, Bauer J, Felts PA, Smith KJ, Misu T, Fujihara K, Bradl M, Lassmann H. 2010. Inflammation induced by innate immunity in the central nervous system leads to primary astrocyte dysfunction followed by demyelination. Acta Neuropathol 120: 223–236.

Singh I, Pahan K, Khan M, Singh AK. 1998. Cytokine-mediated induction of ceramide production is redox-sensitive. Implications to proinflammatory cytokine-mediated apoptosis in demyelinating diseases. J Biol Chem 273: 354–362.

Sorger PK, Dobles M, Tournebize R, Hyman AA. 1997. Coupling cell division and cell death to microtubule dynamics. Curr Opin Cell Biol 9: 807–814.

Stennicke HR, Jurgensmeier JM, Shin H, Deveraux Q, Wolf BB, Yang XH, Zhou Q, Ellerby HM, Ellerby LM, Bredesen D, Green DR, Reed JC, Froelich CJ, Salvesen GS. 1998. Pro-caspase-3 is a major physiologic target of caspase-8. J Biol Chem 273: 27084-27090.

Strasberg P. 1986. Cerebrosides and psychosine disrupt mitochondrial functions. Biochem Cell Biol 64: 485-489.

Subramanian M, Jutila A, Kinnunen PK. 1998. Binding and dissociation of cytochrome c to and from membranes containing acidic phospholipids. Biochem 37: 1394–1402.

Sun Y, Zhao X, Yao Y, Qi X, Yuan Y, Hu Y. 2012. Connexin 43 interacts with Bax to regulate apoptosis of pancreatic cancer through a gap junction-independent pathway. Int J Oncol 41: 941-948.

Suzuki K, Suzuki Y. 1970. Globoid cell leukodystrophy (Krabbe's disease): deficiency of galactocerebroside beta-galactosidase. Proc Natl Acad Sci USA 66: 302-309.

Suzuki K. 1998. Twenty-five years of the "Psychosine Hypothesis": a personal perspective of its history and present status. Neurochem Res 23: 251-259.

Svennerholm L, Vanier MT, Mansson JE. 1980. Krabbe disease: a galactosylsphingosine (psychosine) lipidosis. J Lipid Res 21: 53-58.

Taketomi T, Nishimura K. 1964. Physiological activity of psychosine. Jpn J Exp Med 34: 255-265.

Tanaka K, Webster HD. 1993. Effects of psychosine (galactosylsphingosine) on the survival and the fine structure of cultured Schwann cells. J Neuropathol Exp Neurol 52: 490-498.

Taniike M, Mohri I, Eguchi N, Irikura D, Urade Y, Okada S, Suzuki K. 1999. An apoptotic depletion of oligodendrocytes in the twitcher, a murine model of globoid cell leukodystrophy. J Neuropathol Exp Neurol 58: 644-653.

Tohyama J, Matsuda J, Suzuki K. 2001. Psychosine is as potent an inducer of cell death as C6- ceramide in cultured fibroblasts and in MOCH-1 cells. Neurochem Res 26: 667-671.

Ueda M, Graf R, MacWilliams HK, Schliwa M, Euteneuer U. 1997. Centrosome positioning and directionality of cell movements. Proc Natl Acad Sci USA 94: 9674–9678.

Antwerp DJ, Martin SJ, Kafri T, Green DR, Verma IM. 1996. Suppression of TNF-α-induced apoptosis by NF-kB. Science 274: 787–789.

Vanier M, Svennerholm L. 1976. Chemical pathway of Krabbe disease: the occurrence of psychosine and other neural sphingoglycolipids. Adv Exp Med Biol 68: 115-126.

Vartanian T, Dawson G, Soliven B, Nelson DJ, Szuchet S. 1989. Phosphorylation of myelin basic protein in intact oligodendrocytes: inhibition by galactosylsphingosine and cyclic AMP. Glia 2: 370-379.

Verkhratsky A, Sofroniew MV, Messing A, deLanerolle NC, Rempe D, Rodriguez JJ, Nedergaard M. 2012. Neurological diseases as primary gliopathies: A reassessment of neurocentrism. ASN Neuro 4: 131-149.

Visigalli I, Ungari S, Martino S, Park H, Cesani M, Gentner B, Sergi L, Orlacchio A, Naldini L Biffi A. 2010. The galactocerebrosidase enzyme contributes to the

maintenance of a functional hematopoietic stem cell niche. Blood 116: 1857–1866.

Voccoli V, Tonazzini I, Signore G, Caleo M, Cecchini M. 2014. Role of extracellular calcium and mitochondrial oxygen species in psychosine-induced oligodendrocyte cell death. Cell Death and Disease 5: e152.

Wang X, Zelenski NG, Yang J, Sakai J, Brown MS, Goldstein JL. 1996. Cleavage of sterol regulatory element binding proteins (SREBPs) by CPP32 during apoptosis. EMBO J 15: 1012–1020.

Wenger DA, Rafi A, Luzi P. 1997. Molecular genetics of Krabbe disease (globoid cell leucodystrophy): Diagnostic and clinical implications. Human Mutat.10: 268-279.

White AB, Givogri MI, Lopez-Rosas A, Cao H, van Breemen R, Thinakaran G, Bongarzone ER. 2009. Psychosine accumulates in membrane microdomains in the brain of Krabbe patients, disrupting the raft architecture. J Neurosci 29: 6068-6077.

Widmann C, Gibson S, Jarpe MB, Johnson GL. 1999. Mitogen-activated protein kinase: conservation of a three-kinase module from yeast to human. Physiol Rev 79: 143–180.

Williams K, Ulvestad E, Waage A, Antel JP, McLaurin J. 1994. Activation of adult human derived microglia by myelin phagocytosis in vitro. J Neurosci Res 38: 433-443.

Won JS, Kim J, Paintlia MK, Singh I, Avtar K. Singh AK. 2013. Role of endogenous psychosine accumulation in oligodendrocytes differentiation and survival: implication for Krabbe disease. Brain Res 1508: 44–52.

Wu H, Lozano G. 1994. NF-κB activation of p53. A potential mechanism for suppressing cell growth in response to stress. J Biol Chem 269: 20067–20074.

Wu YP, McMahon EY, Masuda J, Suzuki K, Matsushima GK, Suzuki K. 2001. Expression of immune-related molecules is downregulated in twitcher mice following bone marrow transplantation. J Neurophatol Exp Neurol 60: 1062-1074.

Yamada H, Martin P, Suzuki K. 1996. Impairment of protein kinase C activity in twitcher Schwann cells in vitro. Brain Res 718: 138-144.

Zacchigna S, Lambrechts D, Carmeliet P. 2008. Neurovascular signalling defects in neurodegeneration. Nat Rev Neurosci.9: 169–181.

Zajicek JP, Wing M, Scolding NJ, Compston DA. 1992. Interactions between oligodendrocytes and microglia. A major role for complement and tumor necrosis factor in oligodendrocyte adherence and killing. Brain 115: 1611-1631.

Zaka M, Rafi MA, Rao HZ, Luzi P, Wenger DA. 2005 Insulin-like growth factor-1 provides protection against psychosine-induced apoptosis in cultured mouse oligodendrocyte progenitor cells using primarily the PI3K/Akt pathway. Mol Cell Neurosci 30: 398-407.

Zaka M, Wenger DA. 2004. Psychosine-induced apoptosis in a mouse oligodendrocyte progenitor cell line is mediated by caspase activation. Neurosci Letters 358: 205-209.

Zielasek J, Tausch M, Toyka KV and Hartung HP. 1992. Production of nitrite by neonatal rat microglial cells/brain macrophages. Cell Immunol 141: 111-120.

Zigdon H, Meshcheriakova A, Futerman AH. 2014. From sheep to mice to cells: tools for the study of the sphingolipidoses. Biochim Biophys Acta http://dx.doi.org/10.1016/j.bbalip.2014.02.008: 1-11.

CHAPTER II

Mol Neurobiol. 2016 Dec 5. DOI 10.1007/s12035-016-0312-6

Dedicated to the memory of Carmela Spatafora

HUMAN MESENCHYMAL STEM CELLS FROM ADIPOSE TISSUE DIFFERENTIATED INTO NEURONAL OR GLIAL PHENOTYPE EXPRESS DIFFERENT AQUAPORINS

Rosanna Avola, Adriana Carol Eleonora Graziano, Giovanna Pannuzzo, Venera Cardile*

Department of Biomedical and Biotechnological Sciences, Section of Physiology, University of Catania, Via Santa Sofia 64, 95125 Catania, Italy

Concise and informative title: **Neural differentiation and aquaporins**

Abstract

Aquaporins (AQPs) are 13 integral membrane proteins that provide selective pores for the rapid movement of water, and other uncharged solutes, across cell membranes. Recently, AQPs have been focused for their role in production, circulation and homeostasis of the cerebrospinal fluid and their importance in several human diseases is becoming clear. This study investigated the time course (0, 14, and 28 days) of AQP1, 4, 7, 8 and 9 during the neural differentiation of human mesenchymal stem cells (MSCs) from adipose tissue (AT). For this purpose, two different media, enriched with serum or B-27 and N1 supplements, were applied to give a stimulus toward neural lineage. After 14 days, the cells were cultured with neuronal or glial differentiating medium for further 14 days. The results confirmed that AT-MSCs could be differentiated into neurons, astrocytes and oligodendrocytes, expressing not only the typical neural markers, but also specific AQPs depending on differentiated cell type. Our data demonstrated that at 28 days AT-MSCs express only AQP1, astrocytes AQP1, 4 and 7, oligodendrocytes AQP1, 4, and 8, and finally neurons AQP1, and 7. This study provides fundamental insight into the biology of the mesenchymal stem cells and it suggests that AQPs can be potential neural markers.

Keywords: AQPs, Astrocyte, Cell culture, Neural differentiation, Neuron, Oligodendrocyte.

Introduction

Aquaporins (AQPs) are cell proteinaceous transmembrane water channels with a molecular weight between 28 and 30 kDa that play essential roles in the water permeability, often accounting for up to 90% of it is as in the red cell [1]. In some regions of membrane, these molecules have other function such as the glycerol and small solutes transport [2]. AQPs are members of the superfamily major intrinsic protein (MIP) transmembrane channels and share a common structural organization. They comprise six transmembrane domains connected by five loops and intracellular located N-and C- termini. In biological membranes, AQPs are grouped as homotetramers. Each monomer functions independently as a single channel pore [3]. Mammalian express 13 AQPs isoforms (AQP0-12), based on the primary sequences. They can be divided into three groups: water selective aquaporins (AQP0, 1, 2, 4, 5, 6, and 8), aquaglyceroporins (AQP3, 7, 9, and 10), which transport not only water but also small non-polar molecules like glycerol and urea, and finally superaquaporins (AQP11, 12), which function remains to be clarified [4]. AQPs are widely expressed in many cell types where they have both physiological and pathophysiological relevance [5]. Some AQPs members were found to influence angiogenesis, tumor cell growth, tissue repair, homeostasis, and immune function because they participate in diverse biological processes related to cell migration [6], proliferation [7], apoptosis [8], cell volume-regulation [9], neuronal signal transduction [10], mitochondrial metabolism [11], vesicular swelling [12], and phagocytosis [13]. In the brain, considering that water is about 80%, AQPs play an important role in the production, circulation and homeostasis of the cerebrospinal fluid (CSF). Fluid balance (secretion, removal, fluxes and homeostasis of salts) is important for the brain survival but also neuronal excitability [14]. So far, nine aquaporin subtypes (AQP1, 2, 3, 4, 5, 7, 8, 9, and 11) have been recognized and partially characterized in human brain cell function, but only three aquaporins (AQP1, 4, and 9) have been clearly identified in brain cells *in vivo* [15].

Although the brain have a unique set of AQPs that can modulate water balance and cell volume control and AQPs dysfunction or lack has been described in a variety of neurological diseases, many specific AQPs functions and/or implications are unclear especially in neurogenesis and neural differentiation.

AQPs may contribute also in stem cell differentiation, as stem cells transport considerable amount of water into or out of the cells to achieve rapid volume regulation during differentiation [16]. However, a small number of studies indicated expression and function of AQPs in stem cells [17-20]. AQP3 was reported to express in human fetal airway epithelial progenitor cells [18]. AQP4, 8, and 9 were found in murine adult neural stem cells [17–19]. AQP8 might play a key role in mitochondrial volume regulation during murine adult neural stem cells differentiation [17]. The expression levels and cellular localization of AQP4 and 9 were differentially regulated during murine adult neural stem cells differentiation into neurons and glial cells [19]. AQP4 deletion reduced the proliferation, migration, survival, and neuronal differentiation of neural stem cells of adult mice [20]. Yi et al. [21] discovered the expression of AQP5 in mouse bone marrow-derived mesenchymal stem cells. They demonstrated that AQP5-mediated high plasma membrane water permeability enhances the apoptosis rate of differentiating mouse bone marrow-derived mesenchymal stem cells, thus decreasing their differentiation capacity.

Moreover, AQPs are expressed in a specific age-dependent manner, concomitantly with the intracellular and extracellular water content changes reaching a crucial role during the early postnatal period [22]. In particular, water balance involving AQPs might be important during the neurogenesis. For example during rodent brain development, the most significant period for water transfer across the choroid plexus is likely to be during the prenatal period from embryonic day 13 until birth. During this period, the rapid growth of the choroid plexuses and expansion of the cerebral ventricles occur [16].

Given the great importance of AQPs for the maintenance of cell and tissue homeostasis, in the present study we evaluated the expression of AQPs during the differentiation of human mesenchymal stem cells from adipose tissue (AT-MSCs) toward neural phenotypes. The objective was to determine when and which AQPs are produced during differentiation of AT-MSCs into astrocytes, oligodendrocytes and/or neurons. Other and our previous studies have demonstrated AT-MSCs as an alternative source of stromal cells hold unique regenerative potential as they are self-renewing and capable of differentiating into mesenchymal and non-mesenchymal cells *in vitro*, including neuronal and glial cells [23-28].

Materials and methods

Isolation, culture, and characterization of mesenchymal stem cells from adipose tissue (AT-MSCs)

The adipose tissue has been obtained from donators, from 20 to 30 years of age (mean body mass index of 29 $\pm$ 2.9), not smokers and occasionally taking non-steroidal anti-inflammatory drugs, undergoing liposuction procedures. Lipoaspirates were acquired after the informed consent from the subjects, according to the laws of the Italian Government. Isolation of AT-MSCs, was accomplished as previously described [28]. The lipoaspirate from each patient (50–100 ml) was washed with sterile phosphate buffered saline (PBS; Invitrogen, Milan, Italy) and digested with 0.075% collagenase type I (Invitrogen, Milan, Italy) for 60 min at 37 °C with intermittent shaking. Successively, the digested lipoaspirate was centrifuged at 1200 r.p.m. for 10 min. The pellets were re-suspended in PBS (plus penicillin/streptomycin 1%) and filtered through a 100-μm nylon cell strainer (Falcon BD Biosciences, Milan, Italy). The filtered cells were again centrifuged at 1200 rpm for 10 min, plated in T-75 culture flasks (Falcon BD Biosciences, Milan, Italy) with DMEM-1g (plus 10% FBS and 1% penicillin/streptomycin) containing 1% of MSC growth medium (MSCGS; Science Cell Research Laboratories, Milan, Italy) and incubated at 37 °C with 5% CO_2. Twenty-four hours after the initial plating, non-adherent cells were removed by intensely washing the flasks. After 3 days, culture medium was changed and the cells maintained for 28 days with 2 weekly medium changes.

For phenotype characterization, MSC markers CD44, CD90 and CD105 and hematopoietic cell line markers CD14, CD34 and CD45 were detected by flow cytometry analysis.

For the execution of the flow cytometry, after reaching confluence (80% of total flask surface), AT-MSCs (2^{nd} - 3^{rt} passage) were trypsinized (trypsin-EDTA; Sigma-Aldrich, Milan, Italy) and sub-cultured in 6-well culture dishes for 2 days. Cells were first washed with PBS, again trypsinized, fixed with 2% paraformaldehyde (PFA) for 20 min at 4 °C and permeabilized with 1x Triton (Sigma-Aldrich, Milan, Italy) for 5 min at 4 °C. Subsequently, cells were washed with PBS/BSA 1% and incubated with primary antibodies (Millipore, Milan, Italy) for 60 min at room temperature. Cells were then washed with PBS/BSA 1% and incubated for 60 min at

room temperature in the dark with secondary antibodies (goat anti-mouse or goat anti-rabbit) conjugated with fluorescein (FITC; 1:200; Millipore, Milan, Italy). Samples were analyzed using a Coulter Epics Elite ESP flow cytometer (Cytomics FC 500, Beckman Coulter) and analysis was performed using CXP Analysis software. A minimum of 10000 forward and side scatter gated events were collected per specimen. Samples were excited at wavelength λ= 488 nm and fluorescence was monitored at wavelength λ= 525 nm. Fluorescence was detected using logarithmic amplification. Mean fluorescence intensity (MFI) values were calculated and recorded automatically.

Neural induction

Experimental human AT-MSCs semi-confluent (80% of total flask surface) were trypsinized (Trypsin-EDTA; Sigma–Aldrich, Milan, Italy) and sub-cultured at high density (100 cells/µl) in 24 multiwell plates (500 µl/well). After 24 hours the medium was removed, the cultures were washed with PBS with calcium chloride and magnesium chloride (Sigma-Aldrich, Milan, Italy) and exposed to two neural induction media. One group was maintained with medium DMEM/F12 supplemented with 10% FBS (Invitrogen, Milan, Italy), 1% penicillin/streptomycin, (Sigma-Aldrich, Milan, Italy), 40 ng/ml fibroblast growth factor-basic (FGF-basic; Peprotech, DBA, Milan, Italy), and 20 ng/ml epidermal growth factor (EGF, Peprotech, DBA, Milan, Italy) (medium A). The second group was incubated with medium containing DMEM/F12 enriched of B-27 and N1 growth supplements, 30% glucose, 1 M Hepes buffer, 40 ng/ml fibroblast growth factor-basic (FGF-basic) and 20 ng/ml epidermal growth factor (EGF) (all Peprotech, DBA, Milan, Italy) [17] (medium B). Finally, some cultures of human AT-MSCs, used as a control, were incubated in DMEM-lg supplemented with 10% FBS and 1% penicillin/streptomycin. All groups were cultured for 14 days.

Glial and/or neuronal differentiation

Fourteen days after plating, AT-MSCs pre-treated with medium A or neurospheres obtained after pre-treatment with medium B were transferred from each well into two different 50 ml conical tubes and centrifuged at 300 g for 10 min; the supernatant was removed and 1.0 ml of trypsin-EDTA solution 1x was added into each tube. Cells and medium were mixed using Pasteur pipettes and placed in water

bath at 37 °C for 2-3 min. After, 1.0 ml of FBS was added to cell suspension and centrifuged at 600 g for 5 min. The cells were re-suspended in 0.5 ml of medium (medium A or B, respectively) and plated at high density (100 cells/µl) in 24 multiwell plates (500 µl/well) pre-treated with acid gelatin (2% H_2O). After 24 hours, the medium was removed and the cells were washed with PBS with calcium chloride and magnesium chloride (Sigma-Aldrich, Milan, Italy). Hence, each group of cells pre-treated with medium A or B for neural induction was divided in two groups and maintained for 14 days with neuronal (medium C) or glial differentiating medium (medium D). Medium C contained Neurobasal medium (Gibco, Life Technologies, Milan, Italy) plus 10% FBS, 1% penicillin/streptomycin, 50 ng/ml nerve grown factor -β (NGF-β; Gibco Life Technologies, Milan, Italy), 50 ng/ml brain derived neurotrophic factor (BDNF; Gibco Life Technologies, Milan, Italy) and 10 ng/ml neurotrophin-3 (NT-3; Peprotech, DBA, Milan, Italy). Medium D comprised Neurobasal medium (Gibco, Life Technologies, Milan, Italy) plus 10% FBS, 1% penicillin/streptomycin, 4 mM forskolin (Sigma-Aldrich, Milan, Italy) and 10 ng/ml heregulin β-1 (Peprotech, DBA, Milan, Italy). Thus, the experimental groups at 14 days became four: AT-MSCs pre-treated with medium A were cultured with medium C or D (for neuronal or glial differentiation, respectively) and AT-MSCs pre-treated with medium B were maintained with medium C or D (for neuronal or glial differentiation, respectively) for further 14 days. The identification of specific neural surface markers and AQPs was performed by immunocytochemistry, Western blot analysis and reverse transcription polymerase chain reaction (RT-PCR) at 0, 14, and/or 28 days.

Detection of neural markers and AQPs by immunocytochemistry

To determine cell phenotypes, AT-MSCs were grown under control conditions (AT-MSCs control) or treated with neural (medium A or B), neuronal (medium C) or glial (medium D) differentiation medium. Immunocytochemistry was performed at 0, 14 and 28 days. Briefly, cells were first washed with PBS, then fixed with 4% paraformaldehyde in PBS for 30 min and incubated for 30 min with a 5% solution of normal goat serum (Sigma-Aldrich, Milan, Italy). They were subsequently incubated overnight at 4 °C with primary antibodies direct against the following markers: anti-nestin (Millipore, Milan, Italy), -S100β (Bethyl Laboratories, Tema Ricerca, Bologna), -SOX-2 (Santa Cruz Biotechnology, Santa Cruz, CA), -GFAP.(Millipore,

Milan, Italy), -A2B5 (Millipore, Milan, Italy), -O4 (Millipore, Milan, Italy), -β-tubulin-III (Santa Cruz Biotechnology, Santa Cruz, CA), -PGP 9.5 (Santa Cruz Biotechnology, Santa Cruz, CA), and –NeuN (Millipore, Milan, Italy). In parallel the expression of AQPs was determined by using anti-AQP1, -AQP4, -AQP7, -AQP8, and -AQP9 antibodies (all from Santa Cruz Biotechnology, DBA, Milan, Italy). The following day, cells were washed with PBS and incubated for one hour at room temperature with Cy3-conjugated goat anti-mouse (Cy3; 1: 400 dilution), fluorescein isothiocyanate-conjugated goat anti-rabbit (FITC; 1: 200 dilution), or fluorescein isothiocyanate-conjugated goat anti-mouse (FITC; 1: 400 dilution) antibodies (all from Millipore, Milan, Italy). Cells were then washed with PBS, and incubated with DAPI (1: 10,000 dilution; Invitrogen, Milan, Italy). As a control, the specificity of immunostaining was verified by omitting incubation with the primary or secondary antibody. Digital images were acquired using a Leica fluorescence microscope connected to a digital camera (Spot, Diagnostic Instruments, Sterling Heights, USA) and adjusted for contrast in Corel Draw version 9. Immunoreactivity was evaluated taking into account the signal-to-noise ratio of immunofluorescence.

Detection of neural markers and AQPs by Western blot

The proteins expression was confirmed by Western blot analysis performed at 0, 14 and 28 days. Briefly, the cultures were washed twice with ice-cold PBS and collected with lysing buffer M-PER Mammalian Protein Extraction Reagent (Pierce, Fisher Scientific, Milan, Italy). After cooling for 30 min at 0 °C, the supernatant was collected by centrifugation (15,000 x g, 15 min, and 4 °C). Protein quantification was obtained with bicinchoninic acid assay (BCA assay; Pierce, Fisher Scientific, Milan, Italy). Equal amounts of proteins (30 μg) were separated by 4–12% Novex Bis-Tris gel electrophoresis (NuPAGE; Invitrogen, Milan, Italy). Then, proteins were transferred to nitrocellulose membrane (Invitrogen, Milan, Italy) in a wet system. The transfer of proteins was verified by staining the nitrocellulose membranes with Ponceau S. Membrane was blocked in Tris-buffered saline containing 0.01% Tween-20 (TBST) and 5% non-fat dry milk for 1 hour at room temperature. Appropriate primary antibodies described above were diluted in TBST and membranes were incubated for 24 hours at room temperature. Blots were rinsed three times in PBS and the applicable HRP-conjugated secondary antibody was incubated for 1 hour at room temperature (goat anti-rabbit, 1:20,000; goat anti-

mouse, 1:5000; both from Santa Cruz Biotechnology, DBA, Milan, Italy). Antibodies were detected using enhanced chemiluminescent solution (Pierce, Fisher Scientific, Milan, Italy). Bands were measured densitometrically and their relative density was calculated based on the density of the α-tubulin bands in each sample. Values were expressed as arbitrary densitometric units (A.D.U.) corresponding to signal intensity.

Detection of neural markers and AQPs by reverse transcription polymerase chain reaction (RT-PCR)

Total RNA was prepared from control, medium A or B pre-treated and/or medium C or D differentiated cells using 1 ml Qiazol Reagent (Qiagen, Milan, Italy), 0.2 ml chloroform and 0.5 ml isopropanol. Pellet was washed with 75% ethanol, dried with air and resuspended in RNAse-free water.

Total RNA was purified using the Qiagen RNeasy Mini Kit (Qiagen, Milan, Italy). cDNA was synthesized from total RNA samples using the QuantiTect Reverse Transcription Kit (Qiagen, Milan, Italy). Reaction was terminated by incubation of samples at 95 °C for 5 min. Aliquots of cDNA were amplified using specific primers for AQPs (1, 4, 7, 8, and 9) and a panel of specific neural markers. Oligonucleotide sequences were listed in Table 2. cDNA was used for 40 cycle PCR in Rotor-gene Q real-time analyzer (Corbett, Qiagen, Milan, Italy). Each PCR reaction contained 1x Rotor-Gene SYBR Green PCR Master Mix, template cDNA (≤100 ng/reaction), primers (1 μM), and RNase-free water with a final reaction volume of 25 μl. PCR was performed using the following program: initial activation step 95 °C 10 min, denaturation 95 °C 10 sec, annealing 60 °C 30 sec, extension 72 °C 30 sec (40 cycles), final extension 72 °C 10 min. RT-PCR was followed by melting curve analysis to confirm PCR specificity. Each reaction was repeated three times and threshold cycle average was used for data analysis by Rotor-gene Q software. Target genes were normalized against GAPDH. Amplification products were separated by electrophoresis in a 2% agarose gel in 0.045 M Tris–borate/1mM EDTA (TBE) buffer. Relative expression of target genes of mRNA versus GAPDH was quantified by performing densitometric analysis of amplicons and reported as A.D.U. corresponding to signal intensity.

Statistical analysis

The experiments were repeated independently at least three times in triplicate and the mean ± SEM for each value was calculated. One-way statistical analyses of results [Student's t test for paired and unpaired data; variance analysis (ANOVA)] were used. All statistical analyses were performed using the statistical software package SYSTAT, version 11 (Systat Inc., Evanston IL, USA).

Results

Characterization of AT-MSCs

Primary cell cultures were obtained from samples of human lipoaspirate. After one week, the cultures were homogenous, consisting by population of adherent spindle-shape fibroblastoid cells identified after as MSCs (Figure 1a). To characterize human AT-MSCs, cell surface and specific hematopoietic markers were examined by flow cytometry analysis. The cells did not present labeling for CD45, CD14 and CD34, but they showed positivity for CD44 (H-CAM), CD90 (Thy 1) and CD105 (Endoglin), characteristic MSCs markers (Table 1).

Detection of neural markers and AQPs by immunocytochemistry

To order to verify neural, neuronal and glial differentiation and determine time of appearance and levels of AQPs, control, inducted, and differentiated human AT-MSCs were immunostained with a panel of neural markers and AQPs antibodies at 0, 14 and 28 days. At the beginning of the culture, before starting the differentiation, AT-MSCs expressed AQP1 and nestin and were negative for the other investigated markers (Figure 1b). After exposure (14 days) at two different neural induction media (medium A containing FBS or medium B containing B-27 and N1), AT-MSCs exhibited morphological changes. Medium B promoted the formation of spherical clusters called "neurospheres" from floating cultures of single cells (Figure 2a). These free-floating aggregates similar to neurospheres were nestin positive. To confirm the presence of neural cells in neurospheres, SOX-2 was verified [29]. These clusters of cells resulted positive for SOX-2 and AQP4 and maintained the positivity for AQP1 (Figure 2b).

Immunocytochemistry on cells treated with medium containing FBS showed a similar expression of nestin, SOX-2, AQP1and AQP4 and became positive for AQP7 (Figure 3a and b).

Following treatment with neuronal or glial medium, cells exhibited immunocytochemical changes and expressed neuronal or glial markers. Cells derived from neurospheres and treated with glial medium (D) were immunostained with O4 (Figure 4b). O4 is a marker of oligodendrocyte cell. As regards the AQPs, glial differentiated from B-27- and N1-pre-treated cells (Figure 4a) showed high levels of AQP1, AQP4, and AQP8 (Figure 4b). Immunochemistry revealed that B-27- and N1-pre-treated cells (14 days) and after maintained in medium C for further 14 days (Figure 5a) are β-tubulin-III, and AQP1 positive (Figure 5b).

In parallel, FBS-pre-treated cells for 14 days were examined with same markers of differentiation and AQPs. The results showed that cells treated with glial medium are positive for astrocytes marker (GFAP) and contemporary express AQP1, AQP4, and AQP7 (Figure 6a and b). FBS-pre-treated cells exposed to neuronal medium demonstrated to exhibit PGP9.5 positivity and high levels of AQP1, and AQP7 (Figure 7a and b).

Detection of neural markers and AQPs by Western blot

Western blot was performed at 0 (AT-MSCs), 14 (neural induction), and 28 days (after neuronal or glial differentiation). Human AT-MSCs cells resulted positive for nestin (Figure 1c). After exposure to neural induction medium, B-27 and N1- as well as FBS-treated cells expressed SOX-2, and nestin (Figure 2c and 3c). Western blot analysis confirmed that only cells cultured with glial medium from FBS-treated cells were GFAP positive (Figure 6c).

Cells derived from neurospheres and treated with glial medium (D) expressed AQP1, AQP4, and AQP8 (Figure 4c). AT-MSCs pre-treated with FBS medium and glial medium were positive for GFAP, nestin, AQP1, AQP4, and AQP7 (Figure 6c).

As regards neuronal differentiation, cells demonstrated the presence of nestin, β-tubulin-III, NeuN and PGP9.5. In particular, in neuronal phenotypes from FBS-treated cells were detected a more high expression of β-tubulin-III and PGP9.5 (Figure 7c) compared to neurons from B-27-and N1-treated cells (Figure 5c). NeuN band was detected only in neuronal differentiated FBS-treated cells (Figure 7c).

Finally, Western blot confirmed the presence of AQP1, 4, and 7, in line with the immunocytochemistry findings.

Detection of neural markers and AQPs by RT-PCR

To confirm the occurred differentiation of AT-MSCs and gene transcription of neural markers and AQPs, RT-PCR was performed. The results confirmed those obtained by immunocytochemistry and Western blot in AT-MSCs treated with the different media and examined at the time points (Figure 1d-7d).

Discussion

To the best of our knowledge, this is the first study to compare in parallel a set of surface markers and AQPs in AT-MSCs induced to differentiate into neural phenotypes by using several differentiation protocols. The aim was to investigate whether AT-MSCs can differentiate into neural cells expressing different AQPs isoforms and to try to reproduce an *in vitro* model of human neural development. Importantly, the research showed that AT-MSCs could be differentiated into neurons, astrocytes and oligodendrocytes, expressing not only the typical neural markers, but also specific AQPs depending on differentiated cell type. Here, our data demonstrated that AT-MSCs express only AQP1, astrocytes AQP1, 4 and 7, oligodendrocytes AQP1, 4, and 8, and finally neurons AQP1, and 7.

First of all our findings indicated and confirmed that stem cells from adult adipose stromal tissue retain the capacity to differentiate towards neural lineages presenting morphologic and immunochemical characteristics. To induce neural phenotype and to differentiate in neuronal or glial cells two different protocols, respectively, were applied. The purpose was to verify whether the use of different procedures entails differences in the AT-MSCs differentiation capacity detected at the protein or mRNA level. A protocol of induction involved the use of medium containing serum, the other one the use of medium serum-free added with B-27 and N1 supplements. It is known that the processes of proliferation, allocation, and lineage-specific terminal differentiation are regulated by a complex interplay involving stem cell transcription factors (molecular rheostats), cell-specific transcription factors, and a wide variety of cellular kinases, growth factors, and receptors. Moreover, serum plays an important role in supporting the survival and proliferation of numerous types of cultured cells. We have analyzed the effect of AT-MSCs pre-treatment with a

medium enriched with serum and serum-free, respectively, demonstrating that medium with serum gives rise to GFAP positive astrocytes, while serum-free medium to O4 positive oligodendrocytes.

In this study, we used AT-MSCs for the experiments and observed that at more than 90% of cells expressed CD44, CD90 and CD105, mesenchymal cell markers, but not CD14, CD34 and CD45, hematopoietic cell markers, indicating that most cells are mesenchymal stem cells.

Furthermore, our results showed that both pre-treated AT-MSCs with and without FBS for 14 days resulted nestin positive cells. Nestin, an intermediate filament protein is thought to be expressed at high levels in neural stem cells, although its expression has also been observed in myogenic cells, endothelial cells, and hepatic cells [29]. These cells were also SOX-2 positive, a gene transcriptional activator. Nestin and SOX-2 are unequivocally accepted as markers of proliferation, migration and differentiation during embryonic development and in adult brain [30-33]. The loss of these markers induces cell cycle exit and neuronal differentiation [34, 35] with the concomitant up regulation of other tissue-specific intermediate filament proteins [36]. Our results demonstrated that the pre-treatment with FBS seems to lead to a more mature neural phenotype demonstrated by a general decrease of SOX-2 and nestin proteins, a condition found in the chick neural tube [37].

Although it was reported that a high number of neurospheres from adipose tissue is generated *in vitro* when the culture medium is supplemented with serum and enriched with a combination of EGF and FGF [38, 39], in our experimental conditions, no population of cells was able to organize into spheres growing in suspension. On the contrary, AT-MSCs treated for 14 days with serum-free medium added with B-27 and N1 supplements formed neurospheres aggregates arranged in three-dimensional structures expressing a strong quantity of nestin and SOX-2. These neurospheres treated with glial differentiating medium decreased nestin, lost SOX-2, and differentiated in O4 positive cells, a marker of oligodendrocytes intermediate precursors [40]. AT-MSCs pre-treated with medium enriched with FBS for 14 days and after treated with differentiating glial medium for further 14 days were positive for astrocytes GFAP marker. Neurospheres cultivated with neuronal differentiating medium became β-tubulin-III, and PGP9.5 positive, typical markers of neurons.

Thus, the regulation of neural differentiation of AT-MSCs appears to be a complex process. However, immunocytochemical staining for neural markers in AT-MSCs after neural induction and differentiation was immediate, robust, and Western blot and RT-PCR analysis confirmed neural protein and RNA expression, respectively. In any case, while there are numerous reports on the *in vitro* neural differentiation of AT-MSCs, no study has demonstrated or discussed whether the morphological and gene expression changes are associated to modifications of AQPs expression. Thus, in parallel, to know when and what type of AQPs are expressed during the neural differentiation a systematic study was carried out. In particular, AQPs 1, 4, 7, 8 and 9 were examined. Despite few reports have addressed AQPs expression in the developing mammalian brain [41], we showed that AT-MSCs undergo neural-like morphological changes and express different types of AQPs. We found a correlation between the neural differentiation and the aquaporin expression profile. Thus, it now seems clear that the regulation of water balance by aquaporins plays a critical role not only during CNS development but also during adult neurogenesis and differentiation enough to justify the use the aquaporins as a differentiation marker.

In particular, AT-MSCs and differentiated neuronal or glial cells demonstrated to express AQP1. AQP1, initially identified in red blood cells and renal proximal tubular epithelium, is found to be selectively and constitutively expressed in the apical surface of choroid plexus epithelium (CPE) in the CNS [42]. Our results showed that AQP1 expression is not CPE-specific or in the human CNS under pathological conditions, but in our experimental conditions it was identified in all stem or differentiated cell types even if at a different level. Controversial opinions are object of debate about the expression of AQP1 in astrocytes, because it was reported the association of AQP1 expression with pathological states of astrocytes [43] and meantime others authors described the function role of this protein in astrocytes normal condition [44]. Here, we found that the levels of AQP1 expression did not change during the AT-MSCs treatments, suggesting that AQP1 should be linked to maintaining the physiological homeostasis of cell systems examined.

AT-MSCs–pre-treated with FBS and differentiated in astrocytes co-expressed AQP1, AQP7, and AQP4.

AQP7 is an aquaglyceroporin that serves to transport glycerol as well as water and small-uncharged solutes mainly expressed in the fat. Few information are yet available on the expression of AQP7 in brain, but it was found a strong

immunoreactivity of AQP7 in the choroid plexus in the ventricles, ependymal, pia and same blood vessels during perinatal mouse development. Such as AQP1, AQP7 has a crucial role in the CSF production and in early stage of brain development. In our differentiation models, transcript and protein levels of AQP7 were increased during the glial and neuronal differentiation in AT-MSCs pre-treated with FBS. Since no functional information is yet available, we can hypothesize that its expression in GFAP-positive glial cells and NeuN-positive neuronal cells could be linked to the cell energy metabolism [45]. In particular AQP7 may take part in the lactate shuttle in astrocytes [46] and it could participate in the regulation of the whole body energy balance, such as AQP9 [43].

AQP4 is the predominant form of AQP enriched in the CNS [47] and a key molecule for maintaining water and ion homeostasis associated with neuronal activity in the CNS. It is constitutively expressed in the astroglial endfeet at the perivascular and the subpial membranes where it regulates brain water homeostasis by acting as a key constituent of the blood–brain barrier (BBB) and the blood–CSF barrier [48]. It seems that in astrocytes AQP4 provides the principal route for water transport [49] and for regulation of ionic homeostasis, particularly in removing the excess of extracellular potassium, which occurs after neural excitation [50]. AQP4 could be a positive signal for proliferation, to ensure that proper number of new neural stem cells and their progeny are generated. In our study, AQP4 appears from the earliest stages of pre-induction with both the neural media reaching the highest level of expression in O4 positive glial cells pre-treated with B-27 and N1 in parallel with the expression of AQP8. However, the precise mechanisms of AQP4 in regulating the proliferation and neuronal or glial fate choice of neural stem cells remain to be determined. About the functional role of AQP8 relatively little is known. Recently it was hypothesized that AQP8 may to play a role within the cell such as being implicated in the osmotic homoeostasis of the cytoplasm and in particular in mitochondrial volume regulation [51, 52]. We have confirmed the AQP8 expression in oligodendrocytes [53] where it may play a role in concert with AQP4. In our experimental conditions, no type of cells expressed AQP9 because probably it is present only in mature neurons or pathological condition.

Conclusions

Our results demonstrated that AT-MSCs differentiate into neurons, astrocytes, and oligodendrocytes when treated with appropriate serum and/or serum-free medium and that AQPs are key molecules that take part in all differentiation steps. It should be noted that in spite of the foregoing patient success, the use of stem cells for clinical applications is in its infancy. Researchers and physicians still have much to learn about how more effectively utilizing pluripotent stem cells in their practice for the benefit of patients. Such knowledge includes not only using the most appropriate source for harvesting real stem cells but in improving the means of attracting those stem cells to where they are needed and facilitating their differentiation. New objective data are required to validate stem cells in the present and advance stem cell science into the future. Studies with human stem cells are essential to make progress in the development of treatments for human disease, and this research should continue.

This study provides fundamental insight into the biology of the mesenchymal stem cells and describes the expression of different AQPs in physiological condition during their neural differentiation, suggesting that they are potential neural markers and probably therapeutic targets for neurological metabolic disorders.

References

[1] Hill AE, Schachar-Hill B, Schachar-Hill Y (2004) What are Aquaporins for? J Membrane Biol 197:1-32. doi: 10.1007/s00232-003-0639-6

[2] Zeuthen T, Macaulay N (2002) Passive water transport in biological pores. Int Rev Cytol 215:203-230. PMID: 11952229

[3] Preston GM, Agre P (1991) Isolation of the cDNA for erythrocyte integral membrane protein of 28 kilodaltons: member of an ancient channel family. Proc Natl Acad Sci USA 88:11110–11114. PMC53083

[4] Ishibashi K (2006) Aquaporin superfamily with unusual npa boxes: S-aquaporins (superfamily, sip-like and subcellular-aquaporins). Cell Mol Biol 52:20–27. doi: 10.1016/j.bbamem.2006.02.024

[5] King LS, Konzo D, Agre P (2004) From structure to disease: the evolving tale of Aquaporin biology. Nat Rev Cell Biol 5:687-698. doi: 10.1038/nrm1469

[6] Papadopoulos MC, Saadoun S, Verkman AS (2008) Aquaporins and cell migration. Pflugers Arch 456:693–700. doi: 10.1007/s00424-007-0357-5

[7] Hoque MO, Soria JC, Woo J, et al (2006) Aquaporin 1 is overexpressed in lung cancer and stimulates NIH-3T3 cell proliferation and anchorage-independent growth. Am J Pathol 168:1345–1353. doi: 10.2353/ajpath.2006.050596

[8] Jablonski E, Webb A, Hughes FM (2004) Water movement during apoptosis: a role for aquaporins in the apoptotic volume decrease (AVD). Adv Exp Med Biol 559:179–188. PMID: 18727239

[9] Krane CM, Melvin JE, Nguyen HV, Richardson L, Towne JE, Doetschman T, Menon AG (2001) Salivary acinar cells from aquaporin 5-deficient mice have decreased membrane water permeability and altered cell volume regulation. J Biol Chem 276:23413–23420. doi: 10.1074/jbc.M008760200

[10] Borsani E (2010) Aquaporins in sensory and pain transmission. Curr Neuropharmacol 8:122–127. doi: 10.2174/157015910791233187

[11] Lee WK, Thévenod F (2006) A role for mitochondrial aquaporins in cellular life-and-death decisions? Am J Physiol Cell Physiol 291:C195–202. doi: 10.1152/ajpcell.00641.2005

[12] Cho SJ, Sattar AK, Jeong EH, Satchi M, Cho JA, Dash S, Mayes MS, Stromer MH, Jena BP (2002) Aquaporin 1 regulates GTP-induced rapid gating of water in

secretory vesicles. Proc Natl Acad Sci USA 99:4720–4724. doi: 10.1073/pnas.072083499

[13] Zhu N, Feng X, He C, Gao H, Yang L, Ma Q, Guo L, Qiao Y, Yang H, Ma T (2011) Defective macrophage function in aquaporin-3 deficiency. FASEB J 25:4233–4239. doi: 10.1096/fj.11-182808

[14] Badaut J, Lasbennes F, Magistretti PJ, Regli L (2002) Aquaporins in brain: distribution, physiology, and pathophysiology. J Cereb Blood Flow Metab 22:367–378. doi: 10.1097/00004647-200204000-00001

[15] Tait MJ, Saadoum S, Bell BA, Popadopoulos M (2008) Water movements in the brain: the role of aquaporins. Trends in neurosciences 31:37-43. doi: 10.1016/j.tins.2007.11.003

[16] Oshio K , Watanabe H, Song Y, Verkman AS, Manley GT (2005) reduced cerebrospinal fluid production and intracranical pressure in mice lacking choroid plexus water channel aquaporin-1. FASEB J 19:76-78. doi: 10.1096/fj.04-1711fje

[17] La Porta CA, P Gena, A Gritti, U Fascio, M Svelto, Calamita G (2006). Adult murine CNS stem cells express aquaporin channels. Biol Cell 98:89–94. doi: 10.1042/BC20040153

[18] Avril-Delplanque A, Casal I, Castillon N, Hinnrasky J, Puchelle E, Peault B (2005) Aquaporin-3 expression in human fetal airway epithelial progenitor cells. Stem Cells 23:992–1001. doi: 10.1634/stemcells.2004-0197

[19] Cavazzin C, Ferrari D, Facchetti F, Russignan A, Vescovi AL, La Porta CA, Gritti A (2006) Unique expression and localization of aquaporin-4 and aquaporin-9 in murine and human neural stem cells and in their glial progeny. Glia 53:167–181. doi: 10.1002/glia.20256

[20] Kong H, Fan Y, Xie J, Ding J, Sha L, Shi X, Sun X, Hu G (2008) AQP4 knockout impairs proliferation, migration and neuronal differentiation of adult neural stem cells. J Cell Sci 211:4029–4036. doi: 10.1242/jcs.035758

[21] Yi F, Khan M, Gao H, Hao F, Sun M, Zhong L, Lu C, Feng X, Ma T (2012) Increased differentiation capacity of bone marrow-derived mesenchymal stem cells in aquaporin-5 deficiency. Stem Cells Dev 21:2495–2507. doi: 10.1089/scd.2011.0597

[22] Zelenina M, Zelenin S, Aperia A (2005) A Water channels (aquaporins) and their role for postnatal adaptation. Pediatr Res 57:47R-53R. doi: 10.1203/01.PDR.0000159572.79074.0B

[23] Ashjian PH, Elbarbary AS, Edmonds B, De Ugarte D, Zhu M, Zuk PA, Lorenz HP, Benhaim P, Hedrick MH (2003) In vitro differentiation of human processed lipoaspirate cells into early neural progenitors. Plast Reconstr Surg 111:1922–1931. doi: 10.1097/01.PRS.0000055043.62589.05

[24] Winter A, Breit S, Parsch D, Benz K, Steck E, Hauner H, Weber RM, Ewerbeck V, Richter W (2003) Cartilage-like gene expression in differentiated human stem cell spheroids: a comparison of bone marrow-derived and adipose tissue-derived stromal cells. Arthritis Rheum 48:418–429. doi: 10.1002/art.10767

[25] Guilak F, Estes BT, Diekman BO, Moutos FT, Gimble JM (2010) Multipotent adult stem cells from adipose tissue for musculoskeletal tissue engineering. Clin Orthop Relat Res 468:2530–40. doi: 10.1007/s11999-010-1410-9

[26] Musumeci G, Lo Furno D, Loreto C, Giuffrida R, Caggia S, Leonardi R, Cardile V (2011) Mesenchymal stem cells from adipose tissue which have been differentiated into chondrocytes in three-dimensional culture express lubricin. Exp Biol Med 236:1333–1341. doi: 10.1258/ebm.2011.011183

[27] Musumeci G Mobasheri A, Trovato FM, Szychlinska MA, Graziano AC, Lo Furno D, Avola R, Mangano S, Giuffrida R, Cardile V (2014) Biosynthesis of collagen I, II, RUNX2 and lubricin at different timepoints of chondrogenic differentiation in a 3D in vitro model of human mesenchymal stem cells derived from adipose tissue. Acta Histochem. 116:1407-1417. doi: 10.1016/j.acthis.2014.09.008

[28] Lo Furno D, Pellitteri R, Graziano ACE, Giuffrida R, Vancheri C, Gili E, Cardile V (2013) Differentiation of human adipose stem cells into neural phenotype by neuroblastoma- or olfactory ensheathing cells-conditioned medium. J Cell Physiol 228: 2109–2118. doi: 10.1002/jcp.24386

[29] Zuk PA, Zhu M, Ashjian P, De Ugarte DA, Huang J I, Mizuno H, Alfonso ZC, Fraser J K, Benhaim P, Hedrick MH (2002) Human adipose tissue is a source of multipotent stem cells. Mol Biol Cell 13: 4279–4295. doi: 10.1091/mbc.E02-02-0105

[30] Lendahl U, Zimmerman LB, McKay RD (1990) CNS stem cells express a new class of intermediate filament protein. Cell 60:585–595. PMID: 1689217

[31] Gilyarov AV (2008) Nestin in central nervous system cells. Neurosci Behav Physiol 38:165–169. doi: 10.1007/s11055-008-0025-z

[32] Rex M, Orme A, Uwanogho D, Tointon K, Wigmore PM, Sharpe PT, Scotting PJ (1997) Dynamic expression of chicken Sox2 and Sox3 genes in ectoderm induced to form neural tissue. Dev Dyn 209: 323-332. doi: 10.1002/(SICI)1097-0177(199707)209:3<323::AID-AJA7>3.0.CO;2-K

[33] Graham V, Khudyakov J, Ellis P, Pevny L (2003) SOX2 Functions to Maintain Neural Progenitor. Identity 39:749-765. PMID: 12948443

[34] Bylund M, Andersson E, Novitch B G, Muhr J (2003). Vertebrate neurogenesis is counteracted by Sox1–3 activity. Nat Neurosci 6:1162–1168. doi: 10.1038/nn1131

[35] Hutton SR, Pevny LH (2011) SOX2 expression levels distinguish between neural progenitor populations of the developing dorsal telencephalon. Dev Biol 352:40-47. doi: 10.1016/j.ydbio.2011.01.015

[36] Wiese C, Rolletschek A, Kania G, Blyszczuk P, Tarasov KV, Tarasova Y, Wersto RP, Boheler KR, Wobus AM (2004) Nestin expression--a property of multi-lineage progenitor cells? Cell Mol Life Sci 61: 2510–2522. doi: 10.1007/s00018-004-4144-6

[37] Copp AJ, Greene NDE (2010) Genetics and development of neural tube defects. J Pathol 220: 217–230. doi: 10.1002/path.2643

[38] Ferroni L, Gardin C, Tocco I, Epis R, Casadei A, Vindigni V, Mucci G, Zavan B (2013) Potential for neural differentiation of mesenchymal stem cells. Adv Biochem Eng Biotechnol.129:89-115. doi: 10.1007/10_2012_152

[39] Li YC, Lin YC, Young TH (2012) Combination of media, biomaterials and extracellular matrix proteins to enhance the differentiation of neural stem/precursor cells into neurons. Acta Biomater 8:3035-3048. doi: 10.1016/j.actbio.2012.04.036

[40] Xu L, Ryu J, Hiel H, Menon A, Aggarwal A, Rha E, Mahairaki V, Cummings BJ, Koliatsosn V (2015) Transplantation of human oligodendrocyte progenitor cells in an animal model of diffuse traumatic axonal injury: survival and differentiation. Stem Cell Res Ther 6:93. doi: 10.1186/s13287-015-0087-0

[41] Wen H, Nagelhus EA, Amiry-Moghaddam M, Agre P, Ottersen OP, Nielsen S (1999) Ontogeny of water transport in rat brain: postnatal expression of the aquaporin-4 water channel. Eur J Neurosci 11:935-945. PMID: 10103087

[42] Nielsen S, Smith BL, Christensen EI, Agre P (1993) Distribution of the aquaporin CHIP in secretory and resorptive epithelia and capillary endothelia. Proc Natl Acad Sci USA 90:7275–7279. PMID: 8346245

[43] Benga O, Huber VJ (2012) Brain water channel proteins in health and disease. Mol Aspects Med 33:562-578. 10.1016/j.mam.2012.03.008

[44] Mobasheri A, Marples D (2004) Expression of the AQP-1 water channel in normal human tissues: a semi-quantitative study using tissue mircroarray technology. Am J Physiol 286: C529–537. doi: 10.1152/ajpcell.00408.2003

[45] Badaut J, Regli L (2004) Distribution and possible roles of AQP9 in brain. Neurosci 129: 971–981. doi: 10.1016/j.neuroscience.2004.06.035

[46] Magistretti PJ, Pellerin L, Rothman DL, Shulman RG (1999) Energy on demand. Science 283:496-497. PMID: 9988650

[47] Jung JS, Bhat RV, Preston GM, Guggino WB, Baraban JM, Agre P (1997) Molecular characterization of an aquaporin cDNA from brain: candidate osmoreceptor and regulator of water balance. Proc Natl Acad Sci USA 91:13052–13056. PMID: 7528931

[48] Nielsen S, Nagelhus EA, Amiry-Moghaddam M, Bourque C, Agre P, Ottersen OP (1997) Specialized membrane domains for water transport in glial cells: highresolution immunogold cytochemistry of aquaporin-4 in rat brain. J Neurosci 17:171–180. PMID: 8987746

[49] Solenov E, Watanabe H, Manley GT, Verkman AS (2003) Seven-fold reduced osmotic water permeability in primary astrocyte cultures from aquaporin-4 deficient mice measured by a calcein quenching method. Am J Physiol Cell Physiol 286:426-432. doi: 10.1152/ajpcell.00298.2003

[50] Horio Y (2001) Potassium channels of glial cells: distribution and function. Jpn J Pharmacol 87:1-6. PMID: 11676192

[51] Ferri D, Mazzone A, Liquori GE, Cassano G, Svelto M, Calamita G (2003) Ontogeny, distribution, and possible functional implications of an unusual aquaporin, AQP8, in mouse liver. Hepatology 38:947-957. doi: 10.1053/jhep.2003.50397

[52] Calamita G, Ferri D, Gena P, Liquori GE, Cavalier A, Thomas D, Svelto M (2005) The inner mitochondrial membrane has aquaporin-8 water channels and is highly permeable to water. J Biol Chem 280:17149-17153. doi: 10.1074/jbc.C400595200

[53] Yamamoto N, Yoneda K, Asai K, Sobue K, Tada T, Fujita Y, Katsuya H, Fujita M, Aihara N, Mase M, Yamada K, Miura Y, Kato T (2001) Alterations in the

expression of the AQP family in cultured rat astrocytes during hypoxia and reoxygenation. Brain Res Mol Brain Res 90:26-38. PMID: 11376853

Conflict of interest

The authors declare no conflict of interest.

Acknowledgments

The authors wish to tank Prof. G. Musumeci, University of Catania, Department of Biomedical and Biotechnological Sciences, Section of Anatomy and Histology, and Prof. E. Barbagallo, University of Catania, Department of Drug Sciences, Section of Biochemistry, for having kindly provided AQP1 antibody and lipoaspirates, respectively.

Figures Legend

Figure 2(a) Morphology of AT-MSCs exposed to neural induction medium containing B-27 and N1 growth supplements (**medium A**) for 14 days. Magnification of 10x. (**b)** Immunofluorescence of neurospheres derived from AT-MSCs treated with medium containing B-27 and N1 supplements for the determination of AQP1 (upper panel, red), AQP4 (lower panel, red), SOX-2 (upper and lower panel, green). The nuclei were counterstained with 4',6-diamidino-2-phenylindole (DAPI) (blue). Digital images were acquired using Leica microscope connected to a digital camera. Magnification 40x. (**c)** Western blot analysis of nestin, AQP1, AQP4 and SOX-2 protein expressions in neurospheres derived from AT-MSCs treated with medium containing B-27 and N1 supplements. Data show the relative expression (mean ± S.E.M.) of nestin, AQP1, AQP4 and SOX-2 calculated as arbitrary densitometric units (A.D.U.) collected from three independent experiments. (**d)** Evaluation of of nestin, AQP1, AQP4 and SOX-2 in neurospheres derived from AT-MSCs treated with medium containing B-27 and N1 supplements by RT-PCR. Data show the relative expression (mean ± S.E.M.) of nestin and AQP1 calculated as arbitrary densitometric units (A.D.U.) collected from three independent experiments normalized to GAPDH. **Table** inserted in Figure 2 summarizes the data: neurospheres expressed AQP1 and 4, while AQP7, 8, and 9 were not present; N.D., not determined.

Figure 3(a) Morphology of AT-MSCs exposed to neural induction medium containing serum for 14 days. Magnification of 10x. (**b)** Immunofluorescence of AT-MSCs exposed to neural induction medium containing serum for 14 days for the determination of AQP1 (upper panel, green), AQP7 (middle panel, green), AQP4 (lower panel, green) and nestin (upper, middle and lower panels, red).. The nuclei were counterstained with 4',6-diamidino-2-phenylindole (DAPI) (blue). Digital images were acquired using Leica microscope connected to a digital camera. Magnification 40x. (**c)** Western blot analysis of nestin, AQP1, AQP7, AQP4 and SOX-2 protein expressions in AT-MSCs exposed for 14 days to neural induction medium containing serum. Data show the relative expression (mean ± SEM) of nestin, AQP1, AQP7, AQP4 and SOX-2 calculated as arbitrary densitometric units

(A.D.U.) collected from three independent experiments. (**d)** RT- PCR was used to assess the regulation and confirm the expressions of nestin, AQP7, AQP1, AQP4 and SOX-2 in neural induction medium with serum. Gene expression was normalized to GAPDH and data reported as arbitrary densitometric units (A.D.U.). **Table** inserted in Figure 3 summarizes the data: AT-MSCs exposed to neural induction medium containing serum for 14 days expressed AQP1, 4 and 7, while AQP 8 and 9 were not present; N.D., not determined.

Figure 4(**a**) Morphology of glial cells derived from AT-MSCs exposed for 14 days to neural induction medium enriched of B-27 and N1 growth supplements. Magnification of 10x. (**b)** Immunofluorescence of glial cells derived from AT-MSCs exposed for 14 days to neural induction medium enriched of B-27 and N1 growth supplements for the determination of AQP1 (upper panel, green), AQP8 (middle panel, green) AQP4 (lower panel, green), O4 (upper, middle and lower panel, red). The nuclei were counterstained with 4',6-diamidino-2-phenylindole (DAPI) (blue). Digital images were acquired using Leica microscope connected to a digital camera. Magnification 40x. (**c**) Western blot analysis of nestin, GFAP, AQP1, AQP8, and AQP4 proteins in glial cells derived from AT-MSCs exposed for 14 days to neural induction medium enriched of B-27 and N1 growth supplements. Data calculated as arbitrary densitometric units (A.D.U.) and collected from three independent experiments show the relative expression (mean ± SEM) of nestin, AQP1, AQP8, and AQP4 and the absence of GFAP. (**d**) RT-PCR of O4, nestin, AQP1, AQP4, and AQP8 in glial cells derived from AT-MSCs exposed to neural induction with medium enriched of B-27 and N1 growth supplements. Gene expression was normalized to GAPDH and data reported as arbitrary densitometric units (A.D.U.). **Table** inserted in Figure 4 summarizes the data: glial cells derived from AT-MSCs exposed for 14 days to neural induction medium enriched of B-27 and N1 growth supplements expressed AQP1, 4 and 8, while AQP7 and 9 were not present; N.D., not determined.

Figure 5(**a**) Morphology of neuronal cells derived from AT-MSCs exposed to neural induction medium enriched of B-27 and N1 growth supplements for 14 days, Magnification of 10x. (**b)** Immunofluorescence of neuronal cells derived from AT-MSCs exposed to neural induction medium enriched of B-27 and N1 growth

supplements for 14 days for the expression of AQP1 (red), and β-Tubulin III (green). The nuclei were counterstained with 4',6-diamidino-2-phenylindole (DAPI) (blue). Digital images were acquired using Leica microscope connected to a digital camera. Magnification 40x. (**c**) Western blot analysis of neuronal cells derived from AT-MSCs exposed to neural induction with medium enriched of B-27 and N1 growth supplements for the determination of nestin, AQP1, β-Tubulin III, NeuN and PGP9.5 proteins. Data show the relative expression (mean ± SEM) of nestin, AQP1, β-Tubulin III, PGP9.5, calculated as arbitrary densitometric units (A.D.U.) collected from three independent experiments, and the absence of NeuN. (**d**) RT-PCR of neuronal cells derived from AT-MSCs exposed to neural induction medium enriched of B-27 and N1 growth supplements used to assess the expressions of β-Tubulin III, nestin, and AQP1. Gene expression was normalized to GAPDH and data reported as arbitrary densitometric units (A.D.U.). **Table** inserted in Figure 5 summarizes the data: neuronal cells derived from AT-MSCs exposed to neural induction medium enriched of B-27 and N1 growth supplements expressed AQP1 only.

Figure 6(**a**) Morphology of glial cells derived from AT-MSCs exposed to neural induction medium containing serum for 14 days, Magnification of 10x. (**b**) Immunofluorescence of glial cells derived from AT-MSCs exposed to neural induction medium containing serum for the expression of AQP1 (upper panel, green), AQP7 (middle panel, green), AQP4 (lower panel, green), and GFAP (upper, middle and lower panel, red). The nuclei were counterstained with 4',6-diamidino-2-phenylindole (DAPI) (blue). Digital images were acquired using Leica microscope connected to a digital camera. Magnification 40x. (**c**) Western blot analysis for the determination of nestin, GFAP, AQP1, AQP7, and AQP4 proteins in glial cells derived from AT-MSCs exposed to neural induction medium containing. Data show the relative expression (mean ± SEM) of nestin, GFAP, AQP1, AQP7, and AQP4 calculated as arbitrary densitometric units (A.D.U.) collected from three independent experiments. (**d**) RT-PCR of nestin, GFAP, AQP7, AQP1and AQP4 in glial cells derived from AT-MSCs exposed to neural induction medium with serum. Gene expression was normalized to GAPDH and data reported as arbitrary densitometric units (A.D.U.). **Table** inserted in Figure 6 summarizes the data: glial cells derived from AT-MSCs exposed to neural induction medium containing serum expressed AQP1, 4 and 7, while AQP8 and 9 were not present; N.D., not determined.

Figure 7(**a**) Morphology of neuronal cells derived from AT-MSCs exposed for 14 days to neural induction medium containing serum. Magnification of 10x. (**b)** Immunofluorescence of neuronal cells derived from AT-MSCs exposed to neural induction medium containing serum for the determination of AQP1 (upper panel, green), AQP7 (lower panel, green), and PGP9.5 (upper and lower panel, red). The nuclei were counterstained with 4',6-diamidino-2-phenylindole (DAPI) (blue). Digital images were acquired using Leica microscope connected to a digital camera. Magnification 40x. (**c)** Nestin, β-Tubulin III, NeuN, AQP1, AQP7 and PGP9.5 protein expressions in neuronal cells derived from AT-MSCs exposed to neural induction medium containing serum determined by Western blot analysis. Data show the relative expression (mean ± SEM) calculated as arbitrary densitometric units (A.D.U.) collected from three independent experiments. (**d**) RT-PCR of β-Tubulin III, nestin, SOX-2, AQP1, and AQP7 in neuronal cells derived from AT-MSCs exposed to neural induction medium containing serum. Gene expression was normalized to GAPDH and data reported as arbitrary densitometric units (A.D.U.). **Table** inserted in Figure 7 summarizes the data: neuronal cells derived from AT-MSCs exposed for 14 days to neural induction medium containing serum expressed AQP1 and 7, while AQP4, 8 and 9 were not present; N.D.; not determined.

Table 1 MSCs markers identified by flow cytometric analysis

Cell surface marker	% Positive cells
CD44	**95.4 ± 0.4**
CD90	**90.68 ± 0.5**
CD105	**90.4 ± 1.4**
CD14	**8.3 ± 6.2**
CD34	**10.5 ± 6.3**
CD45	**9.7 ± 6.2**

Table 2 RT-PCR primers

Target gene	Primers sequences	Product length (bp)
AQP1	**Forward5'-CTCTCTGTAGCCCTTGGACACCTC Reverse 5'- GGCATCCAGGTCATACTCCTCCAC**	**252**
AQP4	**Forward 5'-GCTGTGATTCCAAACGGACTGATG Reverse 5'- CTGACTCCTGTTGTCCTCCACCTC**	**329**
AQP7	**Forward 5'-AAATGGTCTCCTGGTCCGTGATAG Reverse 5'- ACA CCA AGG TAG CTC CCAATGTT**	**178**
AQP8	**Forward 5'-TCATTGGAGATGGGAAGACC Reverse 5'-TGAGAAGCAAGGAAGTGGC**	**419**
AQP9	**Forward 5'- GATACTCCTCATAATCGTCTTTGC Reverse 5'- AAGACTGAGTCAGGCTCTGGATGG**	**321**
Nestin	**Forward5'-TCAGAGGGAAGGAGATAGAGAGTC Reverse 5'-AGCCAGAAACCATATGTCAAGAGA**	**174**
GFAP	**Forward 5'- AGATCCGCACGCAGTATGAG Reverse 5'-AGATCCGCACGCAGTATGAG**	**178**
O4	**Forward 5'- CATCCTCCCTGTCTGCATCTGT Reverse 5'-TTCCCTGGTTTCTGCCGATA**	**103**
SOX-2	**Forward 5'-GCCTGGGCGCCGAGTGGA Reverse 5'-GGGCGAGCCGTTCATGTAGGTCTG**	**443**
β–Tubulin III	**Forward 5'-CTCAGGGGCCTTTGGACATC Reverse 5'- CCACAAGCACCACATACTCCTG**	**161**
β–Actin	**Forward 5'-CTGCCGCATCCTCTTCCTC Reverse 5'-CTCCTGCTTGCTGATCCACAT**	**398**
GAPDH	**Forward 5'-TCAACAGCGACACCCAC Reverse 5'-GGGTCTCTCTCTTCCTCTTGTG**	**203**

Figure 1

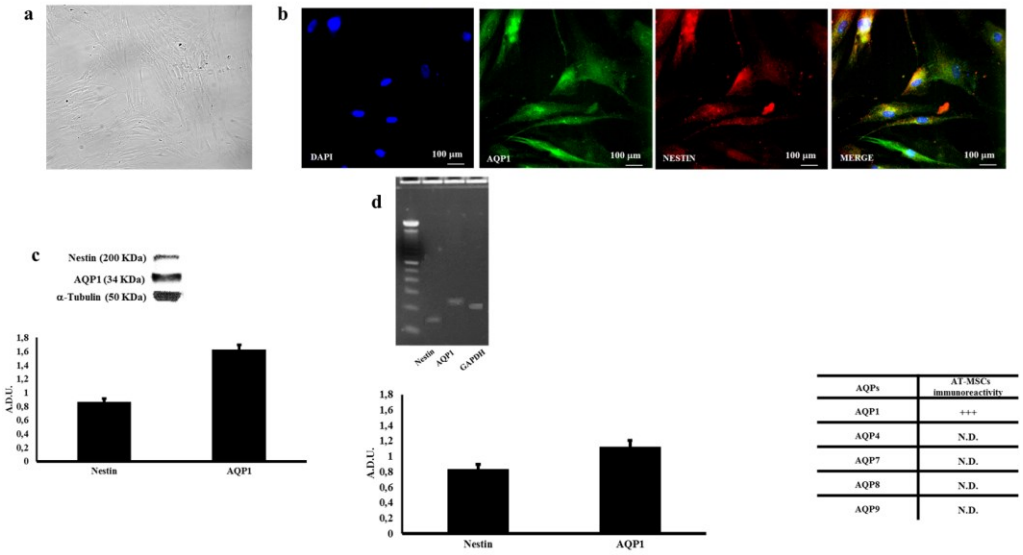

AQPs	AT-MSCs immunoreactivity
AQP1	+++
AQP4	N.D.
AQP7	N.D.
AQP8	N.D.
AQP9	N.D.

Figure 2

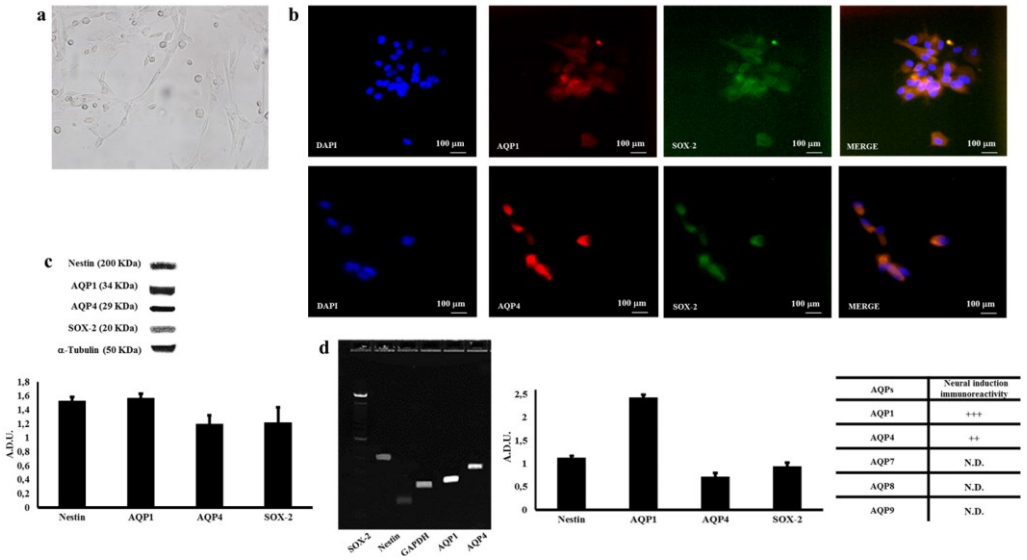

AQPs	Neural induction immunoreactivity
AQP1	+++
AQP4	++
AQP7	N.D.
AQP8	N.D.
AQP9	N.D.

Figure 3

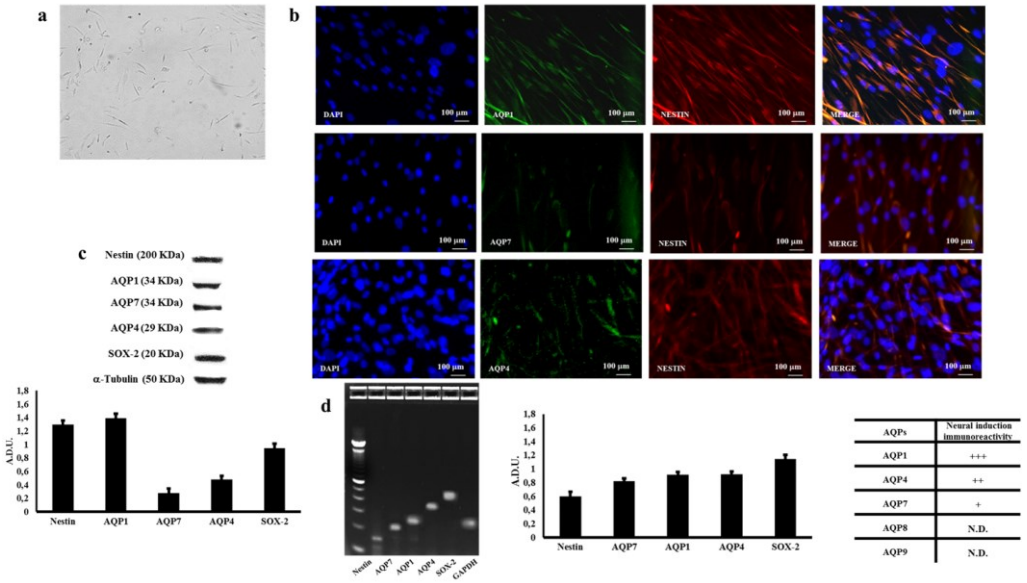

AQPs	Neural induction immunoreactivity
AQP1	+++
AQP4	++
AQP7	+
AQP8	N.D.
AQP9	N.D.

Figure 4

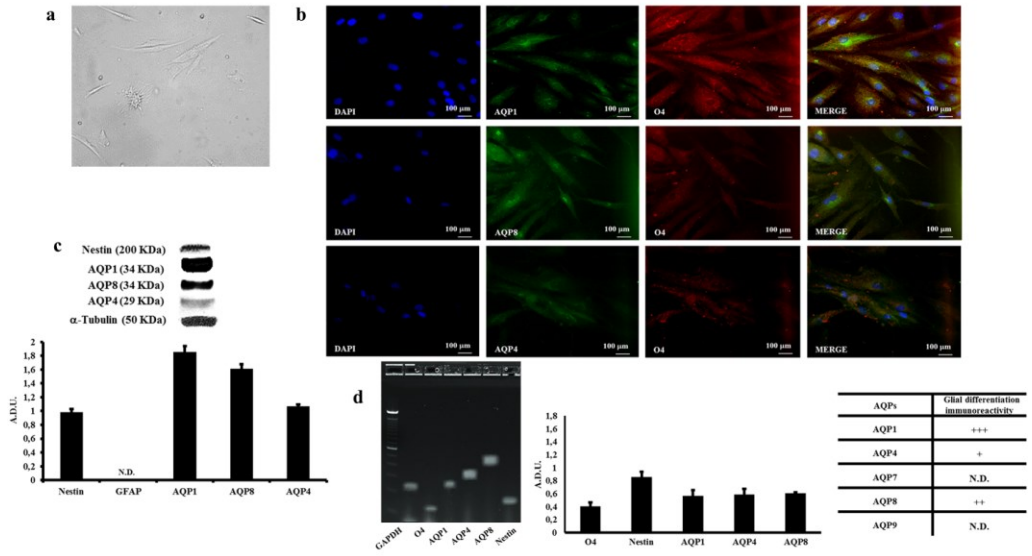

AQPs	Glial differentiation immunoreactivity
AQP1	+++
AQP4	+
AQP7	N.D.
AQP8	++
AQP9	N.D.

Figure 5

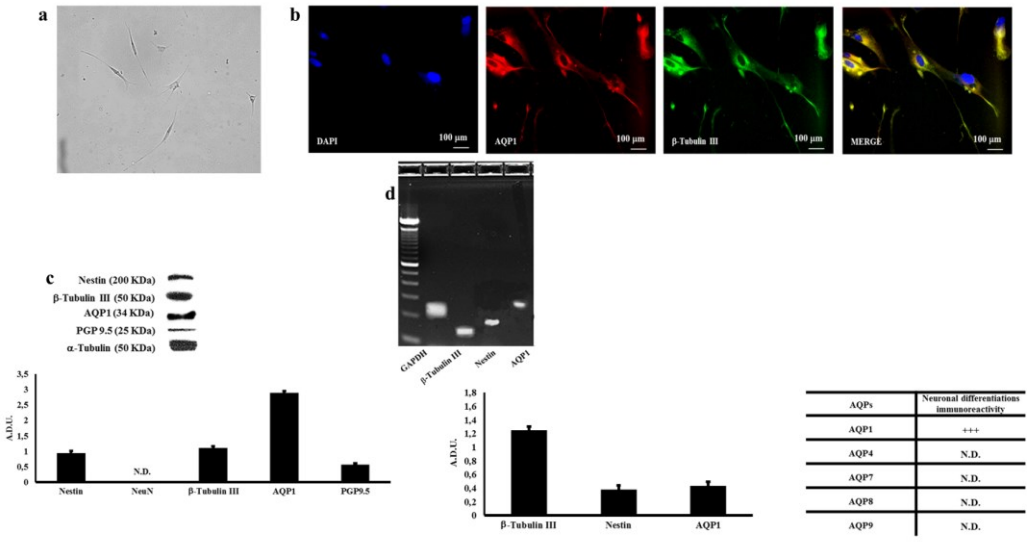

AQPs	Neuronal differentiations immunoreactivity
AQP1	+++
AQP4	N.D.
AQP7	N.D.
AQP8	N.D.
AQP9	N.D.

Figure 6

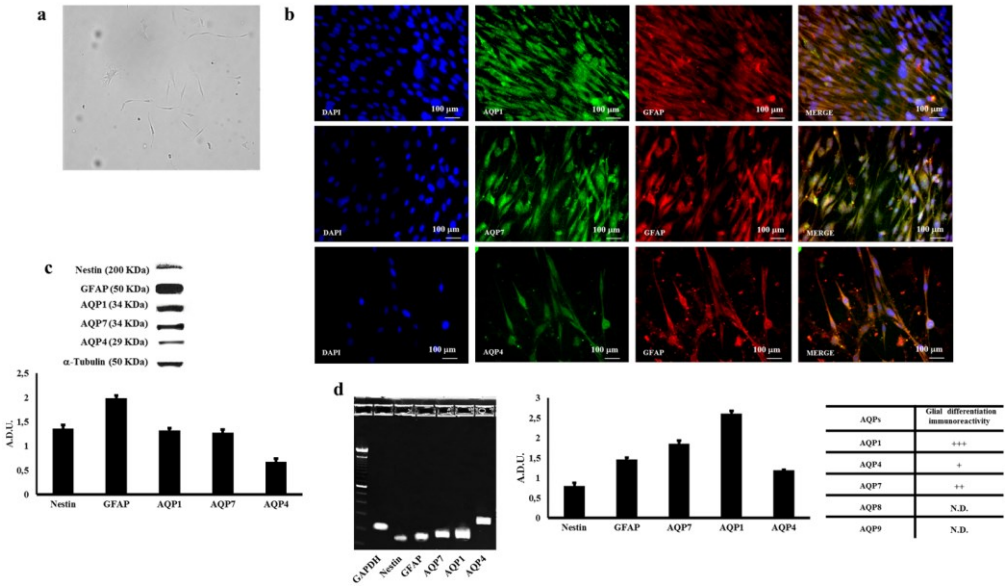
a
b
DAPI
AQP1
GFAP
MERGE
AQP7
AQP4
100 µm
c
Nestin (200 KDa)
GFAP (50 KDa)
AQP1 (34 KDa)
AQP7 (34 KDa)
AQP4 (29 KDa)
α-Tubulin (50 KDa)
A.D.U.
Nestin
GFAP
AQP1
AQP7
AQP4
d
GAPDH
Nestin
GFAP
AQP7
AQP1
AQP4
AQPs
Glial differentiation immunoreactivity
AQP1
+++
AQP4
+
AQP7
++
AQP8
N.D.
AQP9
N.D.

Figure 7

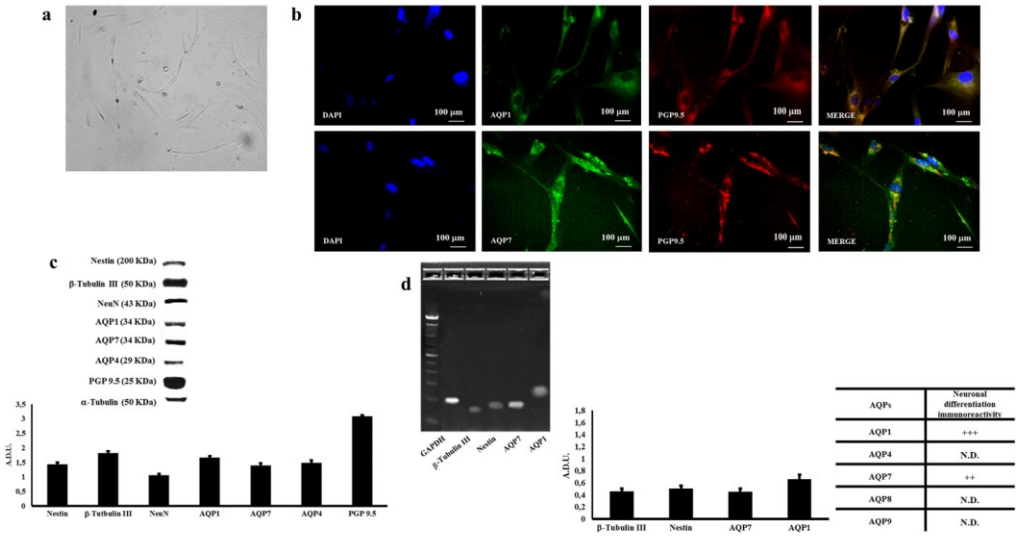

AQPs	Neuronal differentiation immunoreactivity
AQP1	+++
AQP4	N.D.
AQP7	++
AQP8	N.D.
AQP9	N.D.

CHARTER III

Submitted on Disease Models and Mechanisms

Original article

NEW INSIGHTS ON PARKINSON'S DISEASE FROM DIFFERENTIATION OF SH-SY5Y INTO DOPAMINERGIC NEURONS: THE INVOLVEMENT OF AQUAPORIN4 AND 9

Rosanna Avola[1], Adriana Carol Eleonora Graziano[1] Giovanna Pannuzzo[1], Ferdaous Albouchi[2] Venera Cardile[1]*

Running title: **AQP4 and 9 in a Parkinson *in vitro* model**

[1]Department of Biomedical and Biotechnological Science – Section of Physiology, University of Catania, Via Santa Sofia, 97 – 95125 Catania, Italy.
[2]Laboratoire Materiaux Molecules et Applications, Institut Preparatoire au Etude Scientifique et Technique, Faculty of Sciences of Bizerte, University of Carthage, La Marsa 2070, Tunis, Tunisia.

*Corresponding author: V. Cardile; PhD; phone: +390954781318; email: cardile@unict.it

Key words: aquaporin; differentiation; dopaminergic neuron; neuroblastoma; neurodegeneration; Parkinson's disease

Summary statement

We used an *in vitro* cellular model as controlled system that allowed examining some pathophysiological mechanisms and demonstrating the involvement of specific aquaporins in Parkinson's disease.

Abstract

Parkinson's disease is a recurrent neurodegenerative disorder that is associated to a combination of bradykinesia, resting tremor, rigidity, and postural instability. Because of postmortem studies have provided evidences for oxidative damage and alteration of energy and water metabolism, the investigation about key molecules in this area of interest needs to be performed. Aquaporin (AQP) 4 and AQP9 have been found in the brain to maintain homeostatic energy metabolism. To explore the potential role of these AQPs in Parkinson's disease, we used the SH-SY5Y cell line as an *in vitro* cellular model and induced their differentiation into a mature dopaminergic neuron phenotype with retinoic acid (RA) alone or in association with phorbol-12-myristate-13-acetate (MPA). The association RA plus MPA provided the most complete and mature neuron phenotype, as demonstrated by high levels of tyrosine hydroxylase enzyme. After validation of cell differentiation, the neurotoxin 1-methyl-4-phenyl-1, 2, 3, 6-tetrahydropyridine (MPTP) and H_2O_2 were applied to reproduce a Parkinson's-like stress in an oxidative environment. We found that the vulnerability of cells was linked to dynamic changes of AQP4 and AQP9 transcription and expression during treatment steps. In particular, AQP4 and AQP9 appeared to be involved in cell response against MPTP/H_2O_2-induced damage. In conclusion, we suggest a possible application of AQP4 and AQP9 as markers for earlier and later stage of the disease. They may be helpful in diagnosing as well as in the understanding of Parkinson's progression during life without excluding their application for pharmacological approaches.

Introduction

Parkinson's disease (PD) is a neurodegenerative disorder that is caused by the gradual, progressive loss of dopaminergic (DAergic) neurons in the substantia nigra pars compacta (SNpc) that turns into decrease of dopamine (DA) levels in the striatum (caudate and putamen) of the basal ganglia (Lees et al., 2009; Badger et al., 2014). The clinical symptoms of PD are characterized by a combination of bradykinesia, resting tremor, rigidity, and postural instability (Hwang, 2013). Despite the several information about the clinical progression, the pathogenesis of PD and the involved molecular mechanisms are not yet completely understood. To clarify these two aspects and consequently provide the means for therapeutic strategies remain indispensable.

Although the precise mechanisms remain unclear, in the recent years a growing interest has been addressed to neuroinflammation and oxidative stress as key aspects of pathogenesis of disease-associated nigrostriatal degeneration in PD animal models as well in clinical (Cebrian et al., 2015; Wang et al., 2015). Moreover, postmortem studies have provided evidences for both oxidative damage and decrease in the activity of complex I of the mitochondrial electron transport chain in the SNpc (Dunnett and Bjorklund, 1999). In PD, inflammation is primarily a beneficial phenomenon because it is physiologically established to eliminate the irreversibly damaged neurons, but - at later stages - its over-activation can lead to further damage, exacerbate disease responses and prove deadly.

In the central nervous system (CNS), the neuroinflammation is perpetrated not only through activation of initial responders, as macrophages, microglia, astrocytes and endothelial cells, but also it may act through paracrine pathways to accelerate neuronal injury in highly divergent disease (Mosley et al., 2006). Proinflammatory factors, including tumor necrosis factor-α (TNF-α), interleukin-1β (IL-1β), and reactive oxygen species (ROS) have been reported (Gonzalez et al., 2014; Moehle and West, 2015).

Although the cause and pathogenesis of selective loss of DAergic neurons and the accumulation of α-synuclein in PD remain elusive, another emerging aspect points to a convergence in the alteration of energy and water metabolism. In this field, it is well known that abnormalities in water balance and in aquaporins (AQPs) expression play an important role in the pathophysiology of a variety of disorders and, in particular, in neurological diseases (Foglio and Rodella, 2010).

AQPs are a family of water channel proteins that has been identified in mammalian species (Verkman, 2005) to provide a major pathway for osmotically driven water transport through cell membranes. Up to now at least 13 AQPs isoforms (AQP0-AQP12) have been identified. A number of these proteins have been found in the brain, including AQP4 and AQP9 (Badaut et al., 2000; Badaut, 2009; Yang et al., 2009). Specifically, AQP4 is the most abundant water channel found in all brain structures with a highly documented expression on astrocyte plasma membranes domains that face capillaries and pia (Nielsen et al., 1997). Expressed in astrocyte end-feet (Badaut, 2009), AQP4 was also found in the basolateral membranes of ependymal cells (Nielsen et al., 1997). Besides maintaining CNS water balance, AQP4 regulates various astrocytes biological functions, including calcium signal transduction, regulation of neurotransmission, while under neuropathological conditions, AQP4 has a role in astrogliosis and in proinflammatory cytokines secretion (Xiao and Hu, 2014). These findings indicate a possible involvement of AQP4 in the onset and progression of PD, but the role of AQP4 in PD is controversial. To date, a down-regulation of AQP4 expression in striatal glial cells *in vitro* was mediated by the neurotransmitter DA (Kuppers et al., 2008), while an increase in AQP4 mRNA following 6-hydroxidopamine (6-OH-DA) lesion has been observed in the SNpc (Vizuete et al., 1999). Moreover, the AQP4 deficiency was reported as key factor for the increasing sensitivity of DAergic neurons to PD neurotoxin (Yi et al., 2008).

Indeed, AQP9 subtype was mainly observed in astrocytes (Amiry-Moghaddam et al., 2005), catecholaminergic neurons (Badaut, 2009), and subsets of midbrain DAergic and hypothalamic neurons (Amiry-Moghaddam et al., 2005). Even if localized in the mitochondria inner membranes, it has been reported functional evidence against a role for AQPs in mitochondria, suggesting that AQP9 acts in brain energy metabolism as channel permeable to various solutes, including glycerol, lactate and monocarboxylates (Tsukaguchi et al., 1999).

Usually, PD studies are limited by the inaccessibility of the neural tissue and hence the difficulty in obtaining a brain biopsy, until the death of the affected individual. A direct investigation method employs *in vitro* models that offer the advantage of a controlled environment that allows a fast and reproducible exploration of a single pathogenetic mechanism. Furthermore, cellular investigations have the intrinsic

advantage to target directly the specific molecular pathways and the genes/proteins at the basis of the progression of PD (Dawson et al., 2010).

Thus, in this work we used SH-SY5Y, a human neuroblastoma cell line, which not only possess many characteristics of DAergic neurons, but also exhibit properties of stem cells. We induced their differentiation into a mature neuronal phenotype with retinoic acid (RA) alone or in association with phorbol 12-myristate 13-acetate (MPA). Upon treatment, the validation of cell differentiation was performed and the vulnerability to DAergic neurotoxin 1-methyl-4-phenyl-1, 2, 3, 6-tetrahydropyridine (MPTP) was evaluated and compared in all cell groups. H_2O_2 was added in the culture medium to strongly mimic the oxidative environment that characterizes PD neurons *in vivo*.

Considering that the electrical activity and the survival of DAergic neurons are strictly correlated to water, glycerol and lactate balance, we hypothesized a primary involvement of AQP4 and AQP9 in the behavior of DAergic neurons in presence of oxidative stress and PD neurotoxin.

Results

Differentiation of SH-SY5Y into dopaminergic neurons

The SH-SY5Y cell line was differentiated in culture medium enriched with RA or RA+MPA. Cellular morphology was visualized under phase-contrast microscopy. Undifferentiated SH-SY5Y (UN) had a propensity to grow in cluster exhibiting a neuroblast–like morphology (Figure 1A), while SH-SY5Y cells differentiated with RA (Figure 1B) or RA+MPA (Figure 1C) progressively underwent obvious morphological changes showing a clear neuronal morphology with processes extending between them. The differentiation was confirmed by cell viability that showed statistically significant differences between undifferentiated (UN), and RA- or RA+MPA-differentiated SH-SY5Y (Figure 1D). At 14 days of differentiation, cells decreased their proliferating activity, suggesting the effective induction toward a neuronal phenotype. To confirm the mature neuronal phenotypes, the gene expression of neuronal markers was analyzed by RT-PCR (Figure 2). We selected β-tubulin III, a cytoskeleton marker associated with neuronal development, MAP-2, a microtubule-associated protein, and tyrosine hydroxylase (TH), a DAergic neuronal marker. Detection of basal level of neuronal-specific β-Tubulin III, MAP-2 and TH in UN SH-SY5Y should be addressed to their own potential to undergo neuronal

differentiation (Figures 2A-C). Although β-Tubulin III (Figure 2A), and MAP-2 (Figure 2B) mRNA reached high level in RA-differentiated cells, the highest significant increase in TH content, confirmed by immunocytochemistry, was observed in RA+MPA-differentiated SH-SY5Y cells (Figure 2C and 3D).

AQP4 and AQP9 associated to induction of dopaminergic neurons

In order to verify a possible appearance and relationship between AQP4 and AQP9 during neuronal differentiation, we examined their mRNA and protein levels (Figure 3). The differentiation conditions altered the levels of AQP4 and AQP9 protein expression. In particular, these AQPs were almost undetectable in UN SH-SY5Y, but showed an increase in RA+MPA differentiated cells (Figure 3C 1-3). Specifically, in presence of RA alone, cells started to produce AQP4 mRNA (Figure 3A), without protein transduction (Figure 3C 1-2). The RA+MPA-differentiated SH-SY5Y showed a relevant increase of AQP4 expression (Fig. 3C 1-2), and a weak not significant level of AQP9 at both mRNA (Figure 3B) and protein levels (Figure 3C 1-3). At 17th day culture, the DAergic differentiation (TH expression) of SH-SY5Y and the presence of AQP4 or AQP9 were confirmed by immunolabeling (Figure 3D).

Reduction of cell viability by MPTP and H_2O_2 treatments

We apply MPTP on undifferentiated and on RA- or RA+MPA-differentiated SH-SY5Y in presence of an oxidative environment by H_2O_2. This system was double functionalized because of the activation of MPTP and the induction of oxidative stress, both in acute (4 hours) and in chronic (24 hours) condition.

Cell viability assay showed that at 4 hours-treatment UN SH-SY5Y had a viability reduction of 40 ± 6%, and were more vulnerable than RA- or RA+MPA-differentiated SH-SY5Y. Specifically, in acute condition, the mitochondrial activity of RA-differentiated SH-SY5Y was reduced up to 20 ± 7%, while the viability of RA+MPA-differentiated cells did not change (Figure 4A). In chronic condition (24 hours) RA- or RA+MPA-differentiated SH-SY5Y did not show any relevant different sensitivity respect to the undifferentiated (Figure 4A).

As regard TH DAergic marker, the treatment with MPTP/H_2O_2 resulted into a disappearance of its mRNA levels at 24 hours, while only RA+MPA-differentiated SH-SY5Y maintained high level of TH mRNA at 4 hours (Figure 4B).

To verify whether the decrease in viability observed in response to MPTP/H_2O_2 was caspase-dependent or not, after treatment of UN and RA- or RA+MPA-differentiated SH-SY5Y with MPTP/H_2O_2 for 4 and 24 hours, the active form of caspase-3 was investigated. According to viability results, chronic MPTP/H_2O_2 stimulation (24 hours) significantly increased the activation of caspase-3 in all cell groups, whereas in acute condition (4 hours) the caspase-3 activation was detected in UN-SH-SY5Y and in RA-differentiated SH-SY5Y (Figures 4C-D). The RA+MPA-differentiated SH-SY5Y did not report significant change of caspase-3 activation with respect to its own basal level, indicating that the MPTP/H_2O_2-induced decrease in viability was caspase-dependent.

AQP4 and AQP9 modulation during MPTP and H_2O_2 treatments

In order to evaluate a possible involvement of AQP4 an AQP9 in regulating the differences of MPTP/H_2O_2-induced viability in UN SH-SY5Y, RA- or RA+MPA-differentiated SH-SY5Y, we screened their transcription and expression levels in acute and in chronic *in vitro* stimulation. UN SH-SY5Y were the more vulnerable cells reacted to MPTP/H_2O_2 treatment by upregulating mRNA and protein level of AQP9 (Fig. 5B and Fig. 5D), while no change was detected for AQP4 transcription and transduction (Fig. 5A and Fig. 5C). Similar trend was reported after stimulation of RA-differentiated SH-SY5Y, suggesting that higher expression of AQP9 should be linked to MPTP/H_2O_2-induced decrease of cell viability. The RA+MPA-differentiated SH-SY5Y, indeed, showed a time-dependent modulation of AQPs. In acute stimulation characterized by less susceptibility to MPTP/H_2O_2 and inactivation of caspase-3, AQP4 transcription and transduction increased (Fig. 5A and Fig. 5C), while AQP9 maintained a basal level without any significant change with respect to its own unstimulated control (Fig. 5B and Fig. 5D). In chronic condition AQP4 levels drastically decreased (Fig.5C) while AQP9 increased (Fig 5D), reaching approximatively comparable value to those ones reported in UN SH-SY5Y and in RA-differentiated SH-SY5Y. This finding seemed to confirm an AQP9 involvement in MPTP/H_2O_2-induced cell death and advised a putative role of AQP4 in cell protection against MPTP/H_2O_2 damage.

Discussion

Interestingly, this study demonstrated that the vulnerability of human SH-SY5Y cell line, an appropriate cell model for studying neurotoxicity or neuroprotection, was linked to dynamic changes of AQP4 and AQP9 transcription and expression during differentiation toward DAergic neurons and in Parkinson-like stress oxidative conditions.

Most of the current knowledge about PD is gathered from post mortem studies that represent only the end-stage of the disease, and therefore provide a restricted understanding of the development and progression of disease. In other side, although the animal models are capable of producing basic insights, new views of the disease, and preclinical trials of novel therapies, the interspecies differences make difficult accurately simulating the PD neurological development in humans.

The human SH-SY5Y neuroblastoma cell line has been already applied to reproduce *in vitro* some features of the neurons that degenerate in PD. The application of cell system contributed many advances in our comprehension of the pathogenic flow of the disease. In particular, the biochemical pathways, such as oxidative stress, mitochondrial dysfunction and apoptosis have been widely explored (Alberio et al., 2012; Avola et al., 2016; Musumeci et al., 2014). Even if since the early 1980's SH-SY5Y cell line has been widely used as model of neurons in experimental neurological studies (Xie et al., 2010), the choice to use undifferentiated or differentiated SH-SY5Y as PD cell models is more controversial still now.

In the present work, we have used both undifferentiated and differentiated SH-SY5Y and we also compared the efficiency of two different differentiation protocols.

We confirmed that human neuroblastoma SH-SY5Y cell line differentiates into DAergic neurons using RA alone or in association with MPA as differentiating agents. We checked not only the changes in cell morphology, but also we addressed whether RA- and RA+MPA-differentiated SH-SY5Y cells are functionally mature. The detection of markers such as MAP-2, β-Tubulin III and TH (Mullen et al., 1992; Weyer and Schilling, 2003) suggested that the most complete and mature phenotype was reached with RA+MPA inducing agents. We found that RA differentiation increased the protein expression of and β-Tubulin III mRNA levels, while TH levels did not change. According to Encinas and co-workers (2000), we have obtained a comparable expression pattern of MAP-2 between RA-differentiated and undifferentiated SH-SY5Y cells. In this case, the SH-SY5Y differentiation into

cholinergic neurons in presence of RA alone (Lopes et al., 2010) should justify the observed morphological changes. RA together with biologically active phorbol esters such MPA has been reported to induce SH-SY5Y cells differentiation into DAergic phenotypes by the mitogenic control to both human insulin-like growth factor I and II (IGF-I and IGF-II) (Mattsson et al, 1986). In agreement to Mattssons and co-warker, in our experimental condition, RA+MPA-enriched medium differentiated SH-SY5Y with a significant increase of TH, a marker of mature and functional catecholaminergic neurons. These DAergic neurons expressed AQP9 that reached higher values with the contemporary appearance of AQP4 in RA+MPA-differentiated SH-SY5Y.

The *in vitro* model of PD was obtained by stimulation of the cells with MPTP/H_2O_2 for 4 and 24 hours. It is well known that MPTP itself is not toxic, but once inside the brain, MPTP is metabolized into the toxic cationic 1-methyl-4-phenylpyridinium (MPP^+) by the enzyme MAO-B of glial cells. The dopamine transporter moves MPP^+ inside the DAergic neurons, which leads to cell death (Presgraves et al., 2004) and causes the buildup of free radicals, toxic molecules that contribute further to cell destruction. Considering these findings, we applied MPTP on undifferentiated and on RA- or RA+MPA-differentiated SH-SY5Y in presence of an oxidative environment by H_2O_2. This system was double functionalized because of the activation of MPTP and the induction of oxidative stress, both in acute (4 hours) and in chronic (24 hours) conditions. Moreover, the contemporary administration of MPTP with H_2O_2 as oxidative stressor mimed the vulnerability of the cells in PD pathophysiological conditions: DAergic cells are normally exposed to H_2O_2 during dopamine synthesis or catabolism, and 100 μM H_2O_2 did not induce consistent death in SH-SY5Y control cells (Sherer et al., 2002). In acute (4 hours) and in chronic (24 hours) conditions, we found that UN, and RA-differentiated SH-SY5Y reacted to stressor stimulus by decreasing cell viability and by activation of caspase-3. The mature DAergic phenotype, obtained by RA+MPA stimulation, modulated their responsiveness to neurotoxin by altering cell survival only in our experimental chronic condition.

The data about cells viability and caspase-3 protein levels indicated that the cell sensitivity and vulnerability to stimulus were: UN>RA->RA+MPA-differentiated SH-SY5Y. Our results well fit to those reported by Song et al that demonstrated a higher sensitive of SH-SY5Y to neurotoxin showing about 30% cell lethality,

correlated whit mitochondria injury and ultrastructural damage (Song et al., 1997). Moreover, undifferentiated SH-SY5Y cells did not express high levels of TH, the enzyme that synthesizes dopamine, and previous studies suggested that MPTP/H_2O_2 toxicity is realized via non-DAT, accordingly to DAT and monamine oxidase (MAO) activity in SH-SY5Y (Song and Ehrich, 1998), this event contributed to fail the idea of UN SH-SY5Y to be a good PD cell model.

Respect to undifferentiated cells, the RA-differentiated SH-SY5Y showed an higher cell survival and low caspase-3 expression level, because RA can trigger survival signaling pathways in different cell types and it has been demonstrated that up-regulation of survival signaling, like Akt and Erk1/2, can protect neurons from Parkinsonism mimetic (Cheung et al., 2009).

Although RA+MPA-differentiated cells seemed to be less vulnerable to MPTP/H_2O_2-induced Parkinsonism in terms of cells viability in acute condition, they overexpressed the pro-apoptotic proteins caspase-3 in chronic condition, turning into decrease of their viability. These differences were time-dependent, suggesting that probably in this cell system the distribution of neurotoxin should be timely scattered from the culture medium to cell cytoplasm (Song and Ehrich, 1998), perhaps by using specific transporters. Moreover, supporting the finding of a complete induction of DAergic phenotype, we detected a complete loss of TH, after the treatment of RA+MPA-differentiated SH-SY5Y with MPTP/H_2O_2.

In parallel, considering that an emerging aspect points to converge the alteration of energy and water metabolism as a pathophysiological key factor of PD, the AQPs expression was analyzed during the neuronal differentiation and compared in all cell system to detect cell reactions toward MPTP/H_2O_2 Parkinson-like treatment. In particular, AQP4 and AQP9 were examined.

AQP4 is the predominant form of AQP in the CNS (Küppers et al., 2008; Jung et al., 1994). It is a key channel for maintaining water and ion homeostasis associated with neuronal activity and it was found constitutively expressed in glia/astrocytes particularly in the region of subpial vessels, near the brain ventricles and in the SNpc (Benga and Huber, 2012). According to its role and distribution, recently AQP4 has been correlated to PD, in particular down-regulation of AQP4 has been reported to be linked with the role of neurotransmitter dopamine in the proliferation of striatal astrocytes that express AQP4 (Sun et al., 2016). Moreover, AQP4 is involved in the release of inflammatory cytokines and ATP from astrocytes, and then indirectly

regulates microglial activation (Jung et al., 1994) inducing the microgliosis that participates in the neurodegeneration of DAergic neurons (Dzamko et al., 2015, Halliday at al., 2011; Kannarkat et al., 2013). In our experimental condition, we detected the appearance of AQP4 transcriptional levels during the differentiation with RA, and it reached the highest levels during the DAergic differentiation with RA+MPA stimulus. In our *in vitro* PD model, generally a decrease of AQP4 seemed to be correlated with cell death and caspase-3 activation. A higher AQP4 expression was detected only in acute damage of RA+MPA-differentiated-SH-SY5Y. Despite role of AQP4 in PD is not fully understood, our experimental models strongly suggested that AQP4 mediates cell protection against MPTP/H_2O_2 damage by acting as a redox regulated channel, in according to Subburaman and Vanisree, 2011. These data are in line with previous investigation in which AQP4 downregulation in PD models mediated the enhanced sensitivity of DAergic neurons to neurotoxicity/oxidant burden, by the modulation of astrocytes that provide precursors for redox-modulating components and neurotrophic factors (Nakajama et al., 2001). As about AQP9, generally it has been suggested it acts in brain energy metabolism as channel permeable to various solutes, including glycerol, lactate and monocarboxylates (Tsukaguchi et al., 1999) as consequence of its localization in glucose sensitive neurons (Yang et al., 1999; Himmi et al., 2001; Ainscow et al., 2002). In our study, during the SH-SY5Y differentiation, we found a moderate increase of AQP9 that can ensure sufficient cell energy. In our models, AQP9 upregulation following the Parkinson-like induction with MPTP/H_2O_2 seemed to be necessary and it could be linked to a general neuronal damaged. This damage appeared to be an inducible mechanism in catecholaminergic neurons from SH-SY5Y stimulated with RA+MPA. In acute condition, these DAergic neurons did not change AQP9 expression, while it increased in chronic condition.

This data suggested that, in pathological condition, the large amount of lactate and glycerol releases in the extracellular compartment-phenomenon that has been described both in animals as well as in humans (Bertrand et al., 1992; Schulz et al., 2000; Frykholm et al., 2001; Kuo et al., 2003) - should be linked to AQP9. Moreover, considering RA+MPA-differentiated SH-SY5Y stimulated with MPTP/H_2O_2 and comparing their reaction at different time points, we suggest that DAergic neurons orchestrated a fine regulation of AQP4 and AQP9 both during their differentiation and during Parkinson-like damage. As summarized in Table 1,

in all cell systems the inexpression or the downregulation of AQP4 and the upregulation of AQP9 strongly relate with caspase-3 activation and loss of cell viability, whereas AQP4 upregulation and basal level of AQP9 shall link to cell protection against MPTP/H_2O_2-induced damage.

Taken together, these findings evidenced the involvement of AQP4 and AQP9 in MPTP/H_2O_2-induced damage.

Materials and methods

Cell culture

The human neuroblastoma cell line, SH-SY5Y (ATCC, Manassas, VA, USA) was grown in Dulbecco's Modified Eagle's medium and nutrient mixture F-12 (DMEM/F-12 Gibco, life technologies, Milan, Italy) supplemented with 10% fetal bovine serum, (FBS, Sigma-Aldrich, Milan, Italy), 100 U/mL streptomycin, 100 mg/mL penicillin and 100 mg/mL sodium pyruvate (Sigma-Aldrich, Milan, Italy). Cultures were kept at 37 °C in humidified air with 5% CO_2 for 8 days, with a medium change every 3 days. Both adherent and floating cells were collected when cells were passed. Floating cells were removed in culture medium and centrifuged and adherent cells were detached by trypsin-EDTA.

Differentiation protocols

The neuronal differentiation protocol used contained the following steps: pellets and detached cells were firstly gently suspended in normal medium containing DMEM/F-12 with 10% FBS and plate in T-25 flask and in 96-wells plates, at approximately in 1×10^5 cells/cm^2. After 24 hours, the medium was replaced with Neurobasal medium (Gibco, life technologies, Milan, Italy) containing 2% B-27 supplement, 1% L-glutamine (Sigma-Aldrich, Milan, Italy) and 10 μM retinoic acid (RA) for 7 days (RA medium). From day 7 to 14, SH-SY5Y cells were maintained in Neurobasal medium (Gibco, life technologies, Milano, Italy) containing 2% B-27 supplement, 1% L-glutamine (Sigma-Aldrich, Milan, Italy) and 80 nM of phorbol 12-myristate 13-acetate (MPA, Sigma-Aldrich, Milan, Italy) (MPA medium). On day 15, the RA+MPA-differentiated SH-SY5Y cells were treated for 3 days with Neurobasal medium (Gibco, life technologies, Milan, Italy) containing 2% B-27 supplement, 1% L-glutamine (Sigma-Aldrich, Milan, Italy), 10 μM RA and 80 nM of MPA (RA+MPA-differentiated SH-SY5Y). For morphology evaluation, digital

images were acquired using a Leica microscope connected to a digital camera (Spot, Diagnostic Instruments, Sterling Heights, USA).

MPTP treatment

1-methyl-4-phenyl-1, 2, 3, 6-tetrahydropyridine (MPTP) DAergic neurotoxin (M0896, Sigma-Aldrich, Milan, Italy) was dissolved in growth medium at the concentration of 10 mg/mL. For experiments, undifferentiated cells (UN SH-SY5Y), RA- or RA+MPA-differentiated cells were incubated in treatment medium, containing 100 μM of H_2O_2 and 1 mM MPTP for 4 and 24 hours.

Cell viability

Cell viability was evaluated by determining mitochondrial function of living cells on the basis of their ability to reduce the yellow dye, tetrazolium salt 3-(4,5-dimethylthiazol-2-yl)-2,5-diphenyltetrazolium bromide (MTT) (Sigma-Aldrich, Milan, Italy), into dark blue formazan crystal mainly by the mitochondrial dehydrogenases. SH-SY5Y cells were seeded on 96-well plates at a density of 1×10^5 cells/cm^2 and incubate with growing medium, RA medium, RA+MPA medium, cell viability was detected at 0, 7, 14 and 17 days of treatment. The cytotoxic effect of the 1 mM MPTP/H_2O_2 (10 mg/ml MPTP in growth medium 100 μM H_2O_2) was assayed at 4 and 24 hours after treatment. MTT stock solution (5 mg/mL in PBS), as previous described by Lo Furno et al., (2016), was added to each well at one tenth the total media volume and left to incubate at 37 °C for 3 hours. At the end of this incubation, the media was removed and the resulting blue formazan dye was solubilized with 100 μl of dimethylsulphoxide (DMSO). The absorbance was measured in a micro plate reader (Titertek Multiskan, DAS, Italy) at λ= 550 nm. For each sample, three experiments were performed in triplicate, the data were averaged. The data regarding cell viability during differentiation steps were represented as percentage respect to undifferentiated SH-SY5Y. MPTP/H_2O_2 toxicity was represented as a percent of cell viability respect to untreated group of each differentiation condition at two different time points (4 and 24 hours of treatment).

Detection of tyrosine hydroxylase (TH) and AQP4 and 9 by immunocytochemistry

For the experiments, SH-SY5Y were plated on 96-well plates, and incubated with normal medium or RA+MPA medium. Immunocytochemistry was performed at 17

days. Briefly, the cells were first washed with PBS, then fixed with 4% paraformaldehyde in PBS for 30 min and incubated for 30 min with a 5 % solution of normal goat serum (Sigma-Aldrich, Milan, Italy). They were subsequently incubated overnight at 4 °C with primary antibodies direct against the marker of neurons, tyrosine hydroxylase (TH, Abcam, Cambridge, UK), AQP4 and AQP9 (Santa Cruz Biotechnology, Santa Cruz, CA). The following day, cells were washed with PBS and incubated for one hour at room temperature with Cy3-conjugated goat anti-mouse secondary antibody, fluorescein isothiocyanate-conjugated goat anti-rabbit secondary or fluorescein isothiocyanate-conjugated goat anti-mouse secondary antibody (Millipore, Milan, Italy). Cells were then washed with PBS, and incubated with DAPI (1:10,000; Invitrogen). As a control, the specificity of immunostaining was verified by omitting incubation with the primary or secondary antibody using secondary antibodies (goat anti-mouse or goat ant-rabbit) conjugated with fluorescein isothiocyanate (FITC, 1:200; Millipore, Milan Italy) or Cy3-conjugated. Digital images were acquired using a Leica DMRB fluorescence microscope (Leica Microsystems Srl, Milan, Italy) equipped with a computer-assisted Nikon digital camera (Nital SpA, Turin, Italy). Immunoreactivity was evaluated taking into account the signal-to-noise ratio of immunofluorescence.

RT-PCR

Cells were washed twice with 1x PBS buffer and trypsinized at 37 °C for 3 min. Trypsinization was ended by the addition of Dulbecco's Modified Eagle's and nutrient mixture F-12 media (DMEM/F-12 Gibco, Life Technologies, Milan, Italy) supplemented with 10% fetal bovine serum, (FBS, Sigma-Aldrich, Milan, Italy). Then, the cell suspension was centrifuged at 1500× g for 5 min. After centrifugation, the media was removed and the cell pellet was washed with 1x PBS buffer and centrifuged again at 1500 × g for 5 min. Finally, the supernatant was removed and the cell pellet was used to isolate mRNA. Total mRNA was isolated using 1 ml Qiazol Reagent (Qiagen, Milan, Italy), 0.2 ml chloroform and precipitated with 0.5 ml isopropanol. Pellet was washed with 75% ethanol, air-dried and resuspended in RNAse-free water. The cDNAs were synthesized from the total RNA samples by using the QuantiTect Reverse Transcription Kit (Qiagen, Milan, Italy) according to the manufacturer's protocol. Aliquots of cDNA were amplified using specific primers sequences are listed in Table 1. Oligonucleotide cDNA was used for 40

cycle PCR in Rotor-gene Q real-time analyzer (Corbett, Qiagen, Milan, Italy). For PCR analysis, a concentration of 100 ng/reaction of template cDNA was added to the reaction mix containing 1x Rotor-Gene SYBR Green PCR Master Mix (Qiagen, Milan, Italy), 1 μM of each primer (forward and reverse) and RNase-free water to a final reaction volume of 25 μl. PCR was performed using the following program: initial activation step 95 °C 10 min, denaturation 95 °C 10 sec, annealing 60 °C 30 sec, extension 72 °C 30 sec (40 cycles), final extension 72 °C 10 min. RT-PCR was followed by melting curve analysis to confirm PCR specificity. Each reaction was repeated three times and threshold cycle average was used for data analysis by Rotor-gene Q software. Target genes were normalized against GAPDH. Amplification products were separated by electrophoresis in a 2% agarose gel in 0.045 M Tris–borate/1mM EDTA (TBE) buffer. Each amplification was carried out in duplicates in four different experiments. Relative expression of target genes was quantified using $2^{\Delta ct}$ method. We analyzed the mean of the crossing points (or crossing threshold = Ct) of each sample. The Ct represents the number of cycles needed to detect a fluorescence above a specific threshold level and it is inversely correlated to the amount of nucleic acid template present in the reaction. The ΔCt was calculated by normalizing the mean Ct of each sample to the mean Ct of the reference gene measured in the same experimental conditions. The $2^{\Delta ct}$ of each sample was calculated by subtracting calibrator ΔCt to sample ΔCt. The formula $2^{\Delta ct}$ was applied to calculate the fold change.

Western blot analysis

Cell culture were scraped, transferred into 50 ml conical tubes and centrifuged at 1500 × g for 5 min at 4°C (Graziano et al., 2016). After twice washing with 1X PBS, the pellets were treated with lysing buffer M-PER Mammalian Protein Extraction Reagent (Pierce, Fisher Scientific, Milan, Italy) and vortexed for 30 min on ice. Then the lysate was centrifuged at 15,000 × g for 15 min at 4 °C. The supernatants were transferred into a new tube and the protein quantification was performed by the bicinchoninic acid assay (BCA assay; Pierce, Fisher Scientific, Milan, Italy). Equal amounts of proteins were separated by 4–12% Bolt gel electrophoresis (Invitrogen, Milan, Italy). Then, proteins were transferred to a nitrocellulose membrane (Invitrogen, Milan, Italy) in a wet system (Invitrogen, Milan, Italy). The transfer of proteins was verified by staining the nitrocellulose membranes with Ponceau S.

Membrane was blocked in Tris-buffered saline containing 0.01% Tween-20 (TBST) and 5% non-fat dry milk for 1 hour at room temperature. Primary antibodies - anti-caspase-3 active form (Sigma-Aldrich, Milan, Italy), anti-AQP4 and anti-AQP9 (all from Santa Cruz Biotechnology, DBA, Milan, Italy) were diluted in TBST and membranes were incubated overnight at 4 °C. Blots were rinsed three times in PBS and the appropriate HRP-conjugated secondary antibody was incubated for 1 hour at room temperature (goat anti-rabbit, 1:20,000; goat anti-mouse, 1:5000, from both Santa Cruz Biotechnology, DBA, Milan, Italy). A cell lysate (sc-2227, Santa Cruz Biotechnology, Santa Cruz, CA) was used as a positive control. Antibodies were detected using enhanced chemiluminescent solution (Pierce, Fisher Scientific, Milan, Italy) and visualized by Uvitec Alliance LD9 gel imaging system (Uvitec, Cambridge, United Kingdom). Bands were measured densitometrically and their relative density was calculated based on the density of the α-tubulin bands in each sample. Values were expressed as arbitrary densitometric units (ADU) corresponding to signal intensity.

Statistical analysis

The experiment was repeated independently at least three times in triplicate and the mean ± SEM for each value was calculated. One-way statistical analyses of results [Student's t test for paired and unpaired data; variance analysis (ANOVA)] were used. All statistical analyses were performed using the statistical software package SYSTAT, version 11 (Systat Inc., Evanston IL, USA). A value of $p<0.05$ was considered statistical significant.

Abbreviations

PD: Parkinson Disease; SNpc: substantia nigra pars compacta; DA: dopamine; TH: tyrosine hydroxylase; TNF-α: tumor necrosis factor-α; IL-1β: interleukin-1β; FBS: fetal bovine serum; RA: retinoic acid; MPTP: 1-methyl-4-phenyl-1, 2, 3, 6-tetrahydropyridine; MPA: phorbol 12-myristate 13-acetate; DAergic: dopaminergic; DA: dopamine

Authors' contributions

ACEG and RA conceived of, designed the study, performed cell culture, experiments, and analyses, and drafted the manuscript. GP participated in

experiments analyses and technical support. VC conceived of designed the study, performed analyses and drafted the manuscript.
All authors read and approved the final manuscript.

Conflict of interest

The Authors declare that there is no conflict of interest.

References

Ainscow, E. K., Mirshamsi, S., Tang, T., Ashford, M. L. and Rutter G.A. (2002). Dynamic imaging of free cytosolic ATP concentration during fuel sensing by rat hypothalamic neurones: Evidence for ATP-independent control of ATP-sensitive K(+)channels. J Physiol. 544, 429–445.

Alberio, T., Leonardo, Lopiano, L. and Fasano, M. (2010). Cellular models to investigate biochemical pathways in Parkinson's disease. FEBS Journal. 279, 1146-1155.

Amiry-Moghaddam, M., Lindland, H., Zelenin, S., Roberg, B. A., Gundersen, B. B., Petersen, P., Rinvik, E., Torgner, I. A. and Ottersen, O. P. (2005). Brain mitochondria contain aquaporin water channels: evidence for the expression of a short AQP9 isoform in the inner mitochondrial membrane. FASEB J.19, 1459-1467.

Avola, R., A.C.E., Pannuzzo, G., Alvares, E. and Cardile, V. (2016). Krabbe's Leukodystrophy: Approaches and Models In Vitro. Journal of Neuroscience Research. 94, 1284-1292.

Badaut, A., Nehlig, J., Verbavatz, M., Stoeckel, M.J., Freund-Mercier, F. and Lasbennes, F. (2000). Hypervascularization in the magnocellular nuclei of the rat hypothalamus: relationship with the distribution of aquaporin-4 and markers of energy metabolism. J. Neuroendocrinol. 12, 960-969.

Badaut, J. (2009). Aquaglyceroporin 9 in brain pathologies. Neurosci. 168, 1047-1057.

Badaut, J., Verbavatz, J. M., Freund-Mercier, M. J. and Lasbennes, F. (2000). Presence of aquaporin-4 and muscarinic receptors in astrocytes and ependymal cells in rat brain: a clue to a common function? Neurosci. Lett. 292, 75-78.

Badger, J.L., Cordero-Llana, O., Hartfield, E. M. and Wade-Martins, R. (2014). Parkinson's disease in a dish - Using stem cells as a molecular tool. Neuropharmacology. 76, 88-96.

Benga, H. and Huber, V. (2012). Brain water channel proteins in health and disease. Molecular Aspect of Medicine. 33, 562-578.

Bertrand, N., Ishii, H. and Spatz, M. (1992). Regional and temporal glycerol changes induced by forebrain ischemia in gerbils. Neurosci Lett. 148, 81–84.

Cebrián, C., Loike, J. D. and Sulzer, D. (2015). Neuroinflammation in Parkinson's disease animal models: a cell stress response or a step in neurodegeneration? Curr Top Behav Neurosci. 22, 237-70.

Cheung, Y. T., Lau W. K. W., Yu, M. S., Lai, Sau-W., C., Yeung S. C., So, K. F. and Chang, R. C. C. (2009). Effects of all-trans-retinoic acid on human SH-SY5Y neuroblastoma as in vitro model in neurotoxicity research. NeuroToxicology. 30, 127-135-

Dawson, T. M., Ko, H. S. and Dawson, V.L. (2010). Genetic animal models of Parkinson's disease. Neuron. 66, 646-661.

Dunnett, S.B. and Bjorklund, A. (1999). Prospects for new restorative and neuroprotective treatments in Parkinson's disease. Nature. 399 (Suppl.), A32-A39.

Dzamko, N., Geczy, C. L. and Halliday, G. M. (2015). Inflammation is genetically implicated in Parkinson's disease. Neuroscience. 302:89–102.

Encinas, M., Iglesias, M., Liu, Y., Wang, H., Muhaisen, A., Cen˜a, V., Gallego, C., and Comella, J. X. (2000). Sequential Treatment of SH-SY5Y Cells with Retinoic Acid and Brain-Derived Neurotrophic Factor Gives Rise to Fully Differentiated, Neurotrophic Factor-Dependent, Human Neuron-Like Cells. J. Neurochem. 75, 991-1003

Foglio, E. and Rodella, L. F. (2010). Aquaporins and Neurodegenerative. Diseases Current Neuropharmacology. 8, 112-121.

Frykholm, P., Hillered, L., Langstrom, B., Persson, L, Valtysson, J., Watanabe, Y. and Enblad, P. (2001). Increase of interstitial glycerol reflects the degree of ischaemic brain damage: A PET and microdialysis study in a middle cerebral artery occlusion-reperfusion primate model. J Neurol Neurosurg Psychiatry. 71, 455–461.

González-Aparicio, R. and Moratalla, R. (2014). Oleoylethanolamide reduces L-DOPA-induced dyskinesia via TRPV1 receptor in a mouse model of Parkinson´s disease. Neurobiol Dis. 62, 416-425.

Graziano, A.C., Parenti, R., Avola, R. and Cardile, V. (2016). Krabbe disease: involvement of connexin43 in the apoptotic effects of sphingolipid psychosine on mouse oligodendrocyte precursors. Apoptosis. 21, 25-35.

Halliday, G. M. and Stevens, C. H. (2011). Glia: initiators and progressors of pathology in Parkinson's disease. Mov Disord. 26, 6-17.

Himmi, T., Perrin, J., Dallaporta, M. J. and Orsini, C. (2001). Effects of lactate on glucose-sensing neurons in the solitary tract nucleus Physiol Behav. 74, 391–397.

Hwang, O. (2013). Role of oxidative stress in Parkinson's disease. Exp. Neurobiol. 22, 11-17.

Jung, J. S., Bhat, R . V., Preston, G. M., Guggino, W. B., Baraban, J. M and Agre, P. (1997). Molecular characterization of an aquaporin cDNA from brain: candidate osmoreceptor and regulator of water balance. Proc Natl Acad Sci USA. 91, 13052-13056.

Kannarkat, G. T., Boss, J. M. and Tansey, M. G. (2013). The role of innate and adaptive immunity in Parkinson's disease. J Parkinson's Dis. 3, 493-514.

Kuo, J. R., Lin, C. L., Chio, C. C., Wang, J. J. and Lin, M.T. (2003). Effects of hypertonic (3%) saline in rats with circulatory shock and cerebral ischemia after heatstroke. Intensive Care Med. 29, 1567–1573.

Küppers, E., Gleiser, C., Brito, V., Wachter, B., Pauly, T., Hirt, B and Grissmer, S. (2008). AQP4 expression in striatal primary cultures is regulated by dopamine--implications for proliferation of astrocytes. Eur J Neurosci. 28, 2173-2182.

Lees, A. J., Hardy J. and Revesz, T. (2009). Parkinson's disease. Lancet. 373, 2055-2066.

Lo Furno, D., Graziano, A.C.E., Avola, R., Giuffrida, R., Perciavalle, V., Bonina, F., Mannino, G. and Cardile, V. (2016). A Citrus bergamia Extract Decreases Adipogenesis and Increases Lipolysis by Modulating PPAR Levels in Mesenchymal Stem Cells from Human Adipose Tissue. PPAR Res.

Lopes, F. M., Schröder, R., da Frota, M. L., Zanotto-Filho, A., Müller, C. B., Pires, A. S., Meurer, R. T., Colpo, G. D., Gelain, D. P., Kapczinski, F., Moreira, J. C., Fernandes, M. C and Klamt, F. (2010). Comparison between proliferative and neuron-like SH-SY5Y cells as an in vitro model for Parkinson disease studies. Brain Res. 14; 85-94.

Mattsson, M. E., Enberg, G., Ruusala, A. I., Hall, K. and Påhlman, S. (1986). Mitogenic response of human SH-SY5Y neuroblastoma cells to insulin-like growth factor I and II is dependent on the stage of differentiation. J Cell Biol. 102, 1949-1954.

Moehle, M.S. and West, A.B. (2015). M1 and M2 immune activation in Parkinson's Disease: Foe and ally? Neurosci. 302, 59-73.

Mosley, L. R., Benner, E. J., Kadiu, I., Thomas, M., Boska, M. D., Hasa, K., Laurie, C. and Gendelman, H. E. (2006). Neuroinflammation, oxidative stress, and the pathogenesis of Parkinson's disease. Clinical Neuroscience Research. 6, 261-281.

Mullen, R.J., Buck, C.R. and Smith, A.M. (1992). NeuN, a neuronal specific nuclear protein in vertebrates. Development. 116, 201-211.

Musumeci G Mobasheri A, Trovato FM, Szychlinska MA, Graziano AC, Lo Furno D, Avola R, Mangano S, Giuffrida R and Cardile V. (2014). Biosynthesis of collagen I, II, RUNX2 and lubricin at different time points of chondrogenic differentiation in a 3D in vitro model of human mesenchymal stem cells derived from adipose tissue. Acta Histochemica. 116:1407-1417.

Nakajima, K., Hida, H., Shimano, Y., Fujimoto, I., Hashitani, T., Kumazaki, M., Sakurai, T. and Nishino H. (2001). GDNF is a major component of trophic activity in DA-depleted striatum for survival and neurite extension of DAergic neurons. Brain Res. 916, 76-84.

Nielsen, S., Nagelhus, E. A., Amiry-Moghaddam, M., Bourque, C., Agre, P. and Ottersen, O.P. (1997). Specialized membrane domains for water transport in glial cells: high-resolution immunogold cytochemistry of aquaporin-4 in rat brain. J Neurosci. 17, 171-180.

Presgraves, S. P., Ahmed, T., Borwege, S. and Joyce, J. N. (2004). Terminally differentiated SH-SY5Y cells provide a model system for studying neuroprotective effects of dopamine agonists Neurotox Res. 5, 579-598.

Schulz, M.K., Wang, L. P., Tange, M. and Bjerre, P. (2000). Cerebral microdialysis monitoring: Determination of normal and ischemic cerebral metabolisms in patients with aneurysmal subarachnoid hemorrhage. J Neurosurg. 93, 808–814.

Sherer, T. B., Betarbet, R., Stout, A.K., Lund, S., Baptista, M., Panov, A.V., Cookson, M. R. and Greenamyre, J. T. (2002). An in vitro model of Parkinson's disease: linking mitochondrial impairment to altered alpha-synuclein metabolism and oxidative damage. J Neurosci. 22, 7006-7015.

Song, X and Ehrich, M. (1998). Uptake and metabolism of MPTP and MPP· in SH-SY5Y human neuroblastoma cells. In Vitro Toxicology. 18, 341-354.

Song, X., Perkins, S., Jortner B. S., and Ehrich, M. (1997). Cytotoxic Effects of MPTP on SH-SY5Y Human Neuroblastoma Cells. NeuroToxicology. 18, 341-354.

Sun, H., Liang, R., Yang, B., Zhou, Y., Liu, M., Fang, F., Ding, J., Fan, Y., and Hu, G. (2016). Aquaporin-4 mediates communication between astrocyte and

microglia: implications of neuroinflammation in experimental Parkinson's disease. Neuroscience. 317, 65-75.

Subburaman T. T., and Vanisree, A. J. (2011). Oxidative pathology and AQP4 mRNA expression in patients of Parkinson's disease. Annals of Neurosciences. 18, 109-112.

Tsukaguchi, H., Weremowicz, S., Morton, C. C. and Hediger, M. A. (1999) Functional and molecular characterization of the human neutral solute channel aquaporin-9. Am. J. Physiol. 277, 685-696.

Verkman, A.S. (2005). Novel roles of aquaporins revealed by phenotype analysis of knockout mice. Rev Physiol Biochem Pharmacol. 155, 31-55.

Vizuete, M.L., Venero, J.L., Vargas, C., Ilundain, A.A., Echevarria, M., Machado, A. and Cano, J. (1999). Differential upregulation of aquaporin-4 mRNA expression in reactive astrocytes after brain injury: potential role in brain edema. Neurobiol. Dis. 6, 245-258.

Wang, Q., Liu, Y. and Zhou, J. (2015). Neuroinflammation in Parkinson's disease and its potential as therapeutic target. Transl Neurodegener. 4, 1-19.

Weyer, A. and Schilling, K (2003). Developmental and cell type-specific expression of the neuronal marker NeuN in the murine cerebellum. J Neurosci Res. 73, 400-409.

Xiao, M. and Hu, G. (2014). Involvement of aquaporin 4 in astrocyte function and neuropsychiatric disorders. CNS Neurosci Ther. 20, 385-90.

Xie, H., Hu, L. and Li, G. (2010). SH-SY5Y human neuroblastoma cell line: in vitro cell model of dopaminergic neurons in Parkinson's disease. Chin Med J. 123, 1086-1092.

Yang, M., Gao, F., Liu,H., Yu, W.H. and Sun, S.Q. (2009). Temporal changes in expression of aquaporin-3, -4, -5 and -8 in rat brains after permanent focal cerebral ischemia. Brain Res. 1290, 121-132.

Yang, X. J., Kow, L. M., Funabashi, T. and Mobbs, C. V. (1999). Hypothalamic glucose sensor: Similarities to and differences from pancreatic beta-cell mechanisms. Diabetes. 48, 1763–1772.

Yi, F., Hui, K., Xueru, S., Xiulan, S., Jianhua, D., Jie, W. and Gang, H. (2008). Hypersensitivity of aquaporin 4-deficient mice to 1-methyl-4-phenyl-1, 2, 3, 6-tetrahydropyrindine and astrocytic modulation. Neurobiology of Aging. 29, 1226-1236.

Figure legends

Figure 1. Differentiation of SH-SY5Y into dopaminergic neurons.

Morphology of UN-SH-SY5Y (A), RA-differentiated (B) and RA+MPA-differentiated (C) cells under phase-contrast microscopy. SH-SY5Y progressively underwent obvious morphological changes showing a clear neuronal morphology with processes extending between them. (D) Cell viability showed statistically significant differences between UN-, and RA- or RA+MPA-differentiated SH-SY5Y (mean ± S.E.M., $n \geq 3$, $^*p < 0.05$).

Figure 2. Profile of neuronal markers in SH-SY5Y differentiated into dopaminergic neurons.

β-Tubulin III (A), MAP-2 (B), tyrosine hydroxylase (TH) (C) changed their basal levels after differentiation. TH content increased significantly in RA+MPA-differentiated cells (C); β-Tubulin III (A) and MAP-2 (B) mRNA reached high levels in RA+MPA-differentiated SH-SY5Y (mean ± S.E.M., $n \geq 3$, $^*p < 0.05$).

Figure 3. AQP4 and AQP9 were associated to induction of dopaminergic neurons.

AQP4 (A) and AQP9 (B) mRNA levels in UN, RA-, and RA+MPA-differentiated SH-SY5Y. Representative immunoblot of AQP4 and AQP9 proteins (C1) of UN (1), RA- (2), RA+MPA (3)-differentiated SH-SY5Y, and positive control cell lysate (4). The histograms represent the quantification of AQP4 (C2) and AQP9 (C3) expressed as arbitrary densitometric units (A.D.U.) (mean ± S.E.M., $n \geq 3$, $^*p < 0.05$). Immunofluorescence (D) of RA+MPA-differentiated SH-SY5Y for the determination of AQP9 (upper panel, green), AQP4 (lower panel, green), TH (upper and lower panel, red). The nuclei were counterstained with 4',6-diamidino-2-phenylindole (DAPI) (blue). Digital images were acquired using Leica microscope connected to a digital camera. Magnification 40x.

Figure 4. Cell reactions to MPTP and H_2O_2 treatments.

Viability of UN, RA- and RA+MPA-differentiated SH-SY5Y after 4 and 24 hours stimulation with MPTP and H_2O_2 (A). Results show the mean of percentage ± S.E.M. vs. each untreated group ($n \geq 3$, $^*p < 0.05$). TH mRNA levels in all

experimental cell systems (B) expressed as fold change vs each untreated group. Representative immunoblot of active-caspase-3 (C). The histograms represent active-caspase-3 expression as fold change respect to each untreated group ± S.E.M ($n \geq 3$, $^*p < 0.05$).

Figure 5. AQP4 and AQP9 modulation during MPTP and H_2O_2 treatments.
mRNA level of AQP4 (A) and AQP9 (B) in UN, RA- and RA+MPA-differentiated SH-SY5Y after 4 and 24 hours stimulation with MPTP and H_2O_2. Representative immunoblot of AQP4 and AQP9 (C1) expression. Relative quantification of AQP4 (C2) and AQP9 (C3) in MPTP+H_2O_2 stimulated cells was reported as arbitrary densitometric units (A.D.U.) (mean ± S.E.M., $n \geq 3$, $^*p < 0.05$).

Table 1. Dynamic expression of aquaporins

SH-SY5Y	***Basal condition***		***MPTP/H_2O_2 stimulation 4 hours***			***MPTP/H_2O_2 stimulation 24 hours***		
	AQP4	**AQP9**	**AQP4**	**AQP9**	**Caspase-3**	**AQP4**	**AQP9**	**Caspase-3**
Undifferentiated	n.d.	n.d.	n.d.	+	++	n.d.	++	+++
RA-differentiated	n.d.	n.d.	n.d.	+	+	n.d.	++	+++
RA+MPA-differentiated	+	+	++	=	=	--	+++	+++

*n.d., not determined

Table 2. RT-PCR primers

PCR product	Primer sequences	Size (bp)
TH	Forward 5′-TGTGGCCTTTGAGGAGAAGGA Reverse 5′-TCAAACACCTTCACAGCTCGG	169
MAP-2	Forward5'-5′-TGCCATCTTGGTGCCGA Reverse 5'-5′-CTTGACATTACCACCTCCAGGT	307
β-Tubulin III	Forward 5'-CTCAGGGGCCTTTGGACATC Reverse 5'- CCACAAGCACCACATACTCCTG	161
AQP4	Forward 5'-GCTGTGATTCCAAACGGACTGATG Reverse 5'- CTGACTCCTGTTGTCCTCCACCTC	329
AQP9	Forward 5'- GATACTCCTCATAATCGTCTTTGC Reverse 5'- AAGACTGAGTCAGGCTCTGGATGG	321
β–actin	Forward 5'-CTGCCGCATCCTCTTCCTC Reverse 5'-CTCCTGCTTGCTGATCCACAT	398
GAPDH	Forward 5'-TCAACAGCGACACCCAC Reverse 5'-GGGTCTCTCTCTTCCTCTTGTG	203

Figure 1

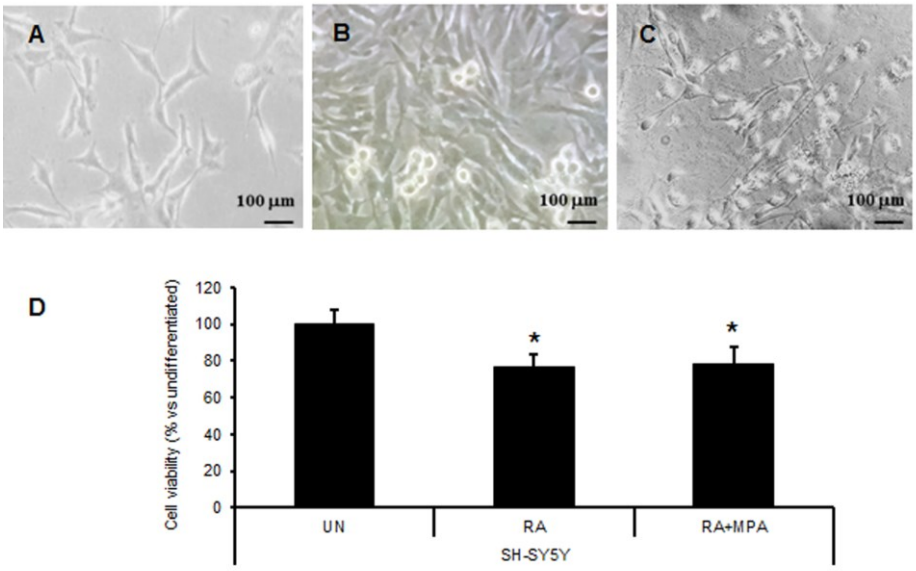
A
100 µm
B
100 µm
C
100 µm
D
Cell viability (% vs undifferentiated)
120
100
80
60
40
20
0
*
*
UN
RA
RA+MPA
SH-SY5Y

Figure 2

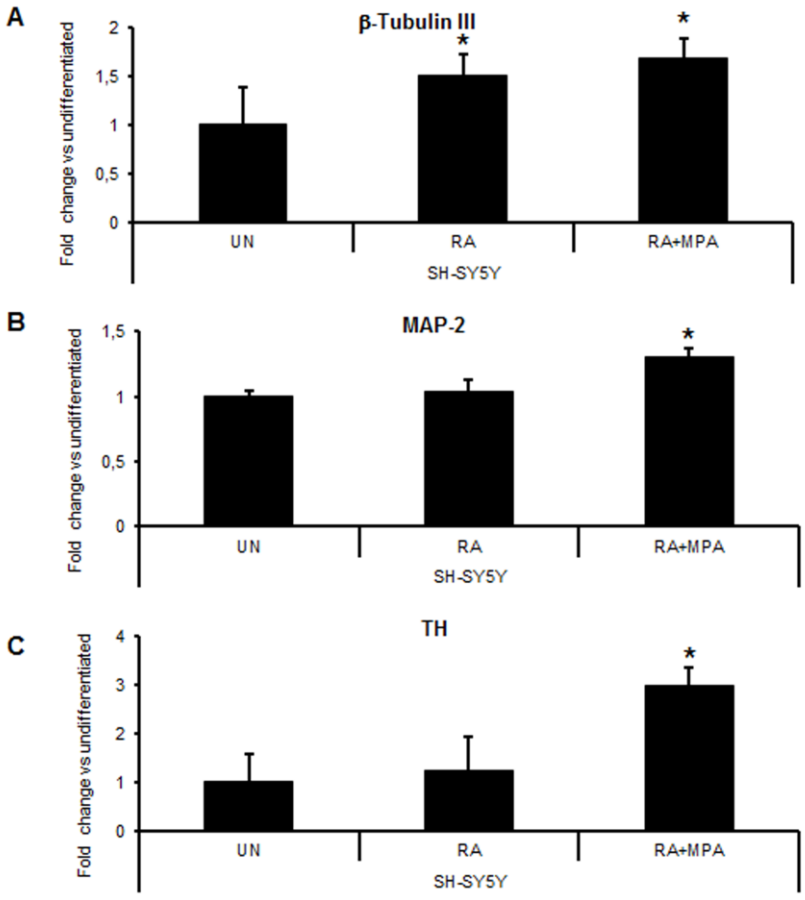
A
β-Tubulin III
Fold change vs undifferentiated
2
1,5
1
0,5
0
*
*
UN
RA
RA+MPA
SH-SY5Y
B
MAP-2
Fold change vs undifferentiated
1,5
1
0,5
0
*
UN
RA
RA+MPA
SH-SY5Y
C
TH
Fold change vs undifferentiated
4
3
2
1
0
*
UN
RA
RA+MPA
SH-SY5Y

Figure 3

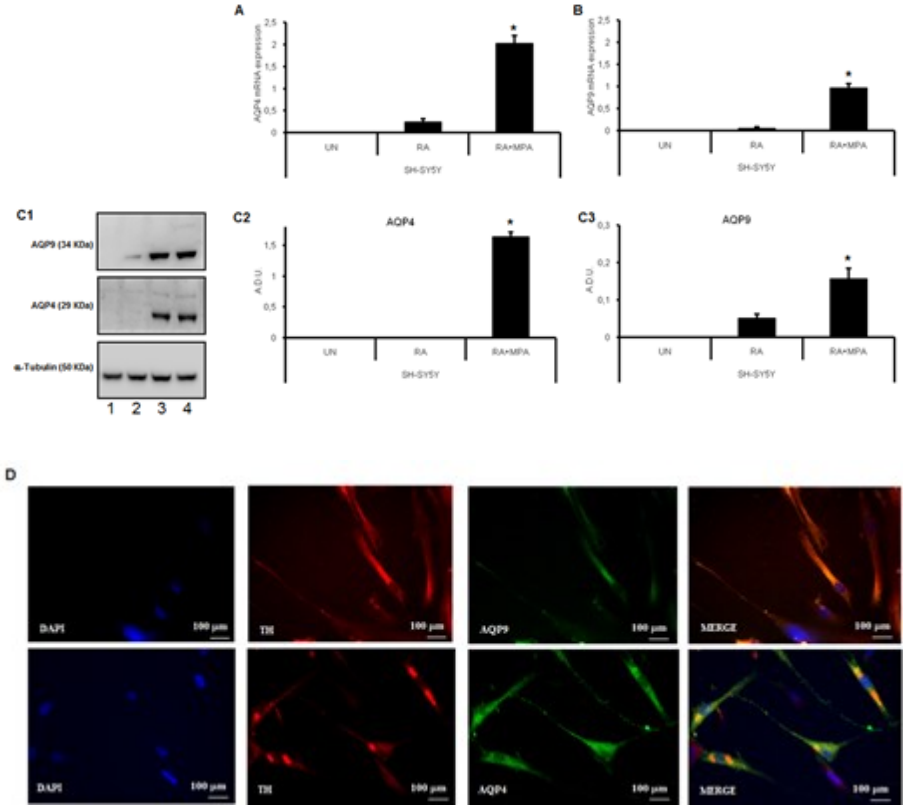
A
B
AQP4 mRNA expression
AQP9 mRNA expression
UN
RA
RA+MPA
SH-SY5Y
C1
AQP9 (34 KDa)
AQP4 (29 KDa)
α-Tubulin (50 KDa)
1 2 3 4
C2
AQP4
C3
AQP9
A.D.U.
D
DAPI
TH
AQP9
AQP4
MERGE
100 µm

Figure 4

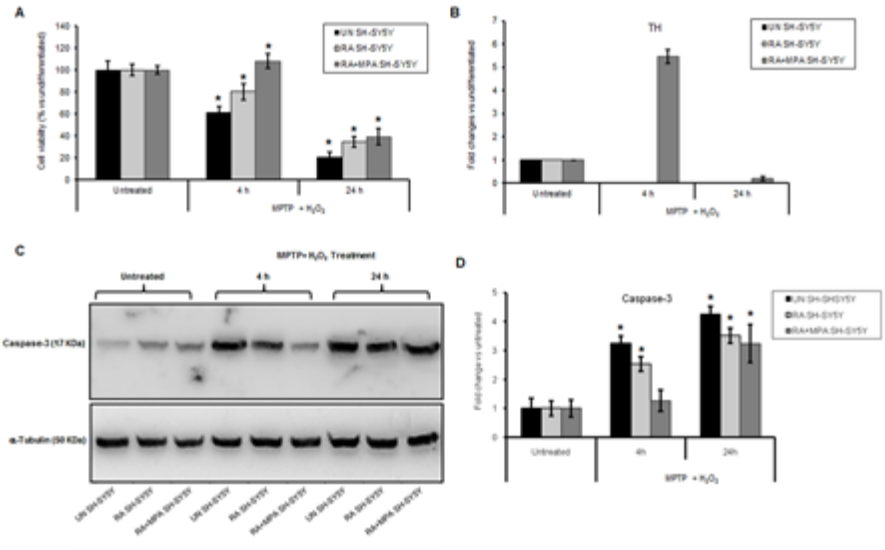
A
B
TH
C
Caspase-3 (17 KDa)
α-Tubulin (50 KDa)
D
Caspase-3
Untreated
4 h
24 h

Figure 5

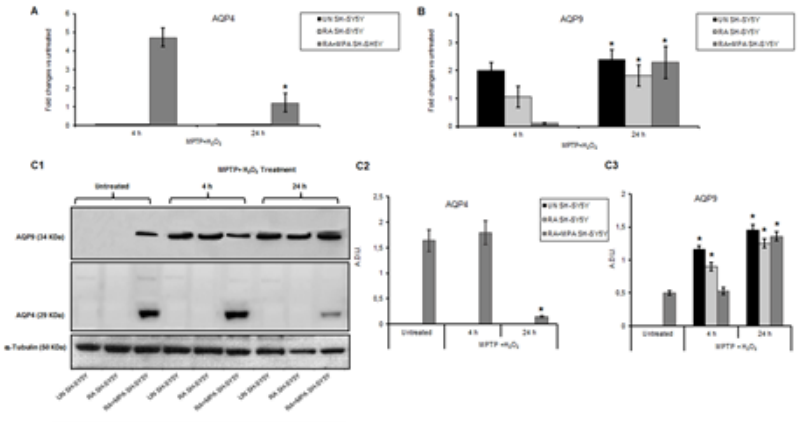
A
AQP4
B
AQP9
C1
Untreated
4 h
24 h
AQP9 (34 KDa)
AQP4 (29 KDa)
C2
AQP4
C3
AQP9

GENERAL DISCUSSION AND CONCLUSION

The purpose of research during the three years of the PhD was identifying in some physiological and pathological conditions, the expression profile of aquaporins (AQPs), a small membrane protein family involved mainly in the transport of water, glycerol and other small solutes through biological membranes.

Since their discovery in 1987 to date more than 300 homologues, well preserved in plants, bacteria and animals have been identified. In vertebrates are known 13 isoforms corresponding to AQP0-AQP12 human proteins, mainly located in epithelial and endothelial cells where they are important players to maintain fluid volume in response to osmotic stimuli and pressure gradients. However, the information regarding AQPs expressed by stem cells during their differentiation is very limited. In order to update the knowledge on stem cells biology, on AQPs related to differentiation and on relationship between specific AQPs and cell phenotype two different *in vitro* approaches were used.

Additionally, during the initial phase of this study to look for the most appropriate experimental protocol to use for the purpose of research, more information on *in vitro* models of some neurodegenerative diseases was carried out. It is known, in fact, that the most of the current knowledge about the central nervous system is gathered from post mortem studies that only represent the end-stage of the disease. Moreover, they provide a restricted understanding of the development and progression of disease. In other side, although the animal models are capable of producing basic insights, new views of the disease, and preclinical trials of novel therapies, the interspecies differences make difficult to accurately simulate the neurological and neuropathological development in humans. Thus, at the start of this study, the great potential of *in vitro* approaches to provide important clues about inflammation, apoptosis and angiogenesis of Krabbe disease was analyzed and reported in a review. The *in vitro* systems described in this review have clarified the mechanistic role of psychosine in the release of cytokines, ROS and NO, in the activation of kinases, caspases and angiogenic factors and the temporal sequence of the development of events involved in Krabbe disease or the contribution and interplay between astrocytes, microglia and oligodendrocytes.

Although in the brain have been identified nine isoforms of AQPs (AQP1, 2, 3, 4, 5, 7, 8, 9 and 11), the published information on neuroscience are limited by direct

analysis complexity, inaccessibility of the nervous tissue and the difficulty in obtaining a biopsy of brain tissue only possible after the death of the individual. Therefore, in order to clarify which specific distribution, the time of appearance and the possible association with certain neurological dysfunction, the expression of AQPs in two different cell models, which allowed reproducing *in vitro* some conditions physiology and pathology of the central nervous system cells, was analyzed.

In one model, the different isoforms of AQPs related to neuronal differentiation of human adult stem cells were examined. The data have confirmed the ability of AT-MSCs to differentiate into 28 days in neurons, astrocytes and oligodendrocytes, demonstrating positivity for typical neural markers associated with specific AQPs expression. In particular, astrocytes express AQP1, 4 and 7, oligodendrocytes AQP1, 4, and 8, and finally neurons AQP1, and 7.

Moreover, the probable role of AQPs in a model that reproduces *in vitro* the toxicity and conditions of oxidative stress in the brain of Parkinson's disease obtained by stimulation of undifferentiated, RA- or RA+MPA-differentiated SH-SY5Y in presence of MPTP/H_2O_2 was analyzed. The results of this study revealed a correlation between the different vulnerability of differentiated and undifferentiated cells and the different expression of AQP4 and 9.

Despite, the precise mechanisms of AQP4 in regulating the proliferation, the neuronal or glial fate choice of neural stem cells and their role in PD remain to be determined, our *in vitro* results strongly suggested that AQP4 could mediate cell protection against MPTP/H_2O_2 damage by acting as a redox-regulated channel. As about AQP9, we found an upregulation induced by MPTP/H_2O_2 that seems to be linked to a general neuronal damage.

This study, showing the expression of different AQPs in physiological and pathophysiological processes during neural differentiation, provides a fundamental contribute to knowledge on new aspects of the biology of the mesenchymal stem cells from human adipose tissue. AQPs could be potential neural markers and probably therapeutic targets for neurological metabolic disorders useful for further researches both *in vitro* and *in vivo*.

REFERENCES

[1] Zaccai G. The effect of water on protein dynamics. Philos Trans R Soc Lond B Biol Sci (2004) 359:1269–1275.

[2] Zeuthen T. General models for water transport across leaky epithelia. Int. Rev. Cytol. (2002) 215:285–317.

[3] Tripathi S., Boulpaep E.L. Mechanisms of water transport by epithelial cells. Q. J.Exp. Physiol. (1989) 74:385–417.

[4] O'Donnell M.J., Maddrell S.H. Paracellular and transcellular routes for water and solute movements across insect epithelia. J. Exp. Biol. (1983) 106:231–253.

[5] Agre P. The aquaporin water channels. Proc Am Thorac Soc. (2006) 3:5–13.

[6] Sidel V.W., Solomon A.K. Entrance of water into human red cells under an osmotic pressure gradient. J. Gen. Physiol. (1957) 41:243–257.

[7] Agre P., Kozono D. Aquaporinwater channels: molecular mechanisms for human diseases. FEBS. Lett. (2003) 555:72–78.

[8] Benga G., Popescu O., Borza V.I., Mureşan A., Mocsy I., Brain A., Wrigglesworth J.M. Water permeability of human erythrocytes. Identification of membrane proteins involved in water transport. Eur. J. Cell. Biol. (1986) 41:252–262.

[9] Denker B.M., Smith B.L., Kuhajda F.P., Agre P. Identification, purification, and partial characterization of a novel Mr 28,000 integral membrane protein from erythrocytes and renal tubules. J. Biol. Chem. (1988) 263:15634–15642.

[10] Preston G.M., Carroll T.P., Guggino W.B., Agre P. Appearance of water channels in Xenopus oocytes expressing red cell CHIP28 protein. Science. (1992) 256:385–387.

[11] Loo D.D., Zeuthen T., Chandy G., Wright E.M. Cotransport of water by the Na+/glucose cotransporter. Proc. Natl. Acad. Sci. U. S. A. (1996) 93:13367–13370.

[12] Nielsen S., Smith B.L., Christensen E.I., Knepper M.A., Agre P. CHIP28 water channels are localized in constitutively water-permeable segments of the nephron. J. Cell Biol. (1993) 120:371–383.

[13] Farmer R., Macey R. Perturbation of red cell volume: rectification of osmotic flow. Biochim. Biophys. Acta - Biomembr. (1970) 196:53–65.

[14] Macey R.I., Karan D. M. Farmer R. E. Properties of water channels in human red cells. Biomembranes. (1972) 3:331–340.

[15] Agre P., Saboori A.M., Asimos A., Smith B.L. Purification and partial characterization of the Mr 30,000 integral membrane protein associated with the erythrocyte Rh (D) antigen. JBC (1987) 262:17497–17503.

[16] Agre P., Sasaki S., Chrispeels M. J. Aquaporins: a family of water channel proteins. Am J Physiol. (1993) 265:F461.

[17] Preston G.M., Agre P. Isolation of the cDNA for erythrocyte integral membrane protein of 28 kilodaltons: member of an ancient channel family. Proc. Natl. Acad. Sci. (1991) 88: 11110–11114.

[18] Heymann J.B., Engel A., Aquaporins: phylogeny, structure, and physiology of water channels. News. Physiol. Sci. (1999) 14:187–193.

[19] Luyten K., Albertyn J., Skibbe W.F., Prior B.A., Ramos J., Thevelein J.M., Hohmann S. Fps1, a yeast member of the MIP family of channel proteins, is a facilitator for glycerol uptake and efflux and is inactive under osmotic stress. EMBO J. (1995):141360–1371.

[20] Krane C.M., Goldstein D.L. Comparative functional analysis ofaquaporins/glyceroporins in mammals and anurans Mamm. Genome. (2007)18:452–462.

[21] Smith B.L., Agre P. Erythrocyte Mr 28,000 transmembrane protein exists as a multisubunit oligo- mer similar to channel proteins. Journal of Biological Chemistry. (1991) 266:6407–6415.

[22] Park J.H., Saier M.H. Phylogenetic characterization of the MIP family of transmembrane channel proteins. J. Membr. Biol. (1996) 153:171–180.

[23] Mathai J.C., Agre P. Hourglass pore-forming domains restrict aquaporin-1 tetramer assembly. Biochemistry. (1999) 38:923–928.

[24] Pao G.M., Wu L.F., Johnson K.D., Hofte H., Chrispeels M.J., Sweet G., Sandal N.N., Saier M.H. Evolution of the MIP family of integral membrane transport proteins. Mol. Microbiol. (1991) 5:33–37.

[25] Zardoya R. Phylogeny and evolution of the major intrinsic protein family. Biol. Cell. (2005) 97:397–414.

[26] Fujiyoshi Y., Mitsuoka K., de Groot B.L., Philippsen A., Grubmuller H., Agre P., Engel A. Structure and function of water channels. Curr. Opin. Struc. Biol. (2002)12:509–515.

[27] Hub J.S., de Groot B.L. Mechanism of selectivity in aquaporins and aquaglyceroporins Proc. Natl. Acad. Sci. U. S. A. (2008) 105:1198–1203.

[28] Heller K.B., Lin E.C., Wilson, T.H. Substrate specificity and transport properties of the glycerol facilitator of Escherichia coli. Journal of Bacteriology. (1980)144:274–278.

[29] Borgnia M.J., Agre P.Reconstitution and functional comparison of purified GlpF and AqpZ, the glycerol and water channels from Escherichia coli. Proc Natl Acad Sci U S A. (2001) 98: 2888–2893.

[30] Fu D., Libson A., Miercke L. J., Weitzman, C., Nollert P., Krucinski J., Stroud R.M. Structure of a glycerol-conducting channel and the basis for its selectivity. Science. (2000) 290:481–486.

[31] Tajkhorshid E., Nollert P., Jensen M.O., Miercke L.J., O'Connell J., Stroud R. M., Schulten K. Control of the selectivity of the aquaporin water channel family by global orientational tuning. Science. (2002) 296:525–530.

[32] Murata K., Mitsuoka K., Hirai T., Walz T., Agre P., Heymann J.B., Engel A., Fujiyoshi, Y. Structural determinants of water permeation through aquaporin-1. Nature. (2000) 407:599–605.

[33] Ren G., Reddy V.S., Cheng A., Melnyk P., Mitra A.K. Visualization of a water-selective pore by electron crystallography in vitreous ice. Proceedings of the National Academy of Sciences USA. (2001) 98:1398–1403.

[34] Sui H., Han B.G., Lee J.K., Walian P., Ja B.K. Structural basis of water-specific transport through the AQP1 water channel. Nature. (2001) 414:872–878.

[35] Gorin M.B., Yancey S.B., Cline J., Revel J. Horwitz P.J., The major intrinsic protein (MIP) of the bovine lens fiber membrane: characterization and structure based on cDNA cloning. Cell (1984) 39:49–59.

[36] Verkman A.S., Mitra A.K., Structure and function of aquaporin water channels. Am. J. Physiol. Renal. Physiol. (2000) 278:F13–28.

[37] Benga G. On the definition, nomenclature and classification of water channel proteins (aquaporins and relatives). Mol Aspects Med. (2012) 33:514–517.

[38] Rojek A., Praetorius J., Frokiaer J., Nielsen S., Fenton R.A. A current view of the mammalian aquaglyceroporins. Annu. Rev. Physiol. (2008) 70:301–327.

[39] Wu B., Beitz E. Aquaporins with selectivity for unconventional permeants. Cell. Mol. Life Sci. (2007) 64:2413–2421.

[40] Liu Z., Shen J., Carbrey J.M., Mukhopadhyay R., Agre P., Rosen BP. Arsenite transport by mammalian aquaglyceroporins AQP7 and AQP9. Proc Natl Acad Sci USA. (2002) 99:6053–6058.

[41] King L.S., Konzo D., Agre P. From structure to disease: the evolving tale of Aquaporin biology. Nat Rev Cell Biol. (2004) 5:687–698.

[42] Verkman A.S. Mammalian aquaporins: diverse physiological roles and potential clinical significance. Expert Rev Mol Med. (2013) 10:1–21.

[43] Endo M., Jain R.K., Witwer B., Brown D. Water channel (aquaporin 1) expression and distribution in mammary carcinomas and glioblastomas. Microvasc Res. (1999) 58:89–98.

[44] Saadoun S., Papadopoulos M.C., Hara-Chikuma M., Verkman A.S. Impairment of angiogenesis and cell migration by targeted aquaporin-1 genedisruption. Nature. (2005) 434: 786–792.

[45] Verkman A.S., Anderson M.O., Papadopoulos, M.C. Aquaporins: important but elusive drug targets. Nat. Rev. Drug Discov. (2014)13:259–277.

[46] Kang S.K., Chae Y.K., Woo J., Kim M.S., Park J.C., Lee J., Soria J.C., Jang S.J., Sidransky D., Moon C. Role of human aquaporin 5 in colorectal carcinogenesis. Am. J. Pathol. (2008) 173: 518–525.

[47] Zhang Z., Chen Z., Song Y., Zhang P., Hu J., Bai C. Expression of aquaporin 5 increases proliferation and metastasis potential of lung cancer. J. Pathol. (2010) 221:210–220.

[48] Lebeck J. Metabolic impact of the glycerol channels AQP7 and AQP9 in adipose tissue and liver. J. Mol. Endocrinol. (2014) 52:R165–178.

[49] Badaut J., Lasbennes .F, Magistretti P.J., Regli L. Aquaporins in brain: distribution, physiology, and pathophysiology. J Cereb Blood Flow Metab. (2002) 22:367–378.

[50] Tait M.J., Saadoum S., Bell B.A., Popadopoulos M. Water movements in the brain: the role of aquaporins. Trends in neurosciences. (2008) 31:37–43.

[51] Pérez E., Barrachina M., Rodríguez A., Torrejón-Escribano B., Boada M., Hernández I., Sánchez M., Ferrer I. Aquaporin expression in the cerebral cortex is increased at early stages of Alzheimer disease. Brain Res. (2007) 1128:164–174.

[52] Satoh J., Tabunoki H., Yamamura T., Arima K., Konno H. Human astrocytes express aquaporin-1 and aquaporin-4 in vitro and in vivo. Neuropathology. (2007) 27:245–256.

[53] Moftakhar P., Lynch M.D., Pomakian J.L., Vinters H.V. Aquaporin expression in the brains of patients with or without cerebral amyloid angiopathy. J Neuropathol Exp Neurol. (2010) 69:1201–1209.

[54] MacAulay N., Zeuthen T. Water transport between CMS compartments: contributions of aquaporins and cotransporters. Neuroscience. (2010) 186:941–956.

[55] Boassa D., Stamer W.D., Yool A.J. Ion channel function of aquaporin-1 natively expressed in choroid plexus. J. Neurosci. (2006) 26:1719–7811.

[56] Redzic Z.B., Preston J.E., Duncan J.A., Chodobski A., Szmydynger-Chodobska J. The choroid plexus-cerebrospinal fluid system: from development to aging. Curr. Top. Dev. Biol. (2005) 71:1–52.

[57] Shields S.D., Mazario J., Skinner K., Basbaum A.I. Anatomical and functional analysis of aquaporin 1, a water channel in primary afferent neurons. Pain. (2007) 131:8–20.

[58] Nagahama M., Ma N., Semba R., Naruse S. Aquaporin 1 immunoreactive enteric neurons in the rat ileum. Neurosci Lett. (2006) 395:206–210.

[59] Ishihara E., Nagahama M., Naruse S., Semba R., Miura T., Usami M., Narita M.Neuropathological alteration of aquaporin 1 immunoreactive enteric neurons in the streptozotocin-induced diabetic rats. Auton Neurosci. (2008) 138:31–40.

[60] Thi M.M., Spray D.C., Hanani M. Aquaporin-4 water channels in enteric neurons. J Neurosci Res. (2008) 86:448–456.

[61] Matsumoto I., Nagamatsu N., Arai S., Emori Y., Abe K. Identification of candidate genes involved in somatosensory functions of cranial sensory ganglia. Brain Res Mol Brain Res. (2004)126:98–102.

[62] Oshio K., Watanabe H., Yan D., Verkman A.S., Manley G.T. Impaired pain sensation in mice lacking aquaporin-1 water channels. Biochem Biophys Res Comm. (2006) 341:1022–1028.

[63] Nandasena B.G., Suzuki A., Aita M., Kawano Y., Nozawa-Inoue K., et al. Immunolocalization of aquaporin-1 in the mechanoreceptive Ruffini endings in the periodontal ligament. Brain Res. (2007) 1157:32–40.

[64] Borsani E., Bernardi S., Albertini R., Rezzani R., Rodella L.F. Alterations of AQP2 expression in trigeminal ganglia in a murine inflammation model. Neurosci Lett. (2009) 449:183–188.

[65] Nielsen S., Smith B.L., Christensen E.I., Agre P. Distribution of the aquaporin CHIP in secretory and resorptive epithelia and capillary endothelia. Proc Natl Acad Sci U S A. (1993) 90:7275–7279.

[66] Kobayashi H., Minami S., Itoh S., Shiraishi S., Yokoo H., Yanagita T., Uezono Y., Mohri M., Wada A. Aquaporin subtypes in rat cerebral microvessels. Neurosci Lett. (2001) 297:163–166.

[67] Nielsen S, Nagelhus EA, Amiry-Moghaddam M, Bourque C, Agre P, Ottersen O.P. Specialized membrane domains for water transport in glial cells: highresolution immunogold cytochemistry of aquaporin-4 in rat brain. J Neurosci. (1997) 17:171–180.

[68] Nagelhus E.A, Mathiisen T.M, Ottersen O.P. Aquaporin-4 in the central nervous system: cellular and subcellular distribution and coexpression with KIR4.1. Neuroscience. (2004) 129:905–913.

[69] Oshio K., Binder D. K., Yang B., Schecter S., Verkman A. S., Manley G. T. Expression of aquaporin water channels in mouse spinal cord. Neuroscience. (2004) 127: 685–693.

[70] Costa C., Tortosa R., Domenech A., Vidal E., Pumarola M., Bassols A. Mapping of aggrecan, hyaluronic acid, heparan sulphate proteoglycans and aquaporin 4 in the central nervous system of the mouse. Journal of Chemical Neuroanatomy. (2007) 33:111–123.

[71] Rash J. E., Yasumura T., Hudson C. S., Agre P., Nielsen S. Direct immunogold labeling of aquaporin-4 in square arrays of astrocyte and ependymocyte plasma membranes in rat brain and spinal cord. Proceedings of the National Academy of Sciences of the United States of America. (1998) 95:11981–11986.

[72] Cavazzin C., Ferrari D., Facchetti F., Russignan A., Vescovi A.L., La Porta C.A., Gritti A. Unique expression and localization of aquaporin-4 and aquaporin-9 in murine and human neural stem cells and in their glial progeny. Glia. (2006) 53:167–181.

[73] Binder D.K., Yao X., Zador Z., Sick T.J., Verkman A.S, Manley G.T. Increased seizure duration and slowed potassium kinetics in mice lacking aquaporin-4 water channels. Glia. (2006) 53:631–636.

[74] Amiry-Moghaddam M., Ottersen O.P. The molecular basis of water transport in the brain. Nat. Rev. Neurosci. (2003) 4:991–1001.

[75] Rash J.E. Molecular disruptions of the panglial syncytium block potassium siphoning and axonal salutatory conduction: pertinence to neuromyelitis optica and other demyelinating diseases of the central nervous system. Neuroscience. (2010) 168:982–1008.

[76] Badaut J., Brunet J.F., Regli L. Aquaporins in the brain: from aqueduct to ‘‘multi-duct’’. Metab. Brain Dis. (2007) 22:251–263.

[77] Padmawar P., Yao X., Bloch O., Manley G.T, Verkman AS. K^+ waves in brain cortex visualized using a long-wavelength K^+-sensing fluorescent indicator. Nat Methods. (2005) 2:825–827.

[78] Saadoun S., Papadopoulos M.C., Watanabe H., Yan D., Manley G.T., Verkman A.S. Involvement of aquaporin-4 in astroglial cell migration and glial scar formation. J. Cell Sci. (2005)18:5691–5698.

[79] Tsukaguchi H., Shayakul C., Berger U. V., Mackenzie B., Devidas S., Guggino W.B., van Hoek A.N., Hediger M.A. Molecular characterization of a broad selectivity neutral solute channel. J Biol Chem. (1998) 273:24737–24743.

[80] Zelenina M. Regulation of brain aquaporins. Neurochem Int. (2010) 57:468–488.

[81] Badaut J., Hirt L., Granziera C., Bogousslavsky J., Magistretti P.J., Regli L. Astrocyte-specific expression of aquaporin-9 in mouse brain is increased after transient focal cerebral ischemia. J Cereb Blood Flow Metab. (2001) 21:477– 482.

[82] Badaut J., Petit J.M., Brunet J.F., Magistretti P.J., Charriaut-Marlangue C., Regli L. Distribution of aquaporin 9 in the adult rat brain: preferential expression in catecholaminergic neurons and in glial cells. Neuroscience. (2004) 128:27–38.

[83] Elkjaer M., Vajda Z., Nejsum L.N., Kwon T., Jensen U.B., Amiry Moghaddam M., Frokiaer J., Nielsen S. Immunolocalization of AQP9 in liver, epididymis, testis, spleen, and brain. Biochem Biophys Res Commun. (2000) 276:1118–1128.

[84] Ribeiro M., Hirt L., Bogousslavsky J., Regli L., Badaut J. Time course of aquaporin expression after transient focal cerebral ischemia in mice. J Neurosci Res. (2006) 83:1231–1240.

[85] McKenna M.C., Bezold L.I., Kimatian S.J., Tildon J.T., Fife M.M. Competition of glycerol with other oxidizable substrates in rat brain: a developmental study of glycerol oxidation by rat brain. Biochem J. (1986) 237:47–51.

[86] Levin B.E., Dunn-Meynell A.A., Routh V.H. Brain glucose sensing and body energy homeostasis: role in obesity and diabetes. Am J Physiol. (1999) 276: R1223-1231.

[87] Penicaud L., Leloup C., Lorsignol A., Alquier T., Guillod E. Brain glucose sensing mechanism and glucose homeostasis. Curr Opin Clin Nutr Metab Care. (2002) 5:539–543.

[88] Magistretti P.J., Pellerin L., Rothman D.L., Shulman R.G. Energy on demand. Science. (1999) 283:496–497.

[89] Nguyen N.H., Brathe A., Hassel B. Neuronal uptake and metabolism of glycerol and the neuronal expression of mitochondrial glycerol-3-phosphate dehydrogenase. J Neurochem. (2003) 85:831–842.

[90] Amiry-Moghaddam M., Lindland H., Zelenin S., Roberg B.A., Gundersen B.B., Petersen P., Rinvik E., Torgner I.A., Ottersen O.P. Brain mitochondria contain aquaporin water channels: evidence for the expression of a short AQP9 isoform in the inner mitochondrial membrane. FASEB. J. (2005) 19:1459–1467.

[91] Shin I., Kim H.J., Lee J.E., Gye M.C. Aquaporin7 expression during perinatal development of mouse brain. Neurosci. Lett. (2006) 409:106–111.

[92] Yamamoto N., Yoneda K., Asai K., Sobue K., Tada T., Fujita Y., Katsuya H., Fujita M., Aihara N., Mase M., Yamada K., Miura Y., Kato T. Alterations in the expression of the AQP family in cultured rat astrocytes during hypoxia and reoxygenation. Brain Res. Mol. Brain Res. (2001) 90:26–38.

[93] Albertini R., Bianchi R. Aquaporins and glia. Curr. Neuropharmacol. (2010) 8:84–91.

[94] Johannes C.M., Schlachetzki S., Wilke S., Pinheiro de Oliveira A.C. Studying neurodegenerative diseases in culture models Revista Brasileira de Psiquiatria. (2013) 35:S92–S100.

[95] Suzuki k., Suzuki Y. Globoid cell leucodystrophy (Krabbe's disease): deficiency of galactocerebroside beta-galactosidase. Proc Natl Acad Sci. (1970) 66:302–309.

[96] Wenger D.A., Suzuki K., Suzuki Y. "Galctosylceramide lipidosis: globoid cell leukodystrophy (Krabbe disease)". In: Scriver CR, Beaudet AL, Sly WS, Valle D, Childs B, Vogelstein B (eds) The metabolic and molecular bases of inherited disease. McGraw Hill, New York. (2011) 37:3669–3694.

[97] Graziano A.C., Parenti R., Avola R., Cardile V. Krabbe disease: involvement of connexin43 in the apoptotic effects of sphingolipid psychosine on mouse oligodendrocyte precursors. Apoptosis. (2016) 21:25–35.

[98] Gibbons H.M., Dragunow M. Adult human brain cell culture for neuroscience research. Int J Biochem Cell Biol. (2010) 42:844–856.

[99] Cebrián C., Loike J.D., Sulzer D. Neuroinflammation in Parkinson's disease animal models: a cell stress response or a step in neurodegeneration?. Curr Top Behav Neurosci. (2015) 22:237–270.

[100] Wang Q., Liu Y., Zhou J. Neuroinflammation in Parkinson's disease and its potential as therapeutic target. Transl Neurodegener. (2015) 4:1-9.

[101] Dawson T.M., Ko H.S., Dawson V.L. Genetic animal models of Parkinson's disease. Neuron. (2010) 66:646–661.

[102] Constantinescu R., Constantinescu A.T., Reichmann H., Janetzky B. Neuronal differentiation and long-term culture of the human neuroblastoma line SH-SY5Y. J Neural Transm Suppl. (2007) 17–28.

[103] Calegari F., Waskow C. Stem Cells: From Basic Research to Therapy, Volume 1: Basic Stem Cell Biology, Tissue Formation during Development, and Model Organisms. CRC Press. (2014).

[104] Weissman I.L., Anderson D.J., Gage F. Stem and progenitor cells: origins, phenotypes, lineage commitments, and transdifferentiations. Annu Rev Cell Dev Biol. (2001) 17:387–403.

[105] Watt SM., Contreras M. Stem cell medicine: umbilical cord blood and its stem cell potential. Semin Fetal Neonatal Med. (2005) 10:209-220.

[106] Reubinoff B.E., Pera M.F., Fong C.Y., Trounson A., Bongso A. Embryonic stem cell lines from human blastocysts: somatic differentiation in vitro. Nat Biotechnol. (2000) 18:399–404.

[107] Schuldiner M., Yanuka O., Itskovitz-Eldor J., Melton D.A., Benvenisty N. Effects of eight growth factors on the differentiation of cells derived from human embryonic stem cells. Proc Natl Acad Sci. (2000) 97:1307–11312.

[108] De Felici M., Farini D., Dolci S. In or out stemness: comparing growth factor signalling in mouse embryonic stem cells and primordial germ cells. Curr Stem Cell Res Ther. (2009) 4:87–97.

[109] Zeidán-Chuliá F., Noda M. Opening'' the mesenchymal stem cell toolbox. Eur J Dent. (2009) 3:240–249.

[110] Friedenstein A.J., Chailakhyan R.K., Latsinik N.V. Panasyuk A.F., Keiliss-Borok I.V. Stromal cells responsible for transferring the microenvironment of the hematopoietic tissue. Transpl. (1974) 17:331–340.

[111] Eaves C.J., Cashman J.D., Sutherland H.J., Otsuka T., Humphries R.K., Hogge D.E., Lansdorp P.L., Eaves A.C. Molecular analysis of primitive hematopoietic cell proliferation control mechanisms. Ann. N. Y. Acad. Sci. (1991) 628:298–306.

[112] Wislet-Gendebien S., Hans G., Leprince P., Rigo J.M., Moonen G., Rogister B. Plasticity of cultured mesenchymal stem cells: switch from nestin-positive to excitable neuron-like phenotype. Stem Cells. (2005) 23:392–402.

[113] Kern S., Eichler H., Stoeve J., Klüter H., Bieback K. Comparative analysis of mesenchymal stem cells from bone marrow, umbilical cord blood, or adipose tissue. Stem Cells. (2006) 24:1294–1301.

[114] Alvarez-Dolado M., Pardal R., Garcia-Verdugo J.M., Fike J.R., Lee H.O., Pfeffer K., Lois C., Morrison S.J., Alvarez-Buylla A. Fusion of bone-marrow-derived cells with Purkinje neurons, cardiomyocytes and hepatocytes. Nature. (2003) 425:968–973.

[115] Ahrens N., Tormin A., Paulus M., Roosterman D., Salama A., Krenn V., Neumann U., Scheding S. Mesenchymal stem cell content of human vertebral bone marrow. Transplantation. (2004) 78:925–929.

[116] Dominici M., Le Blanc K., Mueller I., Slaper-Cortenbach I., Marini F., Krause D., Deans R., Keating A., Prockop Dj., Horwitz E. Minimal criteria for defining multipotent mesenchymal stromal cells. The International Society for Cellular Therapy position statement. Cytotherapy. (2006) 8: 315–317.

[117] Casteilla L., Planat-Bénard V., Cousin B., Silvestre J.S., Laharrague P., Charrière G., Carrière A., Pénicaud L. Plasticity of adipose tissue: a promising

therapeutic avenue in the treatment of cardiovascular and blood diseases? Arch Mal Coeur Vaiss. (2005) 98:922–926.

[118] Oedayrajsingh-Varma M.J., van Ham S.M., Knippenberg M., Helder M.N., Klein-Nulend J., Schouten T.E., Ritt M.J., van Milligen F.J. Adipose tissue derived mesenchymal stem cell yield and growth characteristics are affected by the tissue harvesting procedure. Cytotherapy. (2006) 8:166–177.

[119] Strem B.M., Hicok K.C., Zhu M., Wulur I., Alfonso Z., Schreiber R.E., Fraser J.K., Hedrick M.H. Multipotential differentiation of adipose tissue-derived stem cells. Keio Journal of Medicine. (2005) 54:132–141.

[120] Zuk P.A., Zhu M., Mizuno H., Huang J., Futrell J.W., Katz A.J., Benhaim P., Lorenz H.P., Hedrick M.H. Multilineage cells from human adipose tissue: implications for cell-based therapies. Tissue Engineering. (2001) 7:211–228.

[121] Tholpady S.S., Llull R., Ogle R.C., Rubin J.P., Futrell J.W., Katz A.J. Adipose tissue: stem cells and beyond. Clin Plast Surg. (2006) 33:55–62.

[122] Traktuev D.O., Merfeld-Clauss S., Li J., Kolonin M., Arap W., Pasqualini R., Johnstone B..H, March K.L. A population of multipotent CD34-positive adipose stromal cells share pericyte and mesenchymal surface markers, reside in a periendothelial location, and stabilize endothelial networks. Circ Res. (2008) 102:77–85.

[123] Katz A.J., Tholpady A., Tholpady S.S., Shang H., Ogle R.C. Cell surface and transcriptional characterization of human adipose-derived adherent stromal (hADAS) cells. Stem Cells. (2005) 23:412–423.

[124] Zuk P.A., Zhu M., Ashjian P., De Ugarte D.A., Huang J.I., Mizuno H., Alfonso Z.C., Fraser J.K., Benhaim P., Hedrick M.H. Human adipose tissue is a source of multipotent stem cells. Mol Biol Cell. (2002) 13:4279–4295.

[125] Arrigoni E., Lopa S., de Girolamo L., Stanco D., Brini A.T. Isolation, characterization and osteogenic differentiation of adipose-derived stem cells: from small to large animal models. Cell Tissue Res. (2009) 338:401–411.

[126] Zannettino A.C., Paton S., Arthur A., Khor F., Itescu S., Gimble J.M., Gronthos S. Multipotential human adipose-derived stromal stem cells exhibit a perivascular phenotype in vitro and in vivo. J Cell Physiol. (2008) 214:413–421.

[127] Guilak F., Lott K.E., Awad H.A., Cao Q., Hicok K.C., Fermor B., Gimble J.M. Clonal analysis of the differentiation potential of human adipose-derived adult stem cells. J Cell Physiol. (2006) 206:229–237.

[128] Safwani W.K., Makpol S., Sathapan S., Chua K.H. The impact of long-term in vitro expansion on the senescence-associated markers of human adipose-derived stem cells. Appl Biochem Biotechnol. (2012) 166:2101–2113.

[129] Zuk P. A. The adipose-derived stem cell: looking back and looking ahead. Molecular Biology of the Cell. (2010) 21: 1783–1787.

[130] Romanov Y.A., Darevskaya A.N., Merzlikina N.V., Buravkova L.B. Mesenchymal stem cells from human bone marrow and adipose tissue: isolation, characterization, and differentiation potentialities. Bull Exp Biol Med. (2005) 140:138–143.

[131] Puissant B., Barreau C., Clavel C., Corre J., Bousquet C., Taureau C., Cousin B., Abbal M., Laharrague P., Penicaud L., Casteilla L., Blancher A. Immunomodulatory effect of human adipose tissue-derived adult stem cells: comparison with bone marrow mesenchymal stem cells. Br J Haematol. (2005) 129:118–129.

[132] De Francesco F., Tirino V., Desiderio V., Ferraro G., D'Andrea F., Giuliano M., Pirozzi G., De Rosa A., Papaccio G.Human CD34/CD90 ASCs are capable of growing as sphere clusters, producing high levels of VEGF and forming capillaries. PloS One. (2009) 4:e6537.

[133] Schubert T., Xhema D., Vériter S., Schubert M., Behets C., Delloye C., Gianello P., Dufrane D. The enhanced performance of bone allografts using osteogenic-differentiated adipose-derived mesenchymal stem cells. Biomaterials. (2011) 32:8880–8891.

[134] La fosse A., Desmet C., Aouassar N., Andre W., Hanet M-S., Beauloye C., Vanwijck R., Poirel H.A., Gallez B., Dufrane D. Autologous adipose stromal cells seeded on a human collagen matrix for dermal regeneration in chronic wounds: clinical proof of concept. Plast Reconstr Surg. (2015) 136:279–295.

[135] Ferraro G.A., De Francesco F., Nicoletti G., Paino F., Desiderio V., Tirino V., D'Andrea F. Human adipose $CD34^+$ $CD90^+$ stem cells and collagen scaffold constructs grafted in vivo fabricate loose connective and adipose tissues. J Cell Biochem. (2013) 114:1039–1049.

[136] Tsuji W., Rubin J.P., Marra K.G. Adipose-derived stem cells: Implications in tissue regeneration. World J Stem Cells. (2014) 6:312–321.

[137] Schubert T., Poilvache H., Galli C., Gianello P., Dufrane D. Galactosyl-knock-out engineered pig as a xenogenic donor source of adipose MSCs for bone regeneration. Biomaterials. (2013) 34:3279–3289.

[138] Vériter S., Gianello P., Igarashi Y., Beaurin G., Ghyselinck A., Aouassar N., Jordan B., Gallez B., Dufrane D. Improvement of subcutaneous bioartificial pancreas vascularization and function by coencapsulation of pig islets and mesenchymal stem cells in primates. Cell Transplant. (2014) 23:1349–1364.

[139] Nagaya N., Kangawa K., Itoh T., Iwase T., Murakami S., Miyahara Y., Fujii T., Uematsu M., Ohgushi H., Yamagishi M., Tokudome T., Mori H., Miyatake K., Kitamura S. Transplantation of mesenchymal stem cells improves cardiac function in a rat model of dilated cardiomyopathy. Circulation. (2005) 112:1128–1135.

[140] Moon M.H., Kim S.Y., Kim Y.J., Kim S.J., Lee J.B., Bae Y.C., Sung SM, Jung J.S. Human adipose tissue-derived mesenchymal stem cells improve postnatal neovascularization in a mouse model of hindlimb ischemia. Cell Physiol Biochem Int J Exp Cell Physiol Biochem Pharmacol. (2006) 17:279–290.

[141] Le Blanc K., Ringden O. Immunobiology of human mesenchymal stem cells and future use in hematopoietic stem cell transplantation. Biol Blood Marrow Transplant. (2005)11:321–334.

[142] Javazon E.H., Beggs K.J., Flake A.W. Mesenchymal stem cells: paradoxes of passaging. Exp Hematol. (2004) 32:414–425.

[143] Barry F.P., Murphy J.M. Mesenchymal stem cells: clinical applications and biological characterization. Int J Bioch Cell Biol. (2004) 36:568–584.

[144] Tropel P., Noël D., Platet N., Legrand P., Benabid A.L. Berger F. Isolation and characterization of mesenchymal stem cells from adult mouse bone marrow. Exp Cell Res. (2004) 295:395–406.

[145] Pfeiffer S, McLaughlin D. In vitro differentiation of human amniotic fluid-derived cells: augmentation towards a neuronal dopaminergic phenotype. Cell Biol Int. (2010) 34:959–967.

[146] Portmann-Lanz C.B., Schoeberlein A., Portmann R., Mohr S., Rollini P., Sager R., Surbek D.V. Turning placenta into brain: placental mesenchymal stemcells differentiate into neurons and oligodendrocytes.Am J Obstet Gynecol. (2010) 202:294 e1–294.e11.

[147] Toda A., Okabe M., Yoshida T., Nikaido T. The potential of amniotic membrane/amnion-derived cells for regeneration of various tissues. J Pharmacol Sci. (2007) 105:215–228.

[148] Musumeci G., Mobasheri A., Trovato F.M., Szychlinska M.A., Graziano A.C., Lo Furno D., Avola R., Mangano S., Giuffrida R., Cardile V. Biosynthesis of collagen I, II, RUNX2 and lubricin at different time points of chondrogenic differentiation in a 3D in vitro model of human mesenchymal stem cells derived from adipose tissue. Acta Histochem. (2014) 116:1407–1417.

[149] Lo Furno D., Graziano A.C., Avola R., Giuffrida R., Perciavalle V., Bonina F., Mannino G., Cardile V. A Citrus bergamia Extract Decreases Adipogenesis and Increases Lipolysis by Modulating PPAR Levels in Mesenchymal Stem Cells from Human Adipose Tissue. PPAR Res. (2016) 2016:4563815.

[150] Lo Furno D., Pellitteri R., Graziano A. C., Giuffrida R., Vancheri C., Gili E., Cardile V. Differentiation of human adipose stem cells into neural phenotype byneuroblastoma- or olfactory ensheathing cells-conditioned medium. Journal of Cellular Physiology. (2013) 228:2109–2118.

[151] Ashjian P.H., Elbarbary A.S., Edmonds B., De Ugarte D., Zhu M., Zuk P.A., Lorenz H.P., Benhaim P., Hedrick M.H. In vitro differentiation of human processed lipoaspirate cells into early neural progenitors. Plast Reconstr Surg. (2003) 111:1922–1931.

[152] Winter A., Breit S., Parsch D., Benz K., Steck E., Hauner H., Weber R.M., Ewerbeck V., Richter W. Cartilage-like gene expression in differentiated human stem cell spheroids: a comparison of bone marrow-derived and adipose tissue-derived stromal cells. Arthritis Rheum. (2003) 48:418–429.

[153] Guilak F., Estes B.T., Diekman B.O., Moutos F.T., Gimble J.M. Multipotent adult stem cells from adipose tissue for muscularskeletal tissue engineering. Clin Orthop Relat Res. (2010) 468:2530–2540.

[154] Woodbury D., Schwarz E.J., Prockop D.J., Black I.B. Adult rat and human bone marrow stromal cells differentiate into neurons. J Neurosci Res. (2000) 61:364–370.

[155] Zurita M., Bonilla C., Otero L., Aguayo C., Vaquero J. Neural transdifferentiation of bone marrow stromal cells obtained by chemical agents is a short-time reversible phenomenon. Neurosci Res. (2008) 60:275–280.

[156] Alexanian A. R. Epigenetic modifiers promote efficient generation of neural-like cells from bone marrow-derived mesenchymal cells grown in neural environment.J Cell Biochem. (2007)100:362–371.

[157] Kohyama J., Abe H., Shimazaki T., Koizumi A., Nakashima K., Gojo S., Taga T, Okano H, Hata J, Umezawa A. Brain from bone: efficient "meta-differentiation" of marrow stroma-derived mature osteoblasts to neurons with Noggin or a demethylating agent. Differentiation. (2001) 68:235–244.

[158] Qu T.Y., Dong X.J., Sugaya I., Vaghani A., Pulido J., Sugaya K. Bromodeoxyuridine increases multipotency of human bone marrow-derived stem cells. Restor Neurol Neurosci. (2004) 22:459–468.

[159] Dezawa M., Kanno H., Hoshino M. Cho H., Matsumoto N., Itokazu Y., Tajima N., Yamada H., Sawada H., Ishikawa H., Mimura T., Kitada M., Suzuki Y., Ide C. Specific induction of neuronal cells from bone marrow stromal cells and application for autologous transplantation. J Clin Invest (2004) 113:1701–1710.

[160] Kohyama J, Abe H, Shimazaki T., Koizumi A.,.Nakashima K., Gojo S., Taga T., Okano H., Hata J. Akihiro Umezawa A.Brain from bone: efficient “meta-differentiation” of marrow stroma-derived mature osteoblasts to neurons with Noggin or a demethylating agent. Differentiation. (2001) 68:235–244.

[161] Sanchez-Ramos J., Song S., Cardozo-Pelaez F., Hazzi C., Stedeford T., Willing A., Freeman T.B., Saporta S., Janssen W., Patel N., Cooper D.R., Sanberg P.R. Adult bone marrow stromal cells differentiate into neural cells in vitro. Exp Neurol. (2000) 164:247–256.

[162] Reynolds B.A., Weiss S. Generation of neuron and astrocytes from isolated cells of the adult mammalian central nervous system. Science. (1992) 255:1707–1710.

[163] Johnson N.F., Hubbs A.F. Epithelial progenitor cells in the rat trachea. Am J Respir Cell Mol Biol. (1990) 3:579–585.

[164] La Porta C.A., Gena P., Gritti A., Fascio U., Svelto M., G Calamita. Adult murine CNS stem cells express aquaporin channels. Biol Cell. (2006) 98:89–94.

[165] Avril-Delplanque A., Casal I., Castillon N., Hinnrasky J., Puchelle E., Peault B. Aquaporin-3 expression in human fetal airway epithelial progenitor cells. Stem Cells. (2005) 23:992–1001.

[166] Kong H, Fan Y, Xie J, Ding J, Sha L, Shi X, Sun X, Hu G. AQP4 knockout impairs proliferation, migration and neuronal differentiation of adult neural stem cells. J Cell Sci. (2008) 211:4029–4036.

[167] Yi F., Khan M., Gao H., Hao F., Sun M., Zhong L., Lu C., Feng X., Ma T. Increased differentiation capacity of bone marrow-derived mesenchymal stem cells in aquaporin-5 deficiency. Stem Cells Dev. (2012) 21:2495–2507.

[168] Randell S.H., Comment C.E., Ramaekers F.C., Nettesheim P. Properties of rat tracheal epithelial cells separated based on expression of cell surface alpha-galactosyl end groups. Am J Respir Cell Mol Biol. (1991)4:544–554.

[169] Calamita G., Mazzone A., Bizzoca A., Cavalier A., Cassano G., Thomas D., Svelto M. Expression and immunolocalization of the aquaporin-8 water channel in rat gastrointestinal tract. Eur. J. Cell Biol. (2001) 80:711–719.

[170] Garlid, K.D. Mitochondrial volume control. In Integration of Mitochondrial Function. Plenum. New York (1988) 259–278.

[171] Venero J.L., Vizuete M.L., Ilundain A.A., Machado A., Echevarria M., Cano J. Detailed localization of aquaporin-4 messenger RNA in the CNS: preferential expression in periventricular organs. Neuroscience. (1999) 94:239–250.

[172] Badaut J., Lasbennes F., Magistretti P.J., Regli L. Aquaporins in brain: distribution, physiology, and pathophysiology. J Cereb Blood Flow Metab. (2002) 22:367–378.

[173] Leigh E.W.S., Leigh A.S. Large Pore Ion and Metabolite-Permeable Channel Regulation of Postnatal Ventricular Zone Neural Stemand Progenitor Cells: Interplay between Aquaporins, Connexins, and Pannexins? Stem Cells International. (2012) 454180:1–9.

[174] Meng F., Rui Y., Xu L., Wan C., Jian X., Gang L. Aqp1 Enhances Migration of Bone Marrow Mesenchymal Stem Cells Through Regulation of FAK and b-Catenin. Stem Cells and Development. (2014) 23:1-10.

LIST OF PUBLICATIONS AND SCIENTIFIC CONTRIBUTIONS

Manuscripts submitted

- **Avola R**, Graziano ACE, Pannuzzo G, Cardile V. New insights on Parkinson's disease from differentiation of SH-SY5Y into dopaminergic neurons: the involvement of aquaporin4 and 9. Submitted on Disease Models and Mechanisms.
- Nsir H, Szychlinska MA, Cardile V, Graziano ACE, **Avola R,** Hessafi H, Zarouk M, Castrogiovanni P, Musumeci G. Polar and apolar olive oil extracts and leaf as a promising anti-inflammatory natural treatment for osteoarthritis. Submitted on Molecules.

Publications on international journals

1. Graziano A, Cardile V, **Avola R,** Vicario N, Parenti C, Salvatorelli L, Magro G, Parenti R. Wilms' Tumor Gene 1 silencing inhibits proliferation of human osteosarcoma MG-63 cell line by cell cycle arrest and apoptosis activation. Oncotarget. 2017 Jan 18. DOI: 10.18632/oncotarget.14715.
2. Cardile V, Graziano ACE, **Avola R,** Piovano M, Russo A. Potential anticancer activity of lichen secondary metabolite physodic acid. Chemico-biological interactions 2016 December DOI: 10.1016/j.cbi.2016.12.007.
3. **Avola R**, Graziano ACE, Pannuzzo G, Cardile V. Human mesenchymal stem cells from adipose tissue differentiated into neuronal or glial phenotype express different aquaporins. Mol Neurobiol. 2016 Dec 5. DOI: 10.1007/s12035-016-0312-6.
4. **Avola R,** Graziano ACE, Pannuzzo G, Alvarez E, Cardile V. Krabbe's Leukodystrophy: Approaches and Models In Vitro Journal of Neuroscience Research Epub 2016 Nov. 94:1284–1292.
5. Graziano ACE, **Avola R,** Pannuzzo G, Cardile V. Chaperones as potential therapeutics for Krabbe disease. Journal of Neuroscience Research Epub 2016 Oct. 94:1220–1230.

6. Pannuzzo G, ACE, Pannuzo M, Massman MF **Avola R**, Cardile V. Zoledronate Derivatives as Potential Inhibitors of Uridine Diphosphate- Galactose Ceramide Galactosyltransferase 8: A Combined Molecular Docking and Dynamic Study . Journal of Neuroscience Research Epub 2016 Nov 94:1318–1326.
7. Lo Furno D, Graziano AC, **Avola R**, Giuffrida R, Perciavalle V, Bonina F, Mannino G, Cardile V. A Citrus bergamia Extract Decreases Adipogenesis and Increases Lipolysis by Modulating PPAR Levels in Mesenchymal Stem Cells from Human Adipose Tissue. PPAR Res. 2016; 2016:4563815.
8. Graziano AC, Parenti R, **Avola R**, Cardile V. Krabbe disease: involvement of connexin43 in the apoptotic effects of sphingolipid psychosine on mouse oligodendrocyte precursors. Apoptosis. 2016 Jan; 21(1):25-35.
9. Musumeci G, Mobasheri A, Trovato FM, Szychlinska MA, Graziano AC, Lo Furno D, **Avola R**, Mangano S, Giuffrida R, Cardile V. Biosynthesis of collagen I, II, RUNX2 and lubricin at different time points of chondrogenic differentiation in a 3D in vitro model of human mesenchymal stem cells derived from adipose tissue. Acta Histochem. 2014 Oct; 116(8):1407-17.
10. Castrogiovanni P, Musumeci G, Trovato FM, **Avola R**, Magro G, Imbesi R. Effects of high-tryptophan diet on pre- and postnatal development in rats: a morphological study. Eur J Nutr. 2014 Feb; 53(1):297-308.
11. Musumeci G, Trovato FM, **Avola R**, Imbesi R, Castrogiovanni P. Serotonin/growth hormone/insulin-like growth factors axis on pre- and postnatal development: A contemporary review. OA Anatomy. 2013 Mar; 1(2):12.
12. Musumeci G, Trovato FM, **Avola R,** Imbesi R, Ventimiglia PC. The role of prolactin in the healing process: A preliminary morphological study. OA Anatomy. 2013 Mar; 1(1):9.

Conference procedeedings

1. **Avola R**, Graziano ACE, Pannuzzo G, Cardile V."Identification of water channel aquaporins in human chondrocytes from adipose mesenchymal stem cells". 67th National Congress of the Italian Physiological Society. Catania, September 21th-23th, 2016.
2. Graziano A, Cardile V, **Avola R**, Vicario N, Parenti C, Salvatorelli L, Magro G, Parenti R. "Wilms' Tumor Gene 1 silencing inhibits proliferation of human osteosarcoma MG-63 cell line by cell cycle arrest and apoptosis activation" 67th National Congress of the Italian Physiological Society. Catania, September 21th-23th, 2016**.**
3. **Avola R**, Graziano ACE, Pannuzzo G, Lo Furno D, Cardile V. "Evaluation of aquaporins during glial or neuronal differentiation of human mesenchymal stem cells from human adipose tissue". 66th National Congress of the Italian Physiological Society. Genova, September 16th-18th, 2015.
4. Graziano ACE, Pannuzzo G, **Avola R**, Cardile V**.** "Effects of psychosine on some apoptosis markers in mouse oligodendrocytes precursors". 66th National Congress of the Italian Physiological Society. Genova, September 16th-18th, 2015.
5. **Avola R,** Graziano ACE, Cardile V**.** "Aquaporin1, 4 and 9 expressions during the differentiation of human mesenchymal stem cells into neural phenotype". 13th Summer School of Neuroscience: "Cognition the target" Catania July 11th-17th, 2015.
6. Graziano ACE, Lo Furno D, Pellitteri R, **Avola R**, Giuffrida R, Cardile V. **"**Neural differentiation of human mesenchymal stem cells from adipose tissue treated with conditioned medium from olfactory ensheathing cells (OECS) or neuroblastoma B104 cell line". 27th Annual Conference of Italian Association of Cell Cultures (ONLUS-AICC) - 5th International Satellite Symposium AICC-GISM November 12th-13th, 2014.

7. Lo Furno D, Graziano A, **Avola R**, Giuffrida R, Cardile V. "Time course of chondrogenic differentiation of human mesenchymal stem cells derived from adipose tissue". 65th National Congress of the Italian Physiological Society. Anacapri, September 28th -30th, 2014.
8. Graziano A, Parenti R, **Avola R**, Cardile V. "Analysis of psychosine-induced damage in different cell types with and without GALC mutation". 65th National Congress of the Italian Physiological Society. Anacapri, September 28th-30th, 2014.
9. Musumeci G, Castrogiovanni P, Giunta S, **Avola R**, Pichler K, Weinberg AM, Carnazza ML, Loreto C. The effects of physical activity (treadmill and vibration stimulation training) on RANKL and OPG expression in bone cells, in rats with glucorticoid-induced osteoporosis. 65th National Congress of the Italian Anatomy and Histology Society. Brescia, September 20th-22th, 2013.
10. Musumeci G, Loreto C, Giunta S, **Avola R**, Pichler K, Weinberg AM, Castrogiovanni P, Carnazza ML, Castorina S. The effects of physical activity (treadmill and vibration stimulation training) on Caspase-3 and Lubricin expression in articular cartilage, in rats with glucorticoid-induced osteoarthritis. 65th National Congress of the Italian Anatomy and Histology Society. Brescia, September 20th-22th 2013.